Isolation and Structure Elucidation of Antiproliferative and Antiplasmodial Natural Products from Plants

Ming Wang

Thesis submitted to the faculty of the
Virginia Polytechnic Institute and State University
In partial fulfillment of the requirements for the degree of

Master of Science in Chemistry

David G. I. Kingston, Chair
Paul R. Carlier
Webster L. Santos

December 1, 2016
Blacksburg, Virginia

Keywords: Natural Products, Antiproliferative, Antiplasmodial,
A2780, *Plasmodium falciparum* Dd2

Isolation and Structure Elucidation of Antiproliferative and Antiplasmodial Natural Products from Plants

Ming Wang

ABSTRACT

As part of an International Cooperative Biodiversity Group (ICBG) program and a collaborative research project with the Natural Products Discovery Institute, four plant extracts were investigated for their antiproliferative and antiplasmodial activities. With the guidance of bioassay guided fractionation, two known antiproliferative terpenoids (**2.1** and **2.2**) were isolated from *Hypoestes sp.* (Acanthaceae), four known antiplasmodial liminoids (**3.1**–**3.4**) were isolated from *Carapa guianensis* (Meliaceae), one inactive terpenoid (**4.1**) was isolated from *Erica maesta* (Ericaceae), and four cerebrosides (**4.2-4.5**) were obtained from *Hohenbergia antillana* (Bromeliaceae).

The structures of these compounds were elucidated by using 1D (^{1}H and ^{13}C), 2D (HMBC, HSQC, COSY, NOESY) NMR spectroscopy and mass spectrometry. The structures of the compounds were also confirmed by comparing them with reported values from the literature.

Compounds **2.1** and **2.2** showed moderate antiproliferative activity against the A2780 human ovarian cancer cell line with IC_{50} values of 6.9 μM and 3.4 μM, respectively. They also exhibited moderate antiplasmodial activity against chloroquine-resistant *Plasmodium falciparum* strain Dd2 with IC_{50} values of 9.9 ± 1.4 μM and 2.8 ± 0.7 μM, respectively. Compounds **3.1** to **3.4** had moderate antiplasmodial activity against *Plasmodium falciparum* Dd2 strain with IC_{50} values of 2.0 ± 0.3 μM, 2.1 ± 0.1 μM, 2.1 ± 0.2 μM and 2.8 ± 0.2 μM, respectively. Compounds **4.1** and **4.2** showed very weak antiplasmodial activity against *Plasmodium falciparum* Dd2 strain, with IC_{50} values between 5 and 10 μg/mL.

Isolation and Structure Elucidation of Antiproliferative and Antiplasmodial Natural Products from Plants

Ming Wang

GENERAL AUDIENCE ABSTRACT

Cancer has a major impact all over the world and is one of the leading causes of death. Malaria remains as one of the most severe tropical diseases in the world. It is a common and often fatal disease caused by a parasitic infection. The treatment of cancer and malaria is a significant challenge, and has become a top priority in drug discovery field. The natural products from plants have been used for medicinal purpose for a long time, and a lot of well-known plant based natural product drugs have been discovered, including anticancer drug paclitaxel, and antimalarial drug chloroquine and artemisinin. However, the resistances for these drugs have developed, and it is urgent to find new drug that can take their place. This research is trying to find promising anticancer and antimalarial natural products from plant extracts. From four plant extracts, two antiproliferative compounds and four antiplasmodial compounds were discovered. In this thesis, the isolation and structure elucidation of these compounds will be discussed.

ACKNOWLEGEMENTS

Firstly, I would like to thank my parents and my husband, Long Xia, for their unconditional love and support for my life and study. Secondly, I would like to thank my advisor, Dr. David G. I. Kingston for his invaluable mentorship and encouragement. He helped me develop an interest in natural product isolation and inspired my desire to become a scientist. I would also like to thank my committee, Dr. Paul R. Carlier and Dr. Webster Santos, for their guidance and support throughout the years. I also thank Dr. Maria Belen Cassera and her group for performing the antimalarial assays. I would like to thank Dr. Murthy Shanaiah, Dr. Mehdi Ashraf-Khorassani, and Mr. Bill Bebout who provided the analytical services for my research.

I would also like to thank all the current and former Kingston group members, Yumin Dai, Yixi Liu, Alex Eaton, Qingxi Su, Chris Presley, Yongle Du, Ms. Karen Innanccone and Ms. Peggy Brodie.

Table of Contents

List of Tables

List of Figures

Chapter 1. Introduction

1.1 Introduction to Cancer

Cancer has a major impact all over the world and is one of the leading causes of death. In 2012, 14 million people were diagnosed with cancer, and 8.2 million died from the disease. Because of the increasing and aging population of the world, the worldwide burden of cancer rises every year, and this rise is especially severe in developing countries. More than 60% of cases occurred in Africa, Asia, and Central and South America, and about 70% of deaths from cancer occurred in these regions.[1]

Cancer is a class of diseases caused by uncontrolled cell-growth. Cancer cells are different from normal cells in many ways. Normal cells will mature into different types and have various functions, but cancer cells do not. Normal cells grow and divide into new cells only when the body needs them, and after growing old they die and are replaced of by new cells. Cell death is controlled by a procedure called programmed cell death or apoptosis. For cancer cells, this process breaks down, and cancer cells can ignore the signal that tells cells to stop dividing. Therefore, new cells will be generated even they are not needed, and old or damaged cells will not die, but keep dividing, leading to the appearance of tumors. In addition, cancer cells can induce surrounding cells to form blood vessels to provide oxygen and nutrition for their growth, and take waste away from them.[2]

There are two types of tumor, malignant tumors and benign tumors. Malignant tumors can spread and invade tissues nearby, and even break off and transfer to other parts of the body through blood or the lymph system, and generate new tumors elsewhere. Benign tumors, however, will not spread or invade to other places, but will usually grow large, which would be life-threatening in the brain.[3]

1.1.1 Ovarian Cancer

There are over 100 types of human cancer, and they are classified by the affected tissue or organ. Ovarian cancer happens if cancer cells grow in the ovary. In most cases, cancer cells arise from the epithelium of the ovary. It is the eighth most common cancer among women, and the most lethal cancer among gynecologic cancers.[4]

In the early stages of ovarian cancer, few symptoms are shown, but these become worse and more persistent as the cancer grows. Possible symptoms include pain in the pelvis, the lower side of the body, the lower stomach, and more frequent and urgent urination. Sometimes, patients also suffer from nausea, weight loss and tiredness.[5]

Ovarian cancer is caused by uncontrolled cell division as in other cancers, but it is not known how this disease arises. However, some factors can increase the risk of developing ovarian cancer. First is genetics, since women with a family history of ovarian cancer or breast cancer will have a higher risk of developing ovarian cancer than other women. The number of total lifetime ovulations also has an effect. Women with no children, or who start their periods at an early age or start their menopause later than average are more likely to develop ovarian cancer. In addition, being overweight, having hormone replacement therapy, and environmental factors can also lead to ovarian cancer.[5]

1.1.2 Important Antiproliferative Compounds against Cancer Cells

1.1.2.1 Paclitaxel

The discovery of paclitaxel (Taxol®, **1.1**) is an important event in natural product drug discovery and development. It was isolated from *Taxus brevifolia* (Pacific Yew) bark in 1969,[6] but it was not considered as a promising candidate because of its moderate *in vivo* activity against P388 and L1210 murine leukemia models. Interest in paclitaxel was stimulated in 1976 when

strong activity was found against the B16 melanoma. Further interest was developed after discovering its broad spectrum of activity and its unique mechanism of promoting tubulin polymerization and stabilizing microtubules against depolymerization.[7]

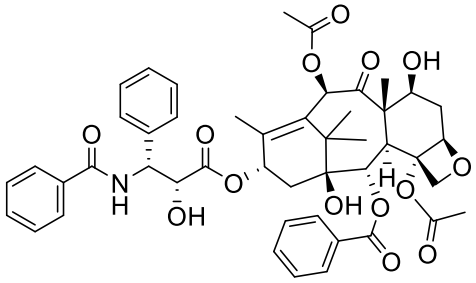

1.1

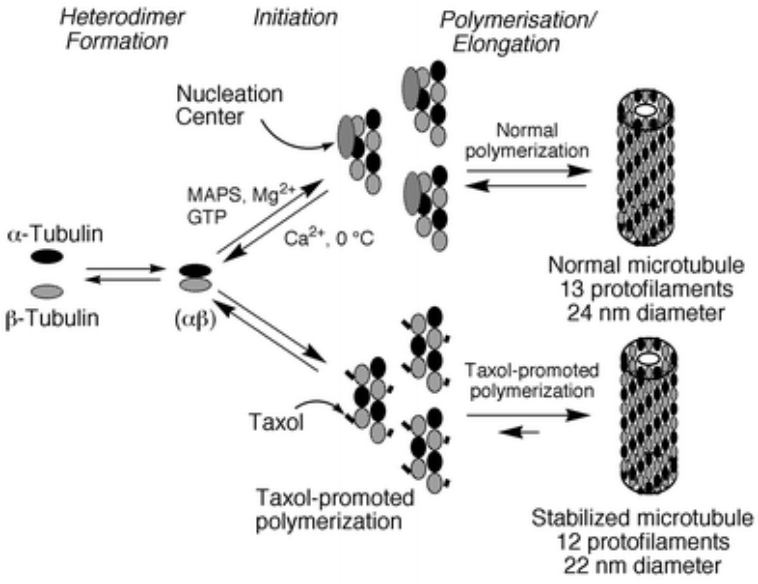

Figure 1-1. Taxol stabilizes tubulin polymerization.[8]
With permission from *Chem. Commun*., **2001**, 867-880. Copyright 2001 Royal Society of Chemistry.

Paclitaxel can bind to the β-tubulin subunits of microtubules in a 1:1 ratio, as shown in Figure 1-1. Unlike some compounds that inhibit the assembly of microtubules, paclitaxel can stabilize the microtubule and prevent it from disassembling. This will stop the formation of the metaphase spindle configuration, and block mitosis.[9] Treated cells will then stop division, and die or reverse back to the G-phase. In addition, after the interruption of microtubule formation, Raf-1

kinase can be activated, which can phosphorylate the antiapoptotic protein Bcl-2 and lead to its inactivation.[10] Also paclitaxel can deactivate Bcl-2 by binding with it directly.

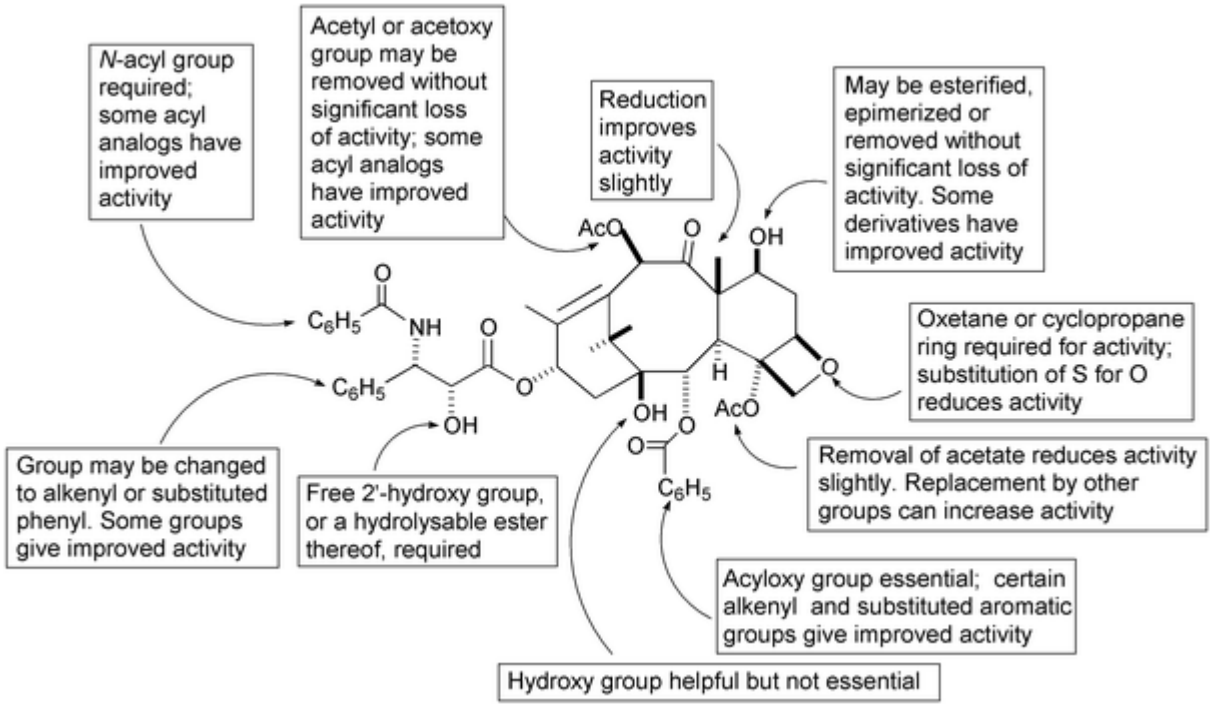

Figure 1-2. Structure-activity relationship of Taxol.[8]
With permission from *Chem. Commun*., **2001**, 867-880. Copyright 2001 Royal Society of Chemistry.

Although paclitaxel is an important anticancer agent, there are still many challenges waiting to be overcome. First is selectivity, since paclitaxel, like other anticancer drugs, is toxic to cancer cells as well as normal cells. Many research groups are thus trying to deliver it in the form of a pro-drug.[11] Another challenge is its low solubility in water; paclitaxel is formulated with Cremophor EL and ethanol or bound with albumin to overcome this problem. To better understand its activity as well as solving these problems, many studies have been done on its structure-activity relationships (SAR), and various analogs of paclitaxel have been produced.[8] Partial SAR information is summarized in Figure 1-2.

In summary, the discovery and development of paclitaxel as an anticancer drug is an important lesson for natural product drug discovery. It provides a new mechanism to treat cancer,

and reveals a new skeleton for structure modification. Some analogs of paclitaxel have even moved to clinical use such as docetaxel. But more work is still required to increase the understanding of how paclitaxel binds with tubulin.

1.2 Introduction to Malaria

Malaria remains as one of the most severe tropical diseases in the world. It is a common and often fatal disease caused by a parasitic infection. The bite of an infected female *Anopheles* mosquito transmits protozoan parasites of the genus *Plasmodium* from the mosquito to an individual. In some cases, transmission may also occur during blood transfusion, or between mother and fetus. Because of these transmission methods, malaria has become a worldwide problem, leading to approximately 214 million infections and 438,000 deaths in 2015.[12]

Although malaria has been eliminated in the United States and most European countries by methods such as vector control and changing land use, it still remains as an important health problem worldwide. There are about 3.2 billion people at a risk of being infected, and 1.2 billion are at high risk. An estimated 90% of all deaths from malaria occur in the WHO African Region.[12] This serious situation may be partially caused by the environment, which is suitable for mosquitos to survive. The *Anopheles* mosquito, as a vector, has a longer lifespan and prefers to feed on human blood. Besides economic limitations, politics and government support problems, and personal willingness to receive treatment can also affect the elimination of malaria in malaria-endemic area.

Over 120 species of *Plasmodia* are known, and among them, five species of *Plasmodium* can infect humans (*Plasmodium falciparum, Plasmodium vivax, Plasmodium ovale, Plasmodium malariae* and *Plasmodium knowlesi*; the first four are the species that infect exclusively human beings). *P. falciparum* is known as the most lethal species, since 90% of malaria related deaths are caused by it.[13] Because of this, most of the current available drugs and drug discovery efforts target

P. falciparum. Although *P. falciparum* is the most devastating species, *P. vivax* is widespread, and is responsible for 25% to 40% of the malarial burden in the world,[14] spreading from South and Southeast Asia to Central and South America. *P. vivax* is not as fatal as *P. falciparum*, and is traditionally known as a benign species. However, it can lead to cerebral malaria, and dormant liver stages, which means patients are under the threat of malarial relapse even after clearance of bloodstream parasites. Very few drugs are able to cure this species of malaria, since it is difficult to culture this parasite and target the hypnozoites in the liver stage.[15] *P. ovale* and *P. malariae* are less common than the previous two species of parasites. *P. ovale* can also form a dormant liver stage, and lead to relapse, while *P. malariae* is the most persistent infection, and can infect other primates. These two species of parasites are usually distinguished by microscopy, since they share similar symptoms.[16] *P. knowlesi* is the cause of a zoonotic malaria in Southeast Asia, and it is less prevalent. However, as *P. knowlesi* only has a 24-hour replication cycle, it would rapidly develop into a severe infection.

1.2.1 Malarial Parasite Biology

All the malarial species have a complex life cycle, and the four human malarial species that are mentioned above are transmitted by the mosquito vector. Taking *P. falciparum* as an example (Figure 1-3),[17] its life cycle consists of two parts with the first part in the human body. After biting by an infected female *Anopheles* mosquito, plasmodial sporozoites are introduced into a human host. In some cases, more than one malarial species will be transmitted into the human body. The sporozoites are brought by the bloodstream to the liver, and invade liver cells. In the liver cell, sporozoites develop into schizonts, which will be released into the bloodstream as merozoites, and infect blood erythrocytes. In erythrocytes, the parasites undergo an asexual replication, developing through three morphological different stages: ring, trophozoite and schizont. Schizonts will then

release new merozoites into the bloodstream again and further infect other blood cells. Some ring stage parasites will differentiate into sexual gametocytes, microgametocytes (male) and macrogametocytes (female). The erythrocytic cycle is significant in diagnosis and treatment, since the symptoms of malaria are mostly related to this stage.

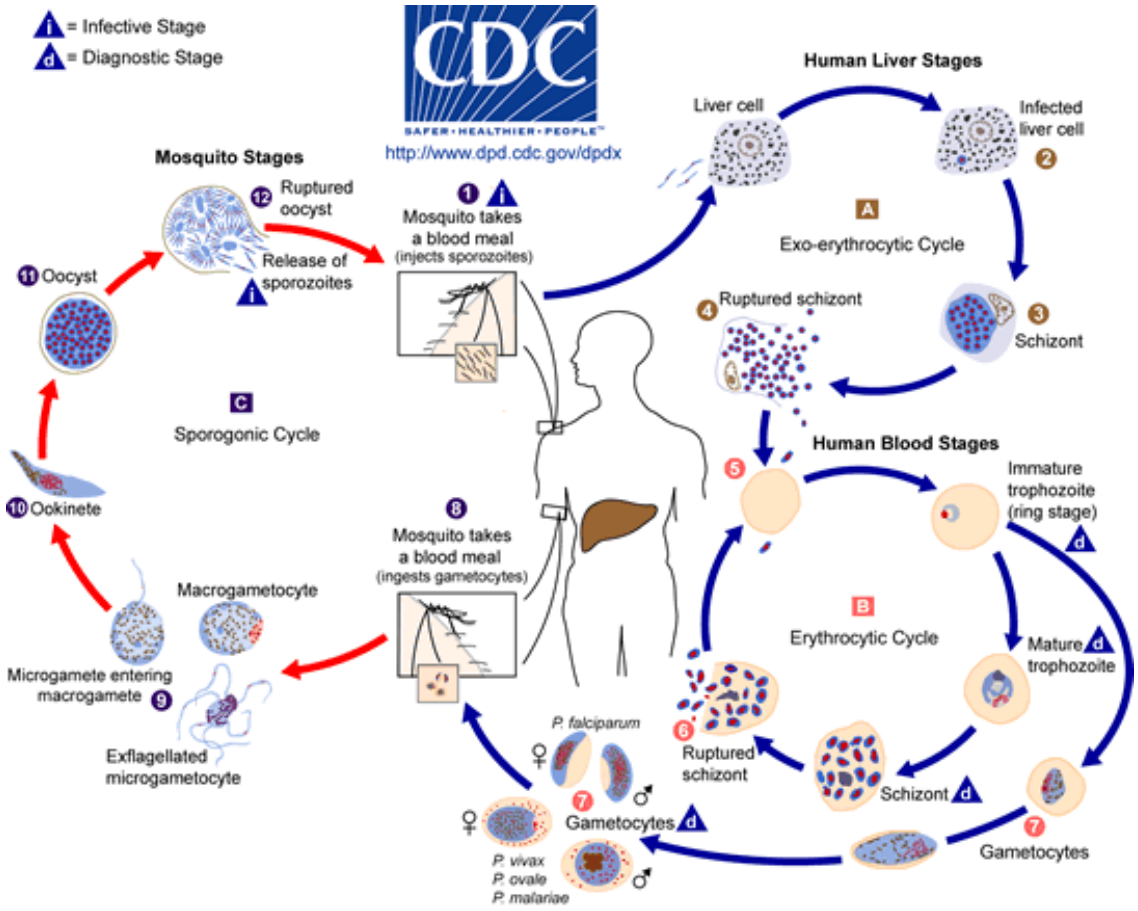

Figure 1-3. Life cycle of malaria. [17]
With permission from *Chem. Rev.*, **2014**, 11138-11163. Copyright 2014 American Chemical Society.

During a blood meal, gametocytes are ingested by a mosquito and begin a further multiplication, known as the sporogonic cycle. In the mosquito's midgut, two sexual gametocytes combine with each other to form zygotes, and then mature into ookinetes. In the midgut, ookinetes develop into oocysts, which further form sporozoites. Sporozoites can migrate to mosquito's salivary glands, where they are available for infecting a new human host.

For the other three species of malarial parasites, there are three main differences in the life cycle. The first one is the liver stage. *P. malariae* is similar to *P. falciparum*, which will rapidly enter the blood stream and process to the erythrocytic cycle. However, *P. vivax* and *P. ovale* form dormant hypnozoites in liver cells,[17] which can be released in the future, and lead to disease relapse. So for the treatment of these two species of parasites, drugs that target hypnozoites are essential. The second difference is the time period for replication. For *P. falciparum* and *P. vivax*, it takes 48 hours for the parasite's replication and initiation of malaria symptoms, while for the benign *P. malariae*, 72 hours are needed. *P. knowlesi* is the most life-threatening, since it replicates within only 24 hours, which means that people infected by this species of malaria suffer from a much more serious periodic fever and other symptoms. The third difference is the time for the appearance of gametocytes.[18] For *P. falciparum*, it takes several days between the initial fever and the appearance of gametocytes. However, for *P. vivax*, the gametocytes appear at almost the same time by asexual replication. Therefore, in order to obtain a better treatment for *P. vivax*, gametocytes need to be killed as well as blood stage parasites.

1.2.2 Important Antimalarial Compounds

1.2.2.1 Quinine

Quinine (**1.2**) was the first antimalarial drug to be used. It was first isolated from the bark of the *Cinchona* tree, which contains many alkaloids,[19] and its structure was determined in the early 20th century. Quinine is an aryl-amino alcohol, and it is an important antimalarial drug for uncomplicated malaria. It can also act quickly against severe malaria, and it is proposed to have a similar mechanism to that of chloroquine (**1.3**), which can bind with heme to inhibit its polymerization.[20] The detailed mechanism will be described for chloroquine.

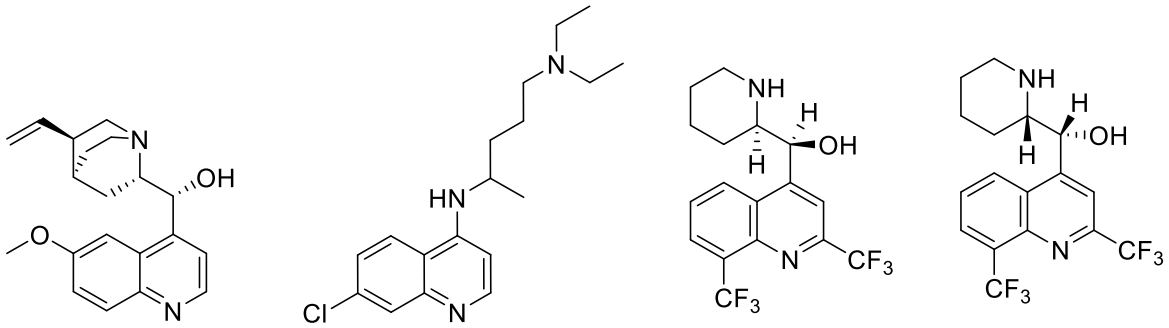

1.2 **1.3** **1.4** **1.5**

Based on the scaffold of quinine, various new kinds of antimalarials have been synthesized, including chloroquine (**1.3**), mefloquine (**1.4** (-)-mefloquine, **1.5** (+)-mefloquine), and other novel drugs under development. However, quinine monotherapy still has some strong disadvantages. The first one is that quinine is toxic to people who have glucose-6-phosphate dehydrogenase (G6PD) deficiency, and it can also lead to some serious side effects, such as low blood sugar, blood in urine, etc.[21] Along with the emergence of resistance, quinine ceased to be an effective treatment option, and more efforts are needed to discover new efficacious derivatives.

1.2.2.2 Chloroquine

Chloroquine (**1.3**) was first introduced in the 1940s, and it is the drug with the longest half-life among currently known antimalarial drugs, approximately 60 days. As an alternative to quinine, chloroquine has a lot of advantages. It can act rapidly against blood stage parasites, and it has good oral bioavailability, water solubility, good distribution and low toxicity. It is very cheap and easy to administer. Because of these strong points, chloroquine became a gold standard treatment for a very long time, and in many countries.

Chloroquine's mechanisms of action have been intensively studied for several decades. It is believed that chloroquine can inhibit heme polymerization and inhibit the free radical detoxification. Figure 1-4a shows the feeding procedure of the parasites. The host hemoglobin is taken in by the cytostome (mouth) of the parasite, and then transferred into the digestive vacuole

(food vacuole). The hemoglobin is then degraded there, and converted to free amino acids to support the parasite's life cycle.

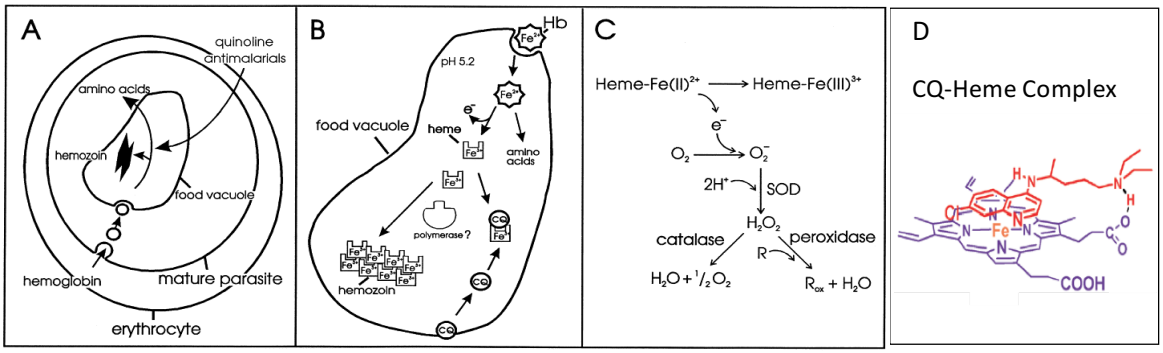

Figure 1-4. Mechanism of chloroquine. a) Hemoglobin degradation. b) Inhibition of heme polymerization. c) Inhibition of free radical detoxification.[22] d) Chloroquine-Heme Complex. With permission from *Pharmacol. Ther.*, **1998**, 55-87. Copyright 1998 Elsevier.

A byproduct, heme (**1.6**) is produced during the degradation of hemoglobin (Figure 1-4b). By oxidation of the central Fe^{2+}, Fe^{3+}-heme is formed, and high concentrations of Fe^{3+}-heme are toxic to the parasite. To deal with this problem, the parasite accumulates heme, and changes it into hemozoin, a nontoxic crystal, by heme polymerization. Chloroquine has been proved to inhibit this polymerization. As a diprotic weak base ($pKa_1 = 8.1$ and $pKa_2 = 10.2$), chloroquine tends to accumulate in the acidic digestive vacuole in the parasite,[23] and forms a complex with heme (CQ-heme), as shown in Figure 1-4d, by a face to face π stacking of porphyrin and quinoline systems. And NMR spectroscopy conducted by Schwedhelm *et al.* showed that chloroquine is in the center position of the Fe^{3+}-heme-CQ 4:1 complex.[24,25] They also found besides of the π-π interactions, the significant van der Waals interactions between side chain and the tetrapyrrole part also plays an important role on the stabilization of Fe^{3+}-heme-CQ 4:1 complex. In this way, chloroquine prohibits the heme polymerization in the parasite. Tilley et al. proved[26] that both free heme and CQ-heme can kill the parasite. This may be caused by acting with target on the membrane of the digestive vacuole, and lead to damage of the membrane. In addition, the CQ-heme complex can

enter the cytosol by passive diffusion. At the higher pH of the cytosol, the salt bridge is destructed, which causes the release of heme, and increase of the concentration of heme in the cytosol. Then chloroquine would reenter the digestive vacuole, and repeat this process. Other 4-aminoquinolines and arylanimo alcohols can also kill the parasite with the same mechanism.

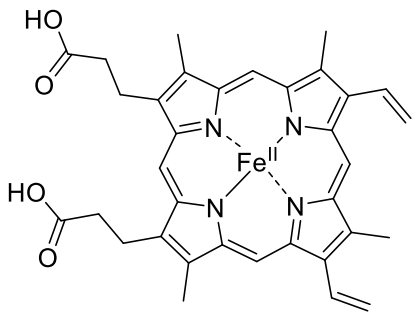

1.6

Free heme can inhibit some enzymes, and can also lead to an oxidative stress to the parasite (Figure 1-4c). After separating from hemoglobin, the central iron oxidizes from $Fe(II)^{2+}$ to $Fe(III)^{3+}$, and along with this, superoxide anion, H_2O_2, and hydroxyl radicals are formed. Malarial parasites are sensitive to oxidative stress. They use antioxidant enzymes, such as superoxide dismutase (SOD), catalase and peroxidase to protect against reactive oxygen species. Traylor et al. reported[27] that free heme also has catalase and peroxidase activity itself. The catalase activity of heme can convert H_2O_2 to H_2O and O_2. Meanwhile, its peroxidase activity can degrade H_2O_2 to H_2O with substrates consumption, such as glutathione (GSH), lipids and proteins. Even though the catalase and peroxidase activities of heme reduce the toxicity of oxidative stress, the substrate consumption is potentially harmful to the parasite. In addition, the results in Riberiro's paper suggested[28] that chloroquine can inhibit the catalase activity of heme by forming a CQ-heme complex. This prolongs the half-life of the reactive oxygen species, which can lead to parasite death. These three mechanisms of chloroquine to kill parasites make it a good antimalarial drug. Despite extensive use, it took 20 years for resistance to chloroquine to develop.

1.2.2.3 Artemisinin

Artemisinins are a family of sesquiterpene trioxane lactone antimalarial drugs. These compounds are derived from the parent structure of artemisinin (**1.7**). Artemisinin is a natural product isolated from the sweet woodworm *Artemisia annua*. It is known to have a short half-life time of 0.5 to 1.5 hours. It is quite efficient, and can rapidly clear parasites in red blood cells as well as gametocytes in the sexual stage. So artemisinin is a good antimalarial drug that can limit malaria transmission.

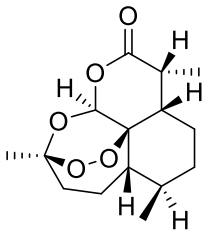

1.7

Artemisinin has a unique structure, since it contains an endoperoxide bond, which is responsible for the antimalarial activity. Several mechanisms of action regarding artemisinins have been proposed, including inhibition of the heme detoxification pathway, alkylation or inhibition of key proteins, and interference with the mitochondrial function of parasites, as shown in Figure 1-5.

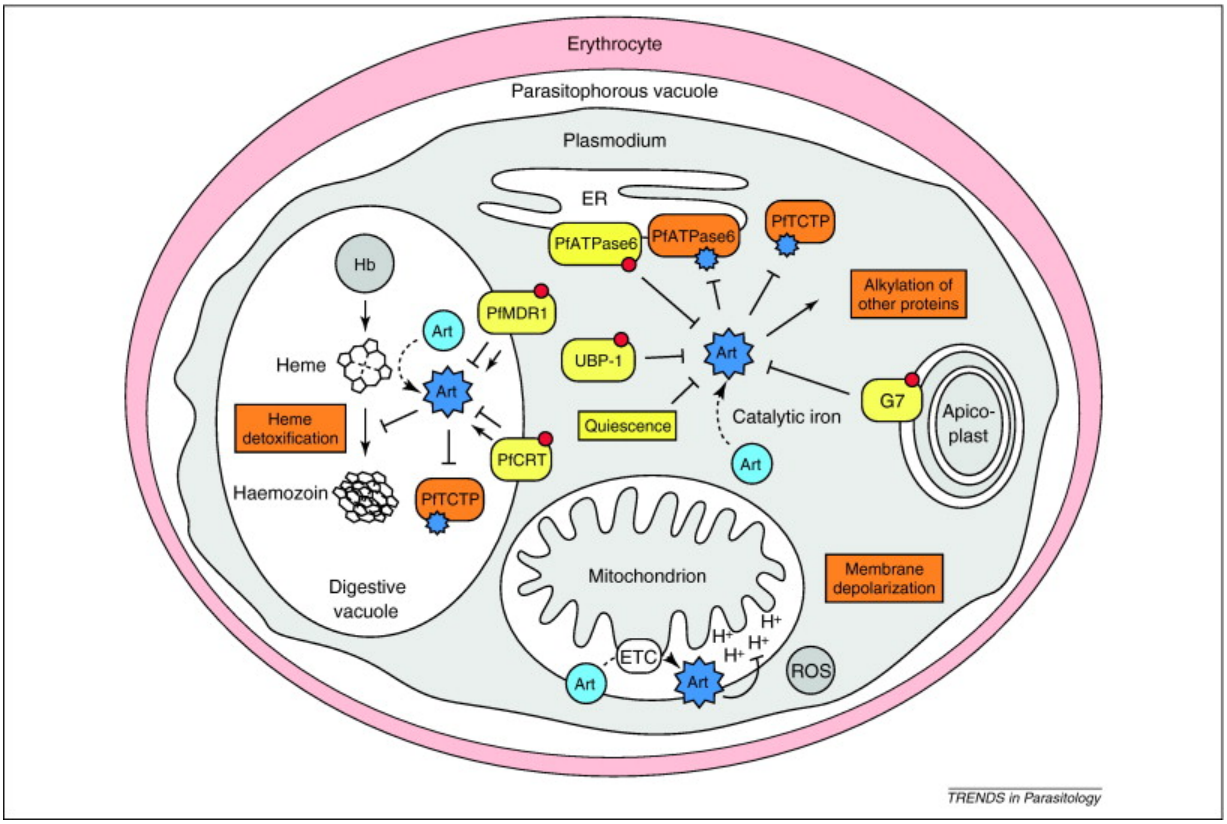

Figure 1-5. Schematic view of postulated artemisinin targets.[38]
With permission from *Trends Parasitol.*, **2011**, 73-81. Copyright 2001 Elsevier.

The first proposed mechanism is that artemisinin inhibits heme (**1.6**) polymerization by alkylation, which is caused by freeing a radical produced during bond cleavage in the digestive vacuole (Figure 1-6). The endoperoxide bond is reductively cleaved by Fe^{2+}-heme, which generates a short-lived alkoxy radical. This is followed by a β-fragmentation, and forms a C-4 radical. The C-4 radical can then interact with one of the four meso carbons on heme to generate an artemisinin-heme complex, which prevents heme polymerization. The free radical of artemisinin can also alkylate other parasite proteins, which gives another route of antimalarial activity. However, this mechanism still has some uncertainties, since blocking hemoglobin degradation does not affect artemisinin's activity.[29]

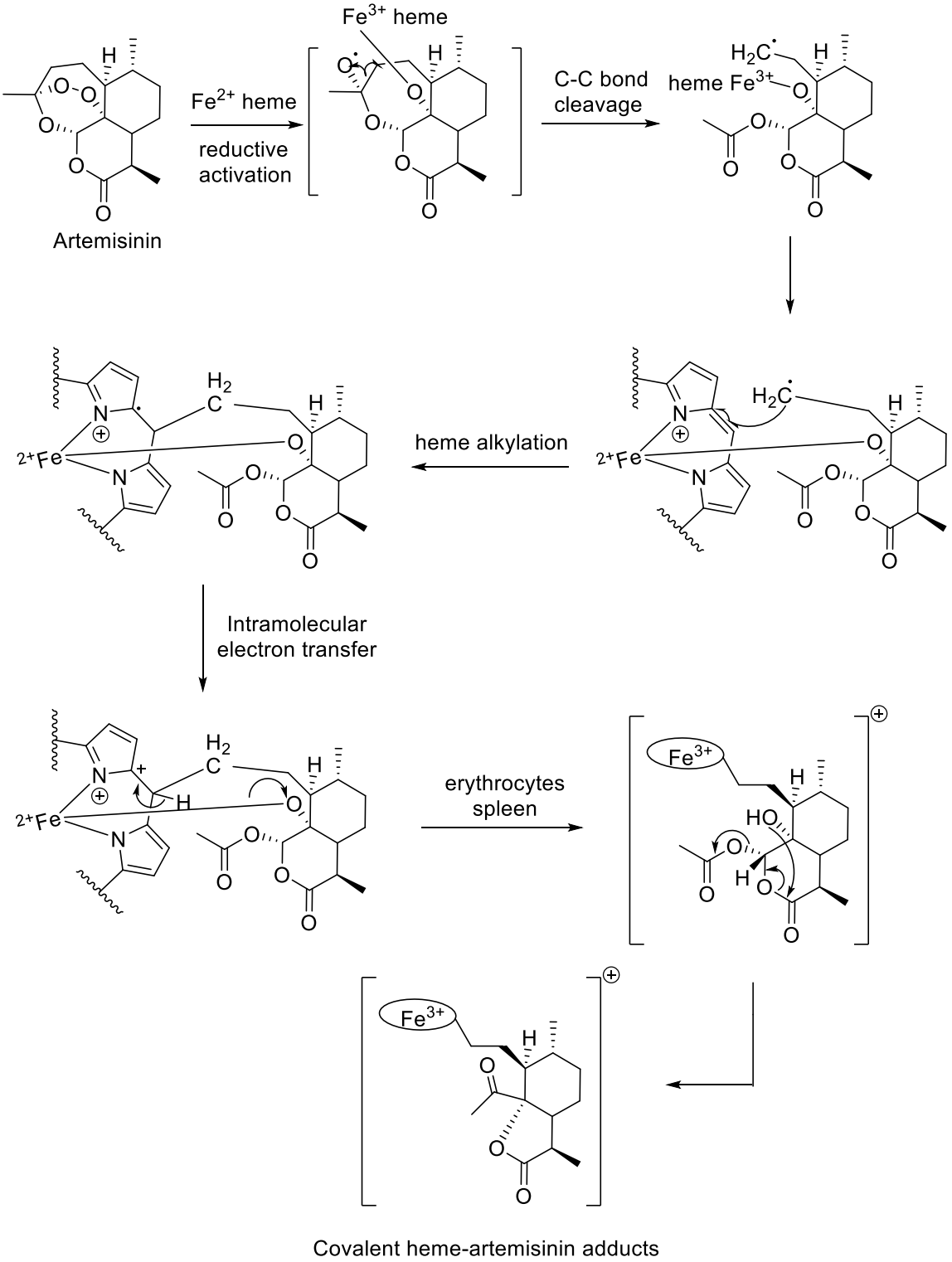

Figure 1-6. Alkylation of heme by artemisinin.[29]
Redrawn from *Acc. Chem. Res.* **2010**, 1444-1451. Copyright 2010 American Chemical Society.

P. falciparum translationally controlled tumor protein (PfTCTP) is an essential protein for parasite growth, and its concentration is 2.5 fold higher in artemisinin-resistant species than wild type. This upregulation may indicate that it is a target of artemisinin.[30] However, this hypothesis has not been proven yet, since there is no evidence showing that *Pf*TCTP is the only protein that increases in this species.

Krishna and co-workers also suggested[31] that the endoperoxide bond of artemisinin can be cleaved after initiation with a metal ion(II) in the cytosol, and that the carbon radical can specifically inhibit an ATP dependent Ca^{2+} pump, *Pf*ATPase6, in the endoplasmic reticulum of the parasite. By mutating the encoding gene, *Pfatpase6*, the sensitivity of malarial species to artemisinin decreased, which supports *Pf*ATPase6 as a target. Although artemisinin is a chiral molecule, both enantiomers have equal antimalarial activity. This phenomenon further indicates that it is the achiral-ferrous species that triggers the antimalarial activity of trioxanes rather than a specific binding with the active site on *Pf*ATPase6.

Artemisinin is also proposed to depolarize the membrane of mitochondria. In return, the level of reactive oxygen species (ROS) would rise to correct and reverse this change. This phenomenon was reported by Wang et al.[32] They also suggested that inference with the mitochondrial electron transport chain (ETC) is caused by artemisinin rather than by other antimalarials.

However, artemisinin has poor water solubility, so it is not suitable for oral administration. This inspired the discovery of artemisinin derivatives, and several semi-synthetic analogues have been developed, including dihydroartemisinin (DHA, **1.8**), artesunate (**1.9**), and arteether (**1.10**), etc. Recently, artemisinin and its derivatives are used in combination with other antimalarial drugs such as pyrimethamine and sulfadoxine, to achieve a better clearance of the parasites.

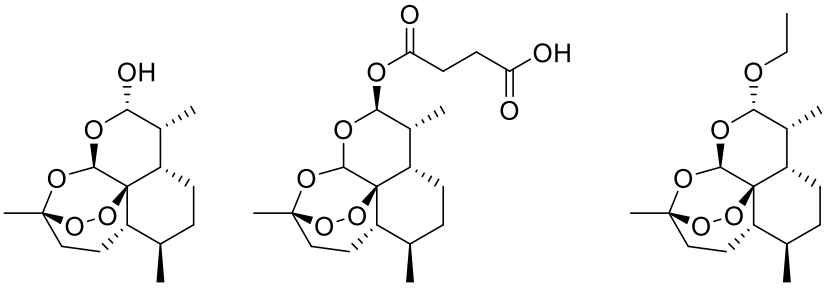

1.8 1.9 1.10

1.3 Bioassay

1.3.1 A2780 Assay

A2780 is a human ovarian cancer cell line. It was obtained from an untreated patient, and it grows as a monolayer on the bottom of surface cell culture flask. In the A2780 assay, a cell plate is set up first by culturing A2780 cells in a 96 well cell culture plate. Then samples are prepared by dissolving in DMSO at 4 mg/mL, and aliquots with varying amounts of sample are incubated at 37 ^{o}C and 5% CO_2 for 48 hours. After that, the incubated cells are treated with Alamar Blue for another 3 hours and the fluorescence intensity in each well is measured. Alamar Blue is reduced to its fluorescent form by reacting with living cells (Figure 1-7); as shown in Figure 1-8, the fluorescence intensity increases along with the cell concentrations and incubation time, and both show a decline at some point due to the over-reduction of resorufin to hydroresorufin. This over-reduction occurs at differing rates, depending on the cell type, and can take from several hours to several days. Since the assay is read after 3 hours, further reduction to the fully reduced non-fluorescent product is not a factor. Cell culture medium is used as blank and paclitaxel is the assay reference. The IC_{50} is the concentration of sample which inhibits cell growth by 50%, and it is calculated based on the dose-response curve of the sample.

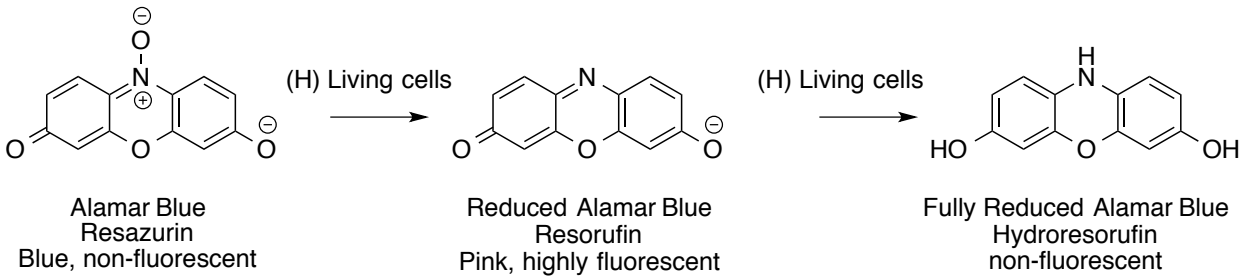

Figure 1-7. The Mechanism of Alamar Blue reacting with living cells.

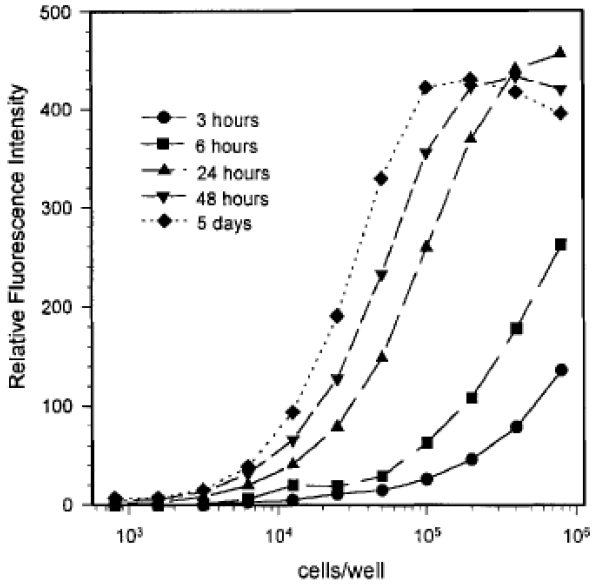

Figure 1-8. Titration of peripheral blood mononuclear cells (PBMC) using the Alamar Blue assay and kinetics of reduction of Alamar Blue reagent.[33] With permission from *J. Clin. Lab. Anal*, **1995**, 89-95. Copyright 1995 John Wiley and Sons.

1.3.2 Antimalarial Assay

The chloroquine/mefloquine resistant *Plasmodium falciparum* strain, Dd2, is used to conduct the antimalarial assay. The first step is culturing *P. falciparum* and setting up the cell plate. Cultures are incubated at 37 ^{o}C, under the gas mixture of 4.99% O_2, 5.06% CO_2, and 89.95% N_2. The level of parasitemia is determined by light microscopy after 3 to 4 days to ensure that the parasites are present in the late-ring stage and early trophozoite stage with no schizonts. The samples are then incubated with parasites for 72 hours, followed by the addition of SYBR Green I (**1.11**). SYBR Green I has a great sensitivity for double-stranded DNA (dsDNA). It binds to

dsDNA and fluoresces strongly, so measurement of the fluorescence intensity in each well enables IC_{50} values to be analyzed with KaleidaGraph software using nonlinear regression curve fitting. Each IC_{50} value was calculated from the average of three independent determinations, and each determination was in duplicate. The IC_{50} values were reported with ± SEM. Artemisinin was used as the positive control with an IC_{50} value of 6.2 ± 1.2 nM.[34,35]

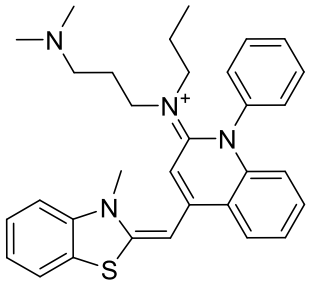

1.11

1.4 Approaches to Natural Product Isolation and Structure Elucidation

1.4.1 Bioassay-Directed Isolation

Bioassay-directed isolation is widely used in natural products research. High-throughput screening is first used to identify the activity of crude extracts, and once they are identified as active, various isolation methods are used to separate them into different fractions for evaluation by bioassay. This approach avoids the isolation of inactive compounds, and leads to the purification of promising active compounds in the extracts.

1.4.2 Liquid-Liquid Partition

Liquid-liquid partition is a method that uses water and organic solvents to separate compounds based on their polarity. This procedure is usually conducted in a separatory funnel. The crude extract is first dissolved in a water and methanol mixture, then less polar solvents, such as hexanes, ethyl acetate and dichloromethane, are used to extract compounds from the methanol/water layer. This procedure is able to separate compounds on the basis of their polarity,

and chlorophyll with very low polarity as well as some very polar compounds which are not active and make it hard for the following separations can be removed by this procedure.

1.4.3 Isolation by Low-Pressure Column Chromatography

Low-pressure liquid column chromatography (LPLC) can use a great diversity of stationary phases, involving adsorption and size-exclusion materials. The adsorption materials separate the compounds by adsorbing them to the stationary phase. And this interaction is controlled by many factors, including hydrogen bonding, van der Waals forces, dipole-dipole interactions, and so on. It is crucial to find a proper stationary phase as well as the best solvents to obtain the optimum separation of fractions. Adsorption LPLC media include silica gel, bonded-phase silica gel (C_{18}, diol, etc.), alumina and polystyrene. Size exclusion techniques separate compounds according to their hydrodynamic volume. Unlike adsorption LPLC, size-exclusion LPLC uses porous non-adsorbing materials, which will not interact with compounds in the mixture. The large compounds will not enter the porous particles, and will elute first from the column. Medium size compounds will partially enter the particles, while small size compounds can freely enter the particles. So size-exclusion LPLC can separate compounds in order of decreasing size. Media for this type of LPLC include polyacrylamide and modified carbohydrates.

1.4.4 Isolation by HPLC

High-performance liquid chromatography (HPLC) is the most widely used technique for final compound purification. Compared with LPLC, it is faster and easier to obtain a pure compound from a complex mixture. The major difference between HPLC and LPLC is the size of particles in the stationary phase. The particles in an HPLC column are much smaller and more uniform in size than those in LPLC. Because of the small size of the particles, high pressure is required to pump solvent through the system, and the high surface adsorption area enables good

separation of compounds. There are four modes of HPLC: normal-phase, reversed phase, gel permeation chromatography and ion exchange chromatography. The columns commonly used in this work were reversed phase C_{18}, and diol columns; the latter can be used in normal-phase as well in reversed phase mode.

1.4.5 Dereplication

The definition of the term "dereplication" was first given by Beutler in 1990 as "a process of quickly identifying known chemotypes".[36] As more and more natural compounds continue to be discovered, it is important to use dereplication tools to make natural compound discovery faster, more accurate and more efficient. Dereplication is usually conducted after the preliminary separation of compounds from the crude mixture. Compounds can be dereplicated by HPLC-MS, HPLC-UV, and NMR.[37] Mass spectrometry (MS) is sensitive, rapid and accurate, and can detect compounds at trace levels. Normally, electrospray ionization (ESI) is used to get the mass of compounds, and since it is a soft ionization method that works in both positive and negative modes, it provides pseudomolecular ions without significant fragmentation. Therefore, the obtained mass can be directly used in database searching, such as the Dictionary of Natural Products (DNP) and SciFinder. With the MS data, we can only determine that it is a new compound in the unlikely event that its mass value is not in any of the databases. If its mass matches a known compound, it could either be a known compound or a new compound with the same mass. In the latter two cases, more information is needed to determine if it is a new compound. The retention time and UV data from HPLC-UV are useful for comparison. UV spectroscopy is also a helpful tool to obtain substructure information. But HPLC retention times depend strongly on the experimental conditions, so an identification on the basis of mass spectroscopic data and HPLC-UV data alone is unusual. The most important tool for dereplication is nuclear magnetic resonance (NMR)

spectroscopy. Structure and substructure information can be quickly obtained from ^{1}H-NMR spectra. After obtaining this information from MS, UV and NMR, they can be input into a database, such as the Dictionary of Natural Product (DNP) or SciFinder, to confirm whether it is a new compound.

1.4.6 Structure Elucidation

Identification of the structure of isolated compounds relies on various kinds of analytical instruments. The common methods that are used to determine the structures of molecules include nuclear magnetic resonance (NMR) spectroscopy, mass spectrometry (MS), infrared (IR) spectroscopy and ultraviolet (UV) spectroscopy. Known compounds can be dereplicated with MS and 1D NMR as described above, while for new compounds, more in-depth analysis of the structure is required. This means that 2D NMR spectra, including COSY, HSQC, HMBC, ROESY and other methods need to be used to reveal the subunit structure and stereochemistry of compounds. If crystals are available, an X-ray crystal structure can be used to determine the structures of compounds.

1.5 References

(1) Stewart, B.; Wild, C. P. World Cancer Report 2014. available at http://www.thehealthwell.info/node/725845?&content=resource&member=572160&catalogue=none&collection=Conditions, Chronic Conditions, Cancer&tokens_complete=true (accessed November 6, 2016).

(2) Hanahan, D.; Weinberg, R. A. The Hallmarks of Cancer. *Cell* **2000**, *100*, 57–70.

(3) Anonymous. Cancer Fact Sheet N 297. available at http://www.who.int/mediacentre/factsheets/fs297/en/ (accessed November 6, 2016).

(4) Chambers, S. K.; Hess, L. M. Ovarian Cancer Prevention. In: *Fundamentals of Cancer*

Prevention, Ed: David, S.; Alberts, M.D.; Lisa, M. **2008**, 447–473.

(5) Holschneider, C. H.; Berek, J. S. Ovarian Cancer: Epidemiology, Biology, and Prognostic Factors. In: *Seminars in Surgical Oncology*, **2000**; Vol. 19, 3–10.

(6) Wani, M. C.; Taylor, H. L.; Wall, M. E.; Coggon, P.; McPhail, A. T. Plant Antitumor Agents. VI. Isolation and Structure of Taxol, a Novel Antileukemic and Antitumor Agent from *Taxus brevifolia*. *J. Am. Chem. Soc.* **1971**, *93*, 2325–2327.

(7) Manfredi, J. J.; Horwitz, S. B. Taxol: An Antimitotic Agent with a New Mechanism of Action. *Pharmacol. Ther.* **1984**, *25*, 83–125.

(8) Kingston, D. G. I. Taxol, a Molecule for All Seasons. *Chem. Commun.* **2001**, 867–880.

(9) Salmon, E. D.; Wolniak, S. M. Taxol Stabilization of Mitotic Spindle Microtubules: Analysis Using Calcium Induced Depolymerization. *Cell Motil.* **1984**, *4*, 155–167.

(10) Haldar, S.; Chintapalli, J.; Croce, C. M. Taxol Induces Bcl-2 Phosphorylation and Death of Prostate Cancer Cells. *Cancer Res.* **1996**, *56*, 1253–1255.

(11) Seligson, A. L.; Terry, R. C.; Bressi, J. C.; Douglass III, J. G.; Sovak, M. A New Prodrug of Paclitaxel: Synthesis of Protaxel. *Anticancer Drugs* **2001**, *12*, 305–313.

(12) Anonymous. World Malaria Report 2015. available at http://www.who.int/malaria/publications/world-malaria-report-2015/report/en/ (accessed November 6, 2016).

(13) Claessens, A.; Adams, Y.; Ghumra, A.; Lindergard, G.; Buchan, C. C.; Andisi, C.; Bull, P. C.; Mok, S.; Gupta, A. P.; Wang, C. W.; Turner, L.; Arman, M.; Raza, A.; Bozdech, Z.; Bowe, J. A. A Subset of Group A-like Var Genes Encodes the Malaria Parasite Ligands for Binding to Human Brain Endothelial Cells. *Proc. Natl. Acad. Sci.* **2012**, *109*, 1772-1781.

(14) Price, R. N.; Tjitra, E.; Guerra, C. A.; Yeung, S.; White, N. J.; Anstey, N. M. Vivax

Malaria: Neglected and Not Benign. *Am. J. Trop. Med. Hyg.* **2007**, *77*, 79–87.

(15) Udomsangpetch, R.; Somsri, S.; Panichakul, T.; Chotivanich, K.; Sirichaisinthop, J.; Yang, Z.; Cui, L.; Sattabongkot, J. Short-Term in Vitro Culture of Field Isolates of *Plasmodium vivax* Using Umbilical Cord Blood. *Parasitol. Int.* **2007**, *56*, 65–69.

(16) Wells, T. N. C.; Alonso, P. L.; Gutteridge, W. E. New Medicines to Improve Control and Contribute to the Eradication of Malaria. *Nat. Rev. Drug Discov.* **2009**, *8*, 879–891.

(17) Njoroge, M.; Njuguna, N. M.; Mutai, P.; Ongarora, D. S. B.; Smith, P. W.; Chibale, K. Recent Approaches to Chemical Discovery and Development against Malaria and the Neglected Tropical Diseases Human African Trypanosomiasis and Schistosomiasis. *Chem. Rev.* **2014**, *114*, 11138–11163.

(18) Santos-Magalhães, N. S.; Mosqueira, V. C. F. Nanotechnology Applied to the Treatment of Malaria. *Adv. Drug Deliv. Rev.* **2010**, *62*, 560–575.

(19) Butler, A. R.; Khan, S.; Ferguson, E. A Brief History of Malaria Chemotherapy. *J. Royal Coll. Phys. Edin.* **2010**, *40*, 172–177.

(20) Combrinck, J. M.; Mabotha, T. E.; Ncokazi, K. K.; Ambele, M. A.; Taylor, D.; Smith, P. J.; Hoppe, H. C.; Egan, T. J. Insights into the Role of Heme in the Mechanism of Action of Antimalarials. *ACS Chem. Biol.* **2012**, *8*, 133–137.

(21) Schlitzer, M. Antimalarial Drugs-What Is in Use and What Is in the Pipeline. *Arch. Pharm.* **2008**, *341*, 149–163.

(22) Foley, M.; Tilley, L. Quinoline Antimalarials: Mechanisms of Action and Resistance and Prospects for New Agents. *Pharmacol. Ther.* **1998**, *79*, 55–87.

(23) Fitch, C. D.; Yunis, N. G.; Chevli, R.; Gonzalez, Y. High-Affinity Accumulation of Chloroquine by Mouse Erythrocytes Infected with *Plasmodium berghei*. *J. Clin. Invest.*

1974, *54*, 24.

(24) Schwedhelm, K. F.; Horstmann, M.; Faber, J. H.; Reichert, Y.; Bringmann, G.; Faber, C. The Novel Antimalarial Compound Dioncophylline C Forms a Complex with Heme in Solution. *ChemMedChem.* **2007**, *2*, 541–548.

(25) Leed, A.; DuBay, K.; Ursos, L. M. B.; Sears, D.; de Dios, A. C.; Roepe, P. D. Solution Structures of Antimalarial Drug-Heme Complexes. *Biochemistry* **2002**, *41*, 10245–10255.

(26) Tilley, L.; Loria, P.; Foley, M. Chloroquine and Other Quinoline Antimalarials. In: *Antimalarial Chemotherapy*; Springer, 2001, 87–121.

(27) Traylor, T. G.; Kim, C.; Richards, J. L.; Xu, F.; Perrin, C. L. Reactions of Iron (III) Porphyrins with Oxidants. Structure-Reactivity Studies. *J. Am. Chem. Soc.* **1995**, *117*, 3468–3474.

(28) de Almeida Ribeiro, M. C.; Augusto, O.; da Costa Ferreira, A. M. Influence of Quinoline-Containing Antimalarials in the Catalase Activity of Ferriprotoporphyrin IX. *J. Inorg. Biochem.* **1997**, *65*, 15–23.

(29) Meunier, B.; Robert, A. Heme as Trigger and Target for Trioxane-Containing Antimalarial Drugs. *Acc. Chem. Res.* **2010**, *43*, 1444–1451.

(30) Krishna, S.; Woodrow, C. J.; Staines, H. M.; Haynes, R. K.; Mercereau-Puijalon, O. Re-Evaluation of How Artemisinins Work in Light of Emerging Evidence of in Vitro Resistance. *Trends Mol. Med.* **2006**, *12*, 200–205.

(31) Eckstein-Ludwig, U.; Webb, R. J.; Van Goethem, I. D. A.; East, J. M.; Lee, A. G.; Kimura, M.; O'Neill, P. M.; Bray, P. G.; Ward, S. A.; Krishna, S. Artemisinins Target the SERCA of *Plasmodium falciparum*. *Nature.* **2003**, *424*, 957–961.

(32) Wang, J.; Huang, L.; Li, J.; Fan, Q.; Long, Y.; Li, Y.; Zhou, B. Artemisinin Directly

Targets Malarial Mitochondria Through its Specific Mitochondrial Activation. *PLoS One.* **2010**, *5*, 9582.

(33) De Fries, R.; Mitsuhashi, M. Quantification of Mitogen Induced Human Lymphocyte Proliferation: Comparison of Alamarbluetm Assay to ^{3}H-Thymidine Incorporation Assay. *J. Clin. Lab. Anal.* **1995**, *9*, 89–95.

(34) Smilkstein, M.; Sriwilaijaroen, N.; Kelly, J. X.; Wilairat, P.; Riscoe, M. Simple and Inexpensive Fluorescence-Based Technique for High-Throughput Antimalarial Drug Screening. *Antimicrob. Agents Chemother.* **2004**, *48*, 1803–1806.

(35) Su, Q.; Dalal, S.; Goetz, M.; Cassera, M. B.; Kingston, D. G. I. Antiplasmodial Phloroglucinol Derivatives from *Syncarpia glomulifera*. *Bioorg. Med. Chem.* **2016**, *24*, 2544–2548.

(36) Beutler, J. A.; Alvarado, A. B.; Schaufelberger, D. E.; Andrews, P.; McCloud, T. G. Dereplication of Phorbol Bioactives: *Lyngbya majuscula* and *Croton cuneatus*. *J. Nat. Prod.* **1990**, *53*, 867–874.

(37) Laatsch, H. Dereplication of Natural Products Using Databases. In: *Marine Biomedicine: From Beach to Beside*, Ed: Baker, B. J. **2015**, 65–86.

(38) Ding, X. C.; Beck, H.-P.; Raso, G. Plasmodium Sensitivity to Artemisinins: Magic Bullets Hit Elusive Targets. *Trends Parasitol.* **2011**, *27*, 73–81.

Chapter 2. Antiproliferative Terpenoids from *Hypoestes sp.* (Acanthaceae)

2.1 Introduction to *Hypoestes sp.* (Acanthaceae)

A crude extract of the leaves and flowers of a *Hypoestes sp.* (Acanthaceae) was prepared in Madagascar from a plant collected there, and shipped to Virginia Tech. The crude extract was reported as having antiproliferative activity against the A2780 ovarian cancer cell line with an IC_{50} value of 14 μg/mL. Fractionation was guided by the A2780 bioassay, and two known antiproliferative compounds (**2.1** and **2.2**) were obtained from the hexane fraction with IC_{50} values against A2780 cells of 6.9 μM and 3.4 μM, respectively. These compounds also exhibited moderate antiplasmodial activity against the chloroquine/mefloquine resistant Dd2 strain of *Plasmodium falciparum* with IC_{50} values of 9.9 μM and 2.8 μM, respectively.

Figure 2-1. Image of *Hypoestes sp.* (Acanthaceae). Photography by Charles Rakotovao, from http://www.tropicos.org/Image/100146648

Hypoestes is a genus of flowering plants of Old World origin, with many species wide spread in the tropical and subtropical region of Africa and Asia. It belongs to the subfamily Acanthoideae of the family Acanthaceae. The plant can grow up to 1 meter in height. Various *Hypoestes sp.* have been used in traditional medicine to treat chest and heart diseases, gonorrhea, and cancer, and for liver protection and as antipyretic and anti-inflammatory agents.[1,2,3]

Various compounds have been isolated from this plant, and have been reported to have different biological activities. Shen *et al.* isolated four diterpenes (**2.3**-**2.6**) from *Hypoestes purpurea*, and compound **2.3** exhibited moderate cytotoxic activity toward the KB cell line.[1] Rasoamiaranjanahary et al. found five isopimarane diterpenes (**2.7-2.11**) from *Hypoestes serpens*, and they all had antifungal activity against both the plant pathogenic fungus *Cladosporium cucumerinum* and the yeast *Candida albicans*.[4] The antiplasmodial fusicoccane diterpene hypoestenonol (**2.12**) was isolated by Musayeib et al. from *Hypoestes forskalei*.[5]

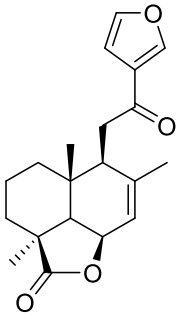

2.3

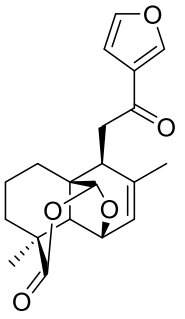

2.4

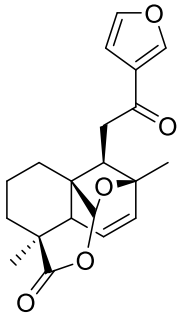

2.5

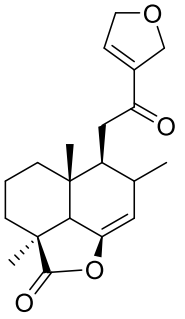

2.6

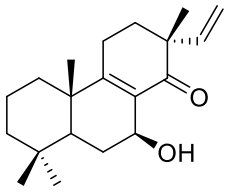

2.7

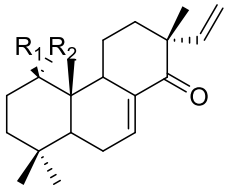

2.8 $R_1=R_2=O$
2.9 $R_1=H;R_2=OH$

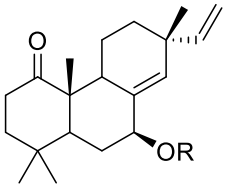

2.10 R=H
2.11 $R=COCH_3$

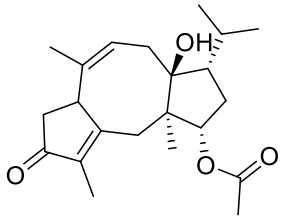

2.12

2.2 Results and Discussion

2.2.1 Isolation of Compounds 2.1 and 2.2

The crude extract was reported to have moderate antiproliferative activity against the A2780 ovarian cancer cell line. After liquid-liquid partition of 2 g of crude extract, 860 mg of the hexanes-soluble fraction was obtained with good antiproliferative activity against the A2780 cell line (IC_{50} = 7.5 μg/mL). The hexanes fraction was further separated by chromatography on Sephadex LH-20 and preparative C_{18} HPLC. The bioactive second fraction from preparative C_{18} HPLC was applied to semi-preparative C_{18} HPLC, and yielded the two diterpenoids **2.1** and **2.2**.

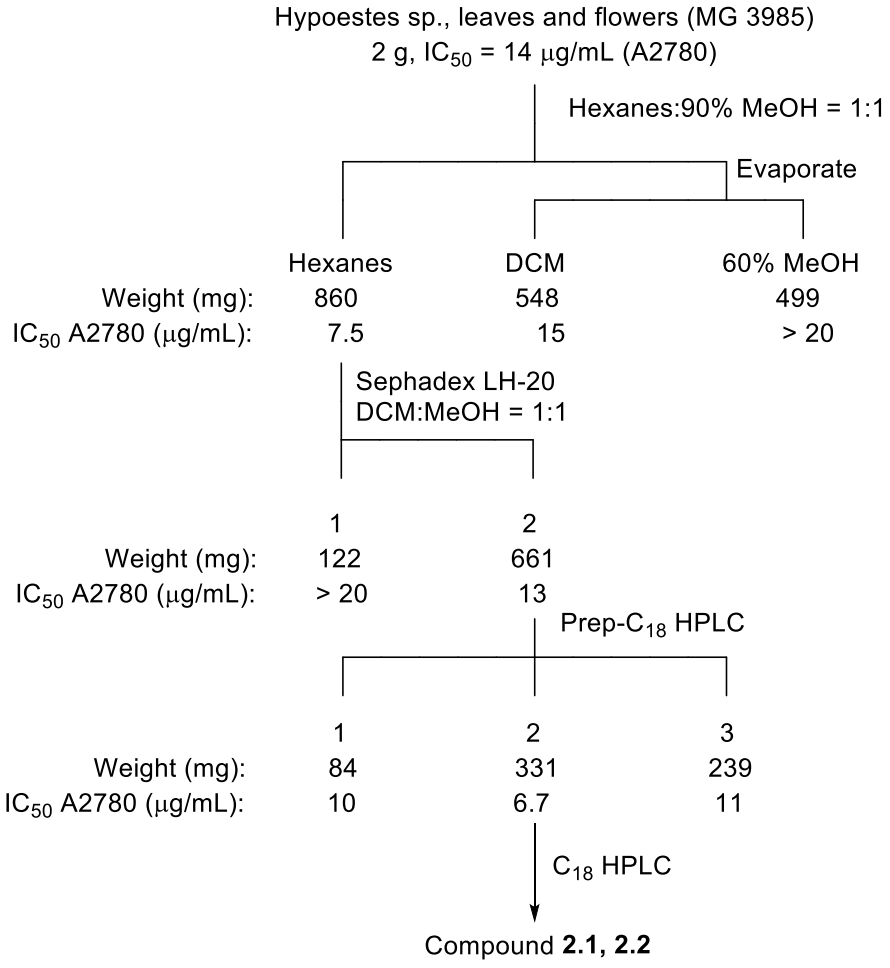

Figure 2-2. Bioassay-guided separation of *Hypoestes sp.*

2.2.2 Structure Elucidation of Compound 2.1

Compound **2.1** was obtained as a white powder. Its molecular formula was determined as $C_{20}H_{32}O$ based on its HRESIMS ion at *m/z* 289.2487 $[M+H]^+$. From the ^{13}C NMR and DEPT spectrum, 20 carbons existed in the structure, with four CH_3 groups, eight CH_2 groups, four CH groups, and four quaternary carbons in the formula, which indicated this compound may be a diterpene.

Since the unsaturated degree of compound **2.1** was five, and there were two double bond protons at δ_H 5.19 (1H, brs), and δ_H 5.62 (1H, t, J = 6.8 Hz), three rings should exist in the structure.

From the ^1H NMR spectrum, signals at δ_H 0.72, 0.80, 0.99, and 1.58 with integrations of three protons each showed the presence of four methyl groups. Only the methyl group with signal at δ_H 0.80 was a doublet (J = 6.1 Hz), all the other three methyl groups were singlets. So the methyl group at δ_H 0.80 was connected to a secondary carbon, and the other three were connected to tertiary carbons.

A quaternary double bond carbon at δ_C 145.1 (C-13) was correlated with a double bond proton at δ_H 5.62 (H-14) in the HMBC spectrum. This proton also correlated with a CH_2 carbon with a signal at δ_C 58.9 (C-15). From the HSQC spectrum, the protons of the carbon at δ_C 58.9 resonated at δ_H 4.20, which indicated that this carbon is an oxygen bearing CH_2 group. Besides, in the HMBC, another CH_2 group with a signal at δ_H 4.17 (H_2-16) was also correlated with the quaternary carbon at δ_C 145.1 (C-13), and its proton chemical shift also indicated its linkage to an oxygen. Therefore, these data suggested the structure of a 2,5-dihydrofuran ring. The HMBC spectrum also showed a correlation between C-13 and H_2-12 (δ_H 1.93), and H_2-12 correlated with

C-11 (δ_C 37.2), and H_2-11(δ_H 1.37) was correlated with C-9 (δ_C 38.8), which was a quaternary carbon. All this information led to the possible partial structure **2.13**.

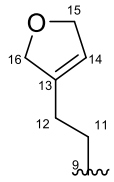

2.13

The double bond and the 2,5-dihydrofuran ring accounted for three degrees of unsaturation, indicating two additional rings. Since the 2,5-dihydrofuran ring and its attaching side chain had six carbons, and there were four methyl groups, only ten carbons remained to be accounted for, suggesting a decalin ring system.

In the HMBC spectrum (Figure 2-3), H_3-17 (δ_H 0.80, 3H, d, J = 6.1 Hz) and H_3-18 (δ_H 1.58, 3H, s) both correlated with the C-9 (δ_C 38.8), which was a ring carbon. And because CH_3-17 was a doublet, it could not be directly connected to C-9. A weak correlation was observed between C-10 (δ_C 46.6) and H_2-11 (δ_H 1.37), giving the partial structure **2.14**.

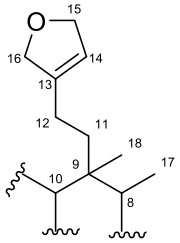

2.14

The COSY spectrum showed that H-10 (δ_H 1.36) correlated with H_2-1 (δ_H 1.40), H_2-1 (δ_H 1.40) correlated with H_2-2 (δ_H 2.01), and H_2-2 (δ_H 2.01) correlated with the double bond proton H-3 (δ_H 5.19). In the HMBC spectrum, H-3 (δ_H 5.19) correlated with the quaternary double bond carbon C-4 (δ_C 144.7), and correlations of H_3-20 (δ_H 0.72) to C-3 (δ_C 120.6), C-4 (δ_C 144.7), and

C-19 (δ_C 20.1) were also observed. Although the 2-bond correlation between H-10 and C-5 was not observed, the correlation between C-10 (δ_C 46.6) and H_3-19 (δ_H 0.99) confirmed that C-10 and C-5 were in a six-membered ring as shown in the partial structure **2.15**. Combination of partial structures **2.14** and **2.15** led to the planar structure of compound **2.1**.

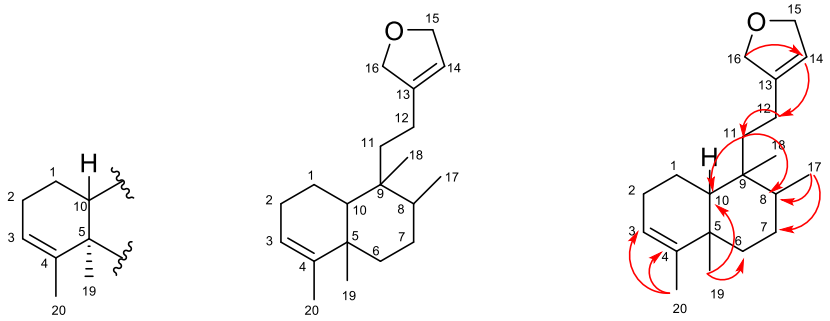

2.15 Planar structure of compound **2.1** HMBC

Table 2-1. NMR spectroscopic data (500 MHz, $CDCl_3$) for compound **2.1**.

	Compound **2.1**		
Position	δ_C, type[b]	δ_H (*J* in Hz)[a]	HMBC
1	18.4, CH_2	1.40, m[c]	2, 10
		1.42, m[c]	
2	27.6, CH_2	2.01, m	1, 3, 4
3	120.6, CH	5.19, m	20
4	144.7, C		
5	38.8, C		
6	37.1, CH_2	1.19, m	5, 10, 19
		1.69, dt (12.8, 2.9)	
7	27.6, CH_2	1.40, m[c]	5, 8
8	37.0, CH	1.51, m[c]	9, 17, 18
9	38.8, C		
10	46.6, CH	1.36, m[c]	19
11	37.2, CH_2	1.37, m[c]	10, 18
12	29.3, CH_2	1.93, m[c]	13, 14, 15
13	145.1, C		
14	126.2, CH	5.62, t (6.8)	12, 13, 15, 16
15	58.9, CH_2	4.20, d (6.8)	13, 14
16	61.5, CH_2	4.17, s	12, 13, 14
17	16.2, CH_3	0.80, d (6.1)	7, 8, 9
18	18.2, CH_3	1.58, s[c]	8, 9, 11
19	20.1, CH_3	0.99, s	5, 6, 10
20	18.5, CH_3	0.72, s	3, 4, 19

[a]Data(δ) measured at 500 MHz; s = singlet, d = doublet, m = multiplet. *J* values are in Hz and are omitted if the signals overlapped as multiplets. The overlapped signals were assigned from HSQC and HMBC spectra.
[b]Data(d) measured at 125 MHz.
[c]Overlaping signal.

NOESY correlations were used to determine the relative stereochemistry of compound **2.1**. The correlation between CH_3-17, CH_3-18 and CH_3-19 indicated that these three methyl groups were cofacial, while the missing correlation between CH_2-11 and CH_3-19 showed that the 2,5-dihydrofuran ring branch was on the opposite face from the CH_3-19 group.

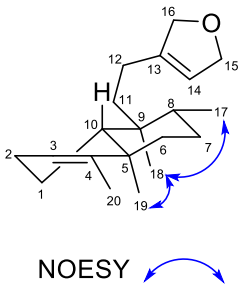

The absolute configuration of **2.1** was determined to be the same as that of the compound isolated by Liu *et al.* in 2014,[6] based on a comparison of the specific rotation of **2.1** ($[\alpha]_D$ -50º (c 0.1, MeOH)) with that of the literature compound ($[\alpha]_D$ -37º (c 0.1, MeOH)). It was reported with significant antibacterial activity against Gram-positive bacteria. The comparison between the ^1H NMR data and ^{13}C NMR data with literature data are summarized in Table 2-2.

Table 2-2. Compare NMR spectroscopic data for compound **2.1** with literature.

	Compound **2.1**		Literature Value for **2.1**[6]	
Position	δ_C, (*J* in Hz)[b]	δ_H, (*J* in Hz)[a]	δ_C, (*J* in Hz)	δ_H (*J* in Hz)
1	18.4, CH_2	1.40, m[c]	18.4, CH_2	1.36, m
		1.42, m[c]		1.42, m
2	27.6, CH_2	2.01, m	27.0, CH_2	2.01, m
3	120.6, CH	5.19, m	120.5, CH	5.17, brs
4	144.7, C		144.6, C	
5	38.8, C		38.3, C	
6	37.1, CH_2	1.19, m	36.9, CH_2	1.17, m
		1.69, dt (12.8, 2.9)		1.69, dt (12.8, 3.0)
7	27.6, CH_2	1.40, m[c]	27.6, CH_2	1.39, m
8	37.0, CH	1.51, m[c]	36.3, CH	1.47, m
9	38.8, C		38.8, C	
10	46.6, CH	1.36, m[c]	46.5, CH	1.36, m
11	37.2, CH_2	1.37, m[c]	37.1, CH_2	1.38, m
12	29.3, CH_2	1.93, m[c]	29.1, CH_2	1.95, m
13	145.1, C		144.9, C	
14	126.2, CH	5.62, t (6.8)	126.0, CH	5.57, t (7.0)
15	58.9, CH_2	4.20, d (6.8)	58.5, CH_2	4.14, d (7.0)
16	61.5, CH_2	4.17, s	60.8, CH_2	4.11, s
17	16.2, CH_3	0.80, d (6.1)	16.1, CH_3	0.79, d (6.3)
18	18.2, CH_3	1.58, s[c]	18.1, CH_3	1.57, brs
19	20.1, CH_3	0.99, s	20.0, CH_3	0.98, s
20	18.5, CH_3	0.72, s	18.5, CH_3	0.71, s

[a]Data(δ) measured at 500 MHz; s = singlet, d = doublet, m = multiplet. *J* values are in Hz and are omitted if the signals overlapped as multiplets. The overlapped signals were assigned from HSQC and HMBC spectra.
[b] Data(δ) measured at 125 MHz;
[c]Overlaping signal.

2.2.3 Structure Elucidation of Compound 2.2

Compound **2.2** was isolated as white powder. Its molecular formula was determined as $C_{20}H_{30}O_3$ based on its HRESIMS ion at *m/z* 341.1985 $[M+Na]^+$. The structure of compound **2.2** was determined by comparing its ^1H NMR spectrum with that of compound **2.1**, as summarized in Table 2-2.

The ^1H NMR spectrum of **2.2** indicates the presence of four methyl groups and the signals in the range from 1.35 ppm to 2.5 ppm were essentially identical with those of **2.1**. These indicated that compound **2.2** had the same ring system as compound **2.1**.

The major difference between compound **2.1** and **2.2** occurred in the range of double bond protons and the H_2-15 (δ_H 4.20) and H_2-16 (δ_H 4.17) protons. As shown in Figure 2-3, in the ^1H NMR spectrum of compound **2.2**, signals for δ_H 4.20 (H-15) and δ_H 4.17 (H-16) were missing from the spectrum. The signal at δ_H 5.60 (H-14) changed from a triplet to a singlet, and moved to δ_H 5.85, and one more singlet proton with δ_H 5.99 appeared in the spectrum. These changes indicated that the protons of H_2-15 and H_2-16 have been replaced. The extra singlet proton with δ_H 5.90 indicated that one H_2-16 proton has been replaced with a hydroxyl group, which made the H_2-16 proton move upfield. The singlet for H-14 and its correlation in the HMBC spectrum with a carbon at δ_C 171.5 indicated that there is a carbonyl group at position 15.

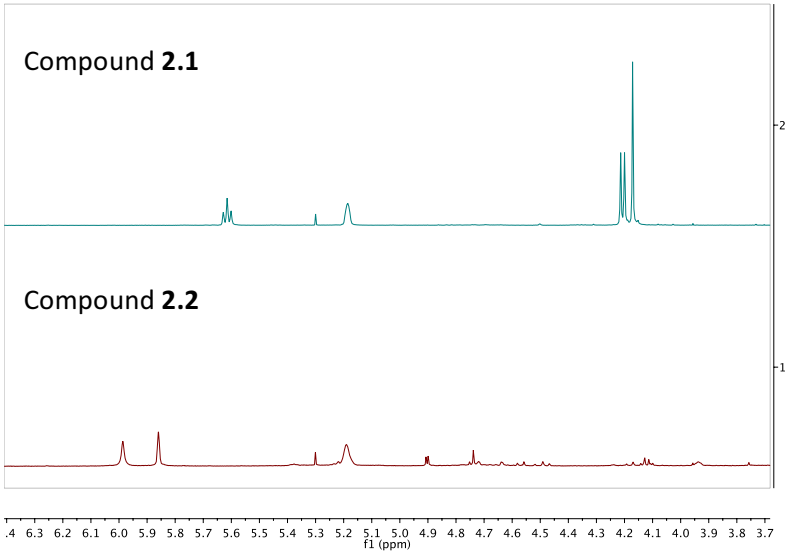

Figure 2-3. Selected range of ^1H NMR spectra of compound **2.1** and **2.2**.

All these data taken together indicated that the structure of compound **2.2** was very similar with that of compound **2.1**. The difference was the structure of 2, 5-dihydrofuran, which changed to 5-hydroxyfuran-2(5H)-furanone moiety.

The absolute structure of compound **2.2** was determined as shown here, by comparing its specific rotation ($[\alpha]_D$ -42° (c 0.1, MeOH)) with that of the compound isolated by Bhattacharya et

al. in 2015 ([α]$_D$ -24.43º (c 0.95, MeOH)).[7] Since the 5-hydroxyfuran-2(5H)-furanone moiety is an intramolecular hemiacetal, and has equivalent between cyclic hemiacetal form and open form, the stereochemistry of the hemiacetal OH group is ambiguous, and compound **2.2** is a mixture of both isomers. Compound 2.2 had been isolated from the plants *Polyalthia longitolia*, *Caryopteris incana*, *Mitrephora thorelii*, and *Polyalthia longifolia*.[7,8,9,10] The comparison between the ^{1}H NMR data with literature data are summarized in Table 2-3.

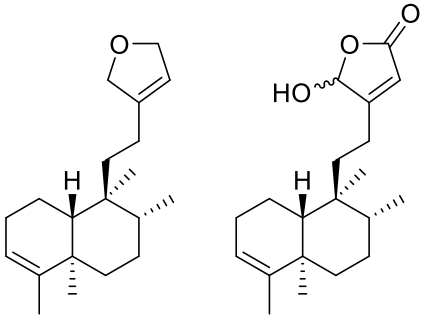

2.1 **2.2**

Table 2-3. Compare NMR spectroscopic data for compound **2.2** with literature.

	Compound **2.2**	Literature Value for **2.2**[7]
Position	δ_H, (*J* in Hz)[a]	δ_H, (*J* in Hz)[a]
1	1.40, m[c]	1.43-1.57, m
	1.42, m[c]	1.43-1.57, m
2	2.01, m	2.01, m
3	5.19, m	5.20, brs
6	1.19, m	1.37-1.19, m
	1.69, dt (12.8, 2.9)	1.65, m
7	1.40, m[c]	1.43-1.57, m
8	1.51, m[c]	1.43-1.57, m
10	1.36, m[c]	1.37-1.19, m
11	1.37, m[c]	1.37-1.19, m
12	2.09, m	2.10, m
14	5.86, s	5.85, m
16	5.99, s	6.07, s
17	0.88, d (6.5)	0.83, d (6.5)
18	1.57, s	1.60, s
19	0.98, s	1.02, s
20	0.73, s	0.79, s

[a]Data(δ) measured at 500 MHz; s = singlet, d = doublet, m = multiplet. *J* values are in Hz and are omitted if the signals overlapped as multiplets. The overlapped signals were assigned from HSQC and HMBC spectra.
[b]Data(δ) measured at 400 MHz.
[c]Overlaping signal.

2.3 Bioactivities

The antiproliferative activities of compound **2.1** and **2.2** were tested against the A2780 ovarian cancer cell line and their antiplasmodial activities were tested against the chloroquine-resistant *Plasmodium falciparum* Dd2 strain. Both compounds **2.1** and **2.2** showed moderate activity against A2780, with IC_{50} values of 6.9 μM and 3.4 μM, respectively. They also displayed good antiplasmodial activity against *Plasmodium falciparum* Dd2. Compound **2.1** had an IC_{50} value of 9.9 ± 1.4 μM, and compound **2.2** had an IC_{50} value of 2.8 ± 0.7 μM. This work reports the first isolation of compound **2.1** from a *Hypoestes sp*. extract, and also the discovery of its antiproliferative activity against ovarian cancer cells and its antiplasmodial activity against

Plasmodium falciparum Dd2. Compound **2.2** has been previously reported to have antifungal,[7] antimalarial,[8] anti-tumor,[9] and anti-inflammatory[10] activities.

Table 2-4. Antiproliferative and antimalarial activity data of compound **2.1** and **2.2**.

Compound	A2780 ovarian cancer cells IC_{50} (μM)	*P. falciparum* Dd2 strain IC_{50} (μM)
2.1	6.9 ± 0.8	9.9 ± 1.4
2.2	3.4 ± 0.5	2.8 ± 0.7

2.4 Experimental Section

2.4.1 General Experimental Procedures

The mass spectra was measured on an Agilent 6220 LC-TOF-MS in the positive ion mode. NMR spectra were obtained in $CDCl_3$ on a Bruker Avance 500 spectrometer. Low pressure column chromatography was performed on Sephadex LH-20 with 1:1 dichloromethane and methanol solvent. The preparative HPLC was performed on an instrument with a Shimadzu SCL-10A controller, Shimadzu LC-8A pumps, and SPD-M10A UV detector with a preparative C_{18} Varian Dynamax column (250 × 21.4 mm). Semi-preparative HPLC was carried out on an instrument with Shimadzu SCL-10A controller, Shimadzu LC-10AT pumps, SPD-M10A UV detector, and SEDEX 75 ELSD detector with a semi-preparative C_{18} Varian Dynamax column (250 × 10 mm).

2.4.2 Plant Material

The *Hypoestes sp.* plant was collected by Stephan Rakotonandrasana from the Orangea forest in Antsiranana, Madagascar, in a thicket on dry sand near the Sakalava Bay on October 3, 2006. The coordinates of collection location is 12º15´S 049º20´E (-12.2500, 49.3333).

2.4.3 Extraction and Isolation

Dried leaves and flowers of *Hypoestes sp.* (Acanthaceae) were ground, extracted with EtOH at room temperature for 24 hours and evaporated to give an extract designated MG 3985. A

sample of 5.47 g of this extract with an IC_{50} value 14.0 μg/mL against the A2780 cell line was shipped to Virginia Tech. A 2 g sample of MG 3985 was suspended in 100 mL 90% aqueous MeOH, and then extracted with hexanes (3 × 100 mL portions) to give 860 mg hexanes-soluble fractions with IC_{50} value of 7.5 μg/mL. The remaining aqueous MeOH fraction was evaporated under vacuum and redissolved in 60% aqueous MeOH. This fraction was then extracted with CH_2Cl_2 (3 × 100 mL portions) to give 548 mg of a CH_2Cl_2–soluble fraction with an IC_{50} value of 15 μg/mL. The residual aqueous MeOH-soluble fraction was evaporated under vacuum, and yielded 499 mg of material with an IC_{50} value over 20 μg/mL. The most active hexanes-soluble fraction was subjected to size exclusion open column chromatography on a Sephadex LH-20 column and elution with 1:1 CH_2Cl_2/MeOH solvent. Two fractions, with masses of 122 mg and 661 mg, were obtained from this procedure. Their activities were > 20 μg/mL and 13 μg/mL, respectively. The fraction with IC_{50} of 13 μg/mL was further fractionated by using the preparative C_{18} HPLC with a preparative C_{18} Varian Dynamax column (250 × 21.4 mm), and eluting with aqueous MeOH from 50% to 100% within 1 hour with a flow rate of 10 mL/min. This gave three fractions, with activities of 10 μg/mL, 6.7 μg/mL and 11 μg/mL, respectively. About 2 mg of the fraction with IC_{50} of 6.7 μg/mL was then subjected to separation on a semi-preparative C_{18} Varian Dynamax HPLC column (10 × 250 mm) and eluted with aqueous MeOH with a gradient from 75% to 85% MeOH over 30 minutes with a flow rate of 2.5 mL/min. Compound **2.1** (0.33 mg) was obtained at 21 min, compound **2.2** (0.19 mg) was obtained at 26 min.

2.4.4 Antiproliferative Bioassays

The antiproliferative bioassays were conducted by testing the compound's activity against the drug-sensitive A2780 ovarian cancer cell line. After culturing for 3 days, the cells grew to around 90% confluency. The cells were then incubated with trypsin for 3-5 minutes and added to

the growth medium (RPMI 1640 supplemented with 10% fetal bovine serum and 2 mM L-glutamine). Cells were then counted by using a hemacytometer and diluted to a concentration of 2.5×10^5 cells per mL in growth medium. The assay was set up in a 96-well microtiter plate and 199 μL cell suspension were added into eleven columns of the plate. The remaining column was plated with growth medium alone (no cells) to serve as background. The cell plate was then incubated for 3 hours at 37 ^oC with 5% CO_2 to allow the cells to adhere to the wells. During this incubation, the drug plate was prepared. The potential antiproliferative agents were dissolved in 50% aqueous DMSO, and made into a series of concentrations at 20 μg/mL, 4 μg/mL, 0.8 μg/mL and 0.16 μg/mL. One column of the drug plate was left empty and four dilutions of paclitaxel were included as positive control. Diluted agents (1 μL each) in the drug plate were then added to the corresponding positions in the cell plate and incubated for another 2 days at 37 ^oC with 5% CO_2. Then the medium in each well was replaced with reaction medium containing 1% AlamarBlue, which reacts with living cells and is converted to its fluorescent form. The fluorescence intensity was measured with a Cytofluor Series 4000 plate reader with an excitation wavelength of 530 nm and an emission wavelength of 590 nm. The fluorescence intensity data were analyzed by linear regression to calculate the IC_{50} value of each sample. For pure active compounds, samples were analyzed in triplicate to provide reliable IC_{50} values.

2.4.5 Antimalarial Bioassays

The antimalarial bioassay was conducted on the Dd2 chloroquine resistant strain of *Plasmodium falciparum*. The parasites were cultured in the gas mixture of 4.99% O_2, 5.06% CO_2, and 89.95% N_2 for 3 to 4 days to reach their ring stage, which was determined by light microscopy. Then after incubation with potential antiplasmodial agents for another 72 hours, SYBR Green I was added to determine the amount of DNA present. SYBR Green I bonds with double strand

DNA to generate a fluorescent complex. The IC_{50} values were calculated based on the fluorescence intensity of diluted samples. The IC_{50} values of pure active compounds were determined in duplicate, and expressed with ±SEM.

2.4.6 Spectroscopic Properties

Compound **2.1**: white powder; $[\alpha]_D$ -50º (c 0.1, MeOH), [lit.[6] $[\alpha]_D$ -37º (c 0.1, MeOH)]; ^{1}H NMR (500 MHz, $CDCl_3$) see Table 2-1; HRESIMS *m/z* 289.2485 $[M+H]^+$ (calcd for $C_{20}H_{33}O^+$, 289.2487).

Compound **2.2**: white powder; $[\alpha]_D$ -42º (c 0.1, MeOH), [lit.[7] $[\alpha]_D$ -24.43º (c 0.95, MeOH)]; ^{1}H NMR (500 MHz, $CDCl_3$) see Table 2-2; HRESIMS *m/z* 341.1985 $[M+Na]^+$ (calcd for $C_{20}H_{30}O_3Na^+$, 341.2087).

2.5 Supporting Information

2.5.1 ^{1}H NMR spectrum of 2.1 ($CDCl_3$, 500 MHz)

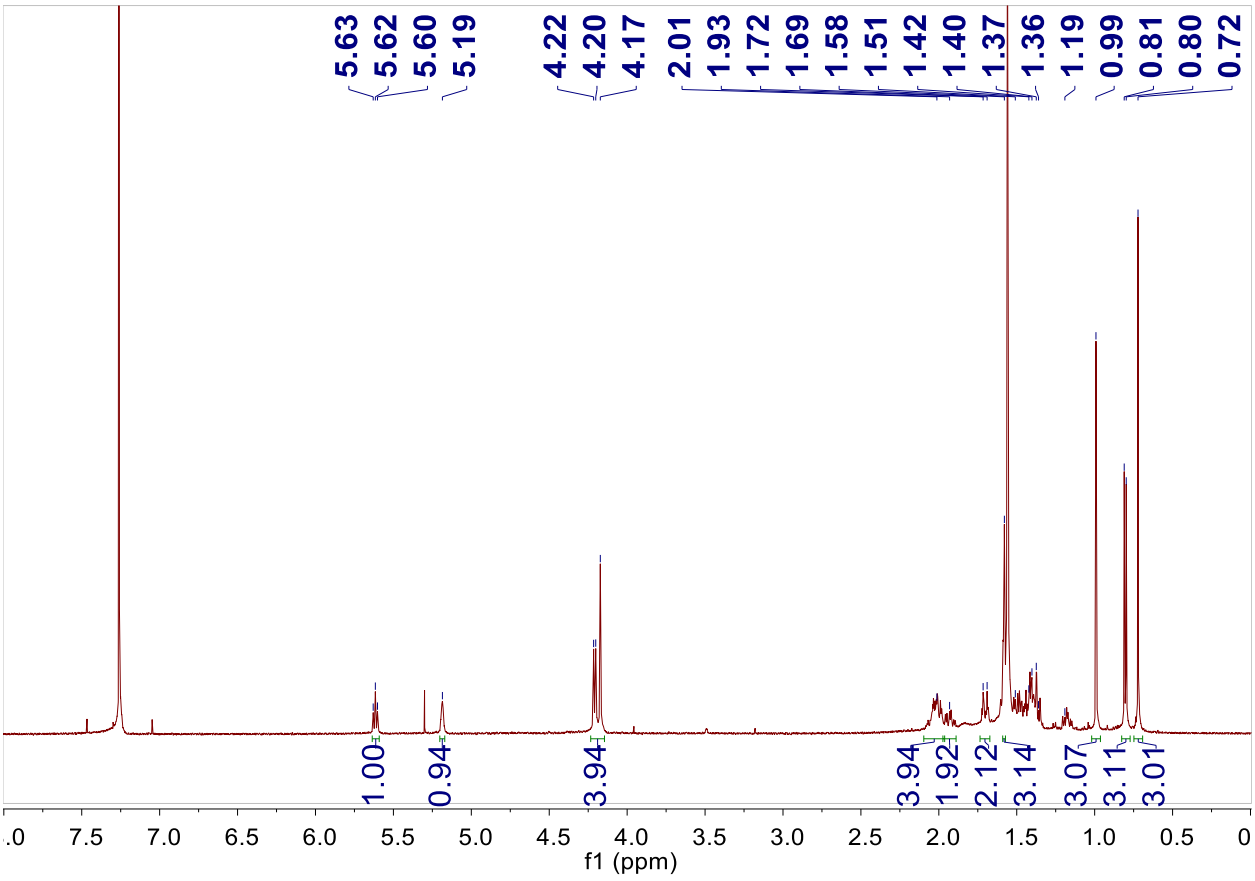

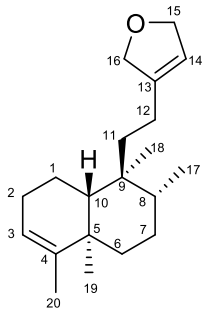

2.5.2 ^{13}C NMR spectrum of 2.1 ($CDCl_3$, 125 MHz)

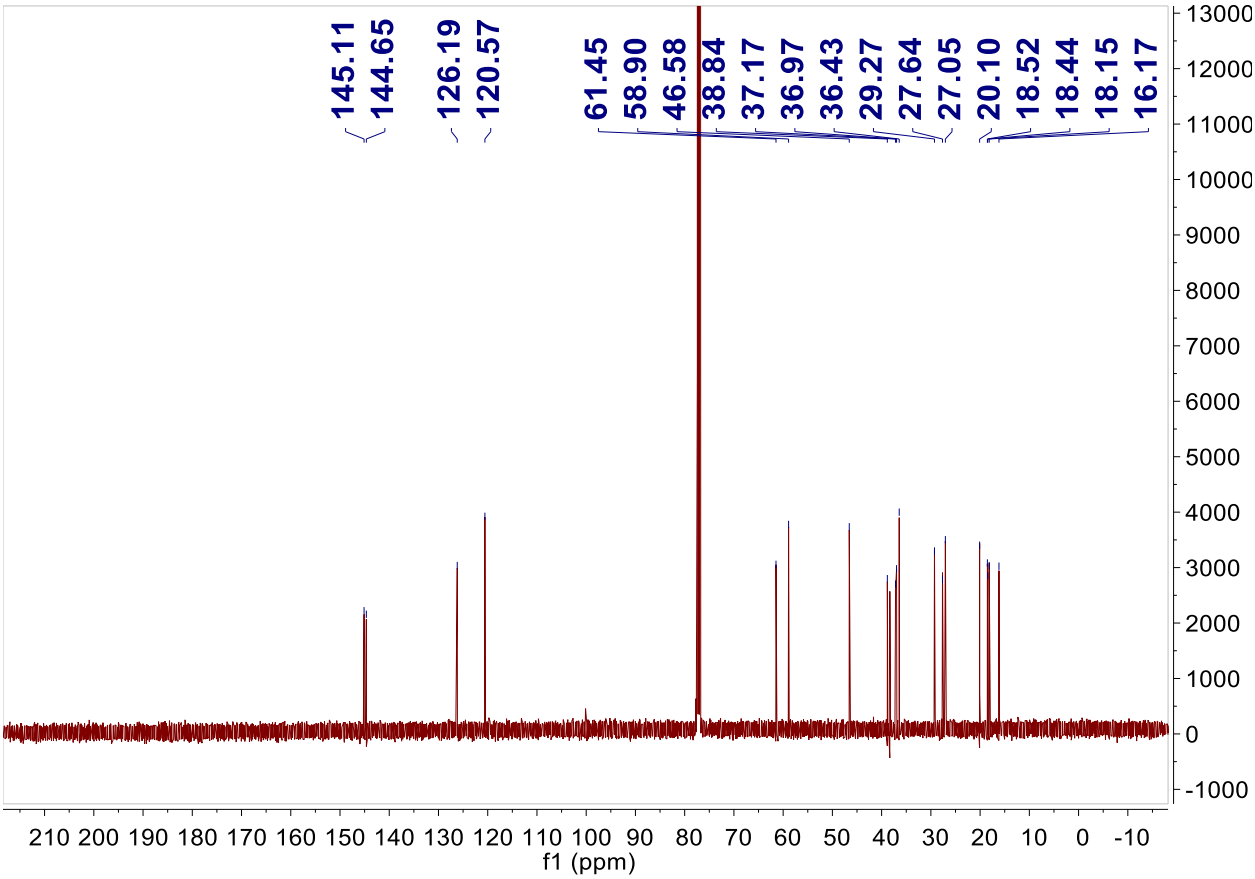

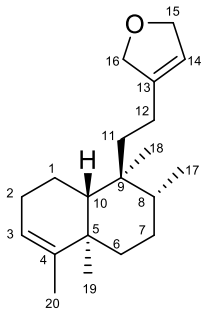

2.5.3 COSY spectrum of 2.1 ($CDCl_3$, 500 MHz)

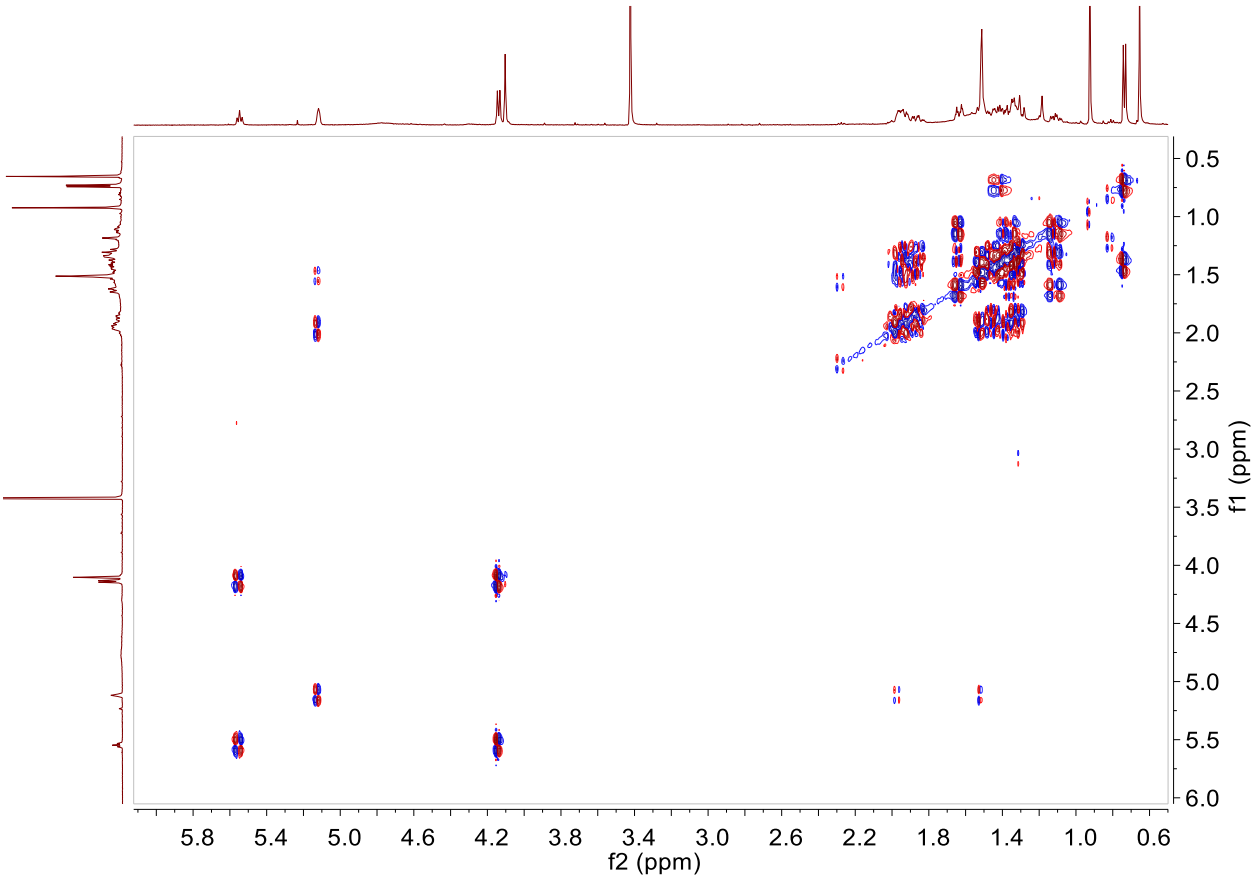

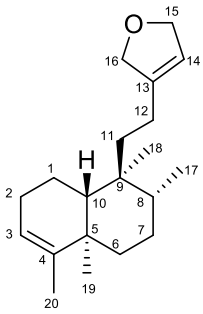

2.5.4 HSQC spectrum of 2.1 ($CDCl_3$, 500 MHz, 125 MHz)

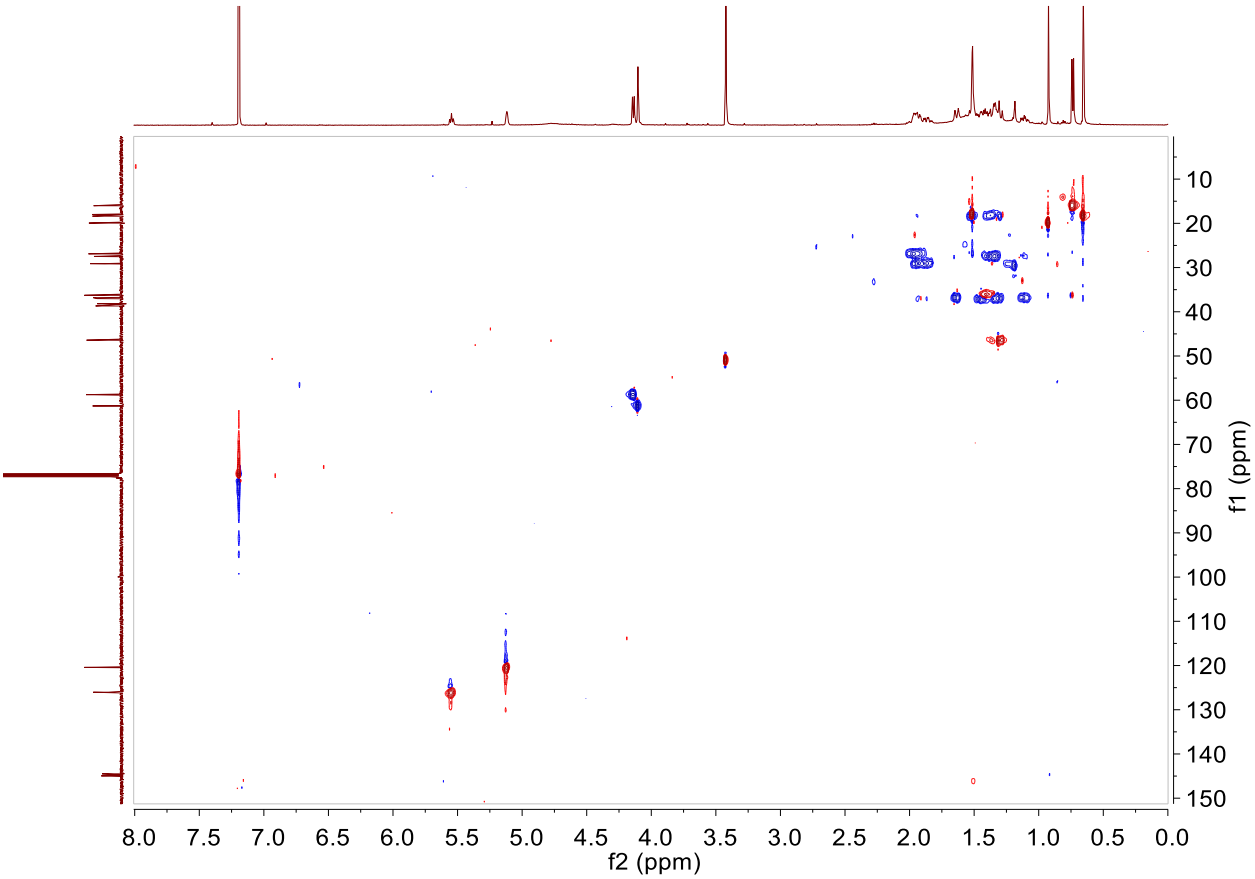

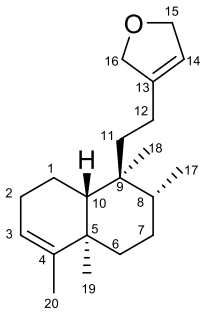

2.5.5 HMBC spectrum of 2.1 ($CDCl_3$, 500 MHz, 125 MHz)

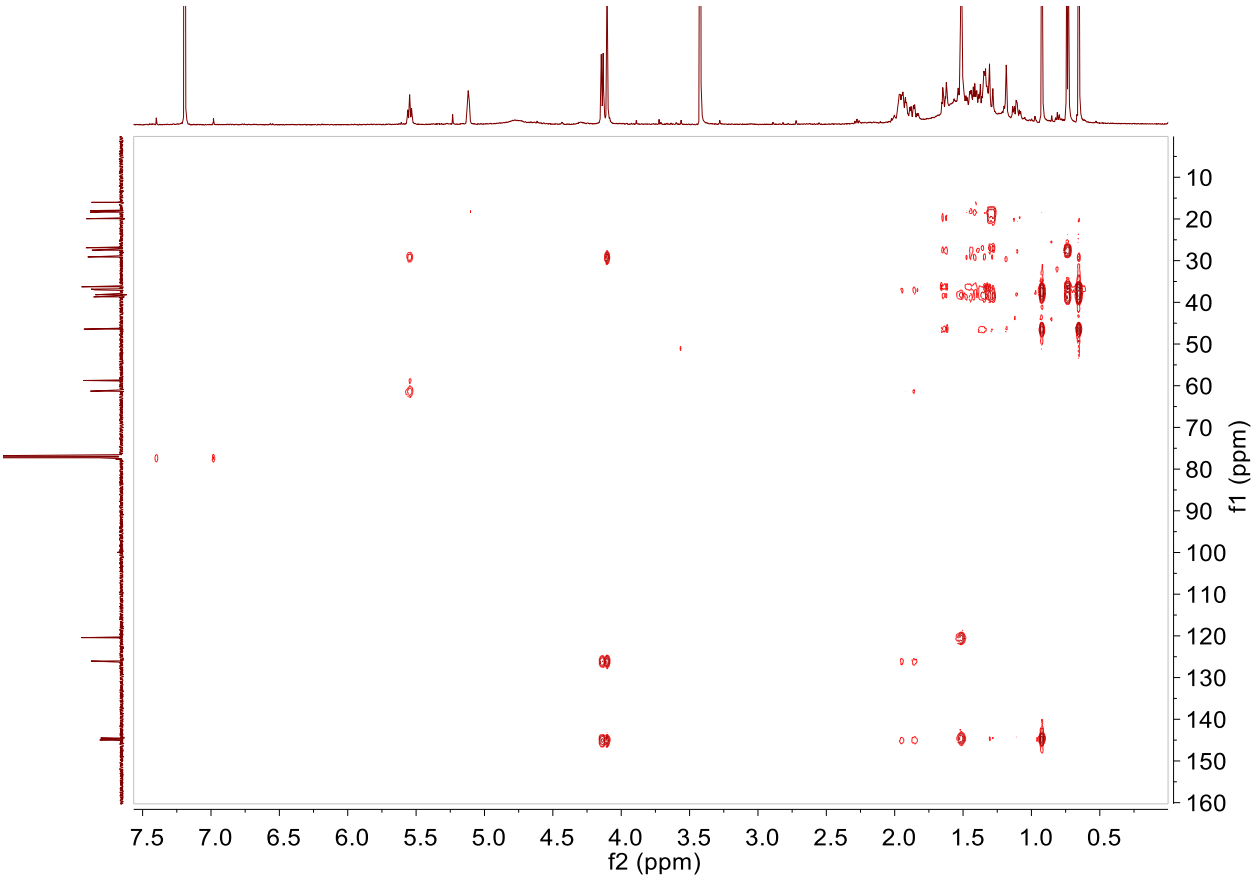

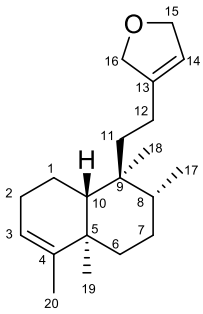

2.5.6 ^{1}H NMR spectrum of 2.2 ($CDCl_3$, 500 MHz) not pure

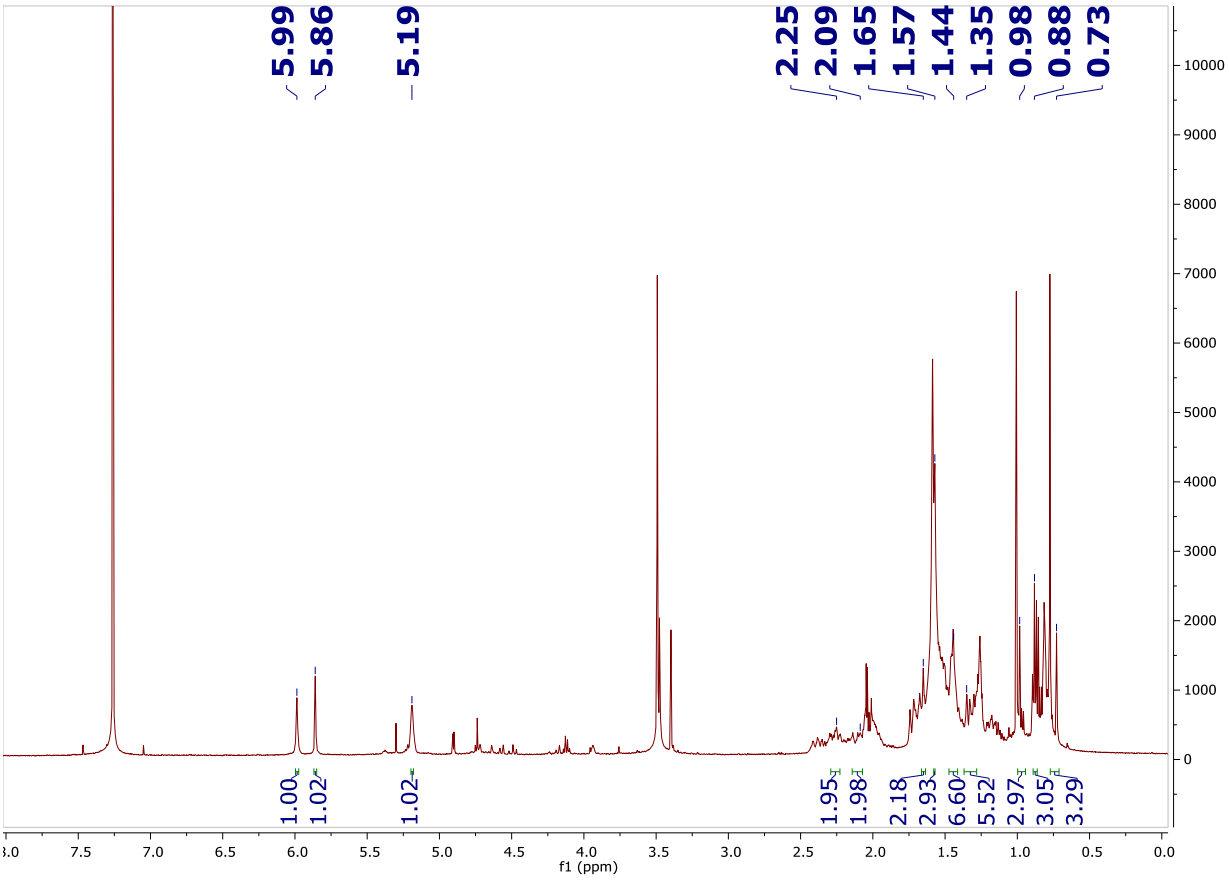

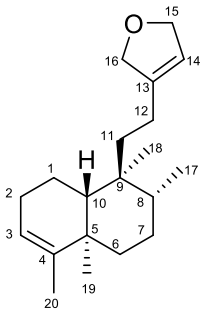

2.6 References

(1) Shen, C.C.; Ni, C.L.; Huang, Y.L.; Huang, R.L.; Chen, C.C. Furanolabdane Diterpenes from *Hypoestes purpurea*. *J. Nat. Prod.* **2004**, *67*, 1947–1949.

(2) Al-Rehaily, A. J.; Al-Yahya, M. A.; Mirza, H. H.; Ahmed, B. Verticillarone: A New Seco-Fusicoccane Diterpenoid Ketonepoxide from *Hypoestes verticillaris*. *J. Asian Nat. Prod. Res.* **2002**, *4*, 117–122.

(3) Muhammad, I.; Mossa, J. S.; Al-Yahya, M. A.; El-Feraly, F. S.; McPhail, A. T. Hypoestenone: A Fusicoccane Diterpene Ketone from *Hypoestes forskalei.* *Phytochemistry* **1997**, *44*, 125–129.

(4) Rasoamiaranjanahary, L.; Guilet, D.; Marston, A.; Randimbivololona, F.; Hostettmann, K. Antifungal Isopimaranes from *Hypoestes serpens*. *Phytochemistry* **2003**, *64*, 543–548.

(5) Al Musayeib, N. M.; Mothana, R. A.; Mohamed, G. A.; Ibrahim, S. R. M.; Maes, L. Hypoestenonols A and B, New Fusicoccane Diterpenes from *Hypoestes forskalei*. *Phytochem. Lett.* **2014**, *10*, 23–27.

(6) Liu, C.-P.; Xu, J.-B.; Zhao, J.-X.; Xu, C.-H.; Dong, L.; Ding, J.; Yue, J.-M. Diterpenoids from *Croton laui* and Their Cytotoxic and Antimicrobial Activities. *J. Nat. Prod.* **2014**, *77*, 1013–1020.

(7) Bhattacharya, A. K.; Chand, H. R.; John, J.; Deshpande, M. V. Clerodane Type Diterpene as a Novel Antifungal Agent from *Polyalthia longifolia* Var. *pendula*. *Eur. J. Med. Chem.* **2015**, *94*, 1–7.

(8) Yoshikawa, K.; Harada, A.; Iseki, K.; Hashimoto, T. Constituents of *Caryopteris incana* and Their Antibacterial Activity. *J. Nat. Med.* **2014**, *68*, 231–235.

(9) Meng, D.H.; Xu, Y.P.; Chen, W.L.; Zou, J.; Lou, L.G.; Zhao, W.M. Anti-Tumour

Clerodane-Type Diterpenes from *Mitrephora thorelii*. *J. Asian Nat. Prod. Res.* **2007**, *9*, 679–684.

(10) Chang, F.R.; Hwang, T.L.; Yang, Y.L.; Li, C.E.; Wu, C.C.; Issa, H. H.; Hsieh, W.B.; Wu, Y.C. Anti-Inflammatory and Cytotoxic Diterpenes from Formosan *Polyalthia longifolia* Var. *pendula*. *Planta Med.* **2006**, *72*, 1344–1347.

Chapter 3. Antiplasmodial Limonoids from *Carapa guianensis* (Meliaceae)

3.1 Introduction to *Carapa guianensis* (Meliaceae)

A crude extract from the wood of *Carapa guianensis* (Meliaceae) collected from Guyana, was provided by the Natural Product Discovery Institute (NPDI). The crude extract had antiplasmodial activity against *Plasmodium falciparum* with an IC_{50} of 2.5 μg/mL. Fractionation was guided by antimalarial bioassay and the four known antiplasmodial compounds (**3.1**, **3.2**, **3.3** and **3.4**) were obtained from the combined hexanes and dichloromethane fractions. Their IC_{50} values against chloroquine-resistant *Plasmodium falciparum* strain, Dd2, were 2.0 ± 0.3 μM, 2.1 ± 0.1 μM, 2.1 ± 0.2 μM and 2.8 ± 0.2 μM, respectively.

Figure 3-1. Image of *Carapa guianensis* (Meliaceae). Photography by A. Gentry, from http://www.tropicos.org/Image/100109184

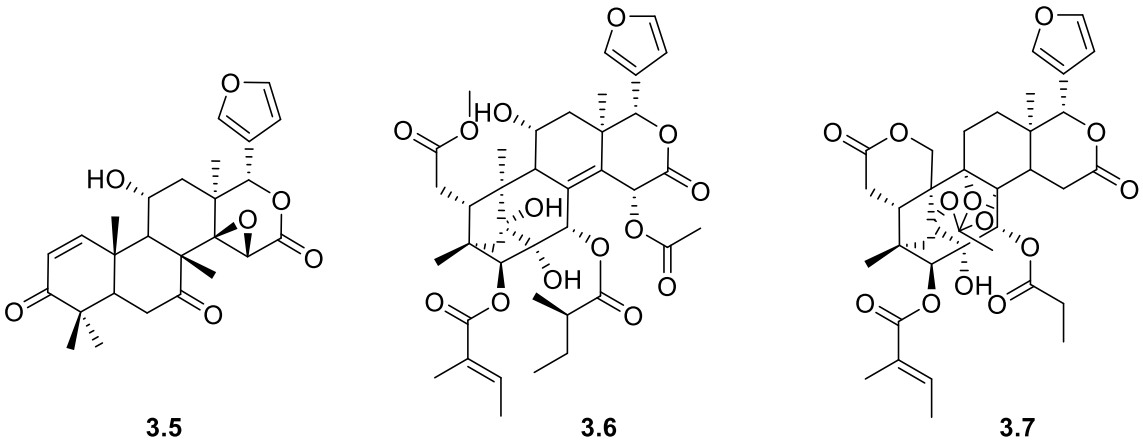

3.5 **3.6** **3.7**

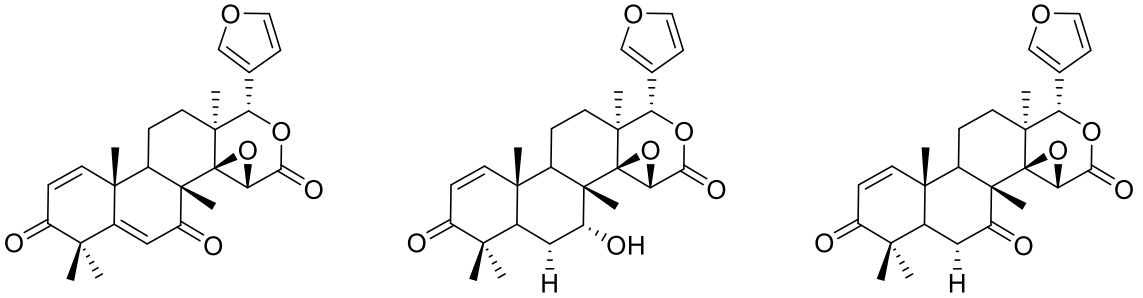

3.8 **3.9** **3.10**

Carapa guianensis is also called andiroba.[1] It is a flowering plant in the Meliaceae family, and it can grow up to 40 meters in height. It has large and textured leaves, and it produces brown, woody nuts, which look like chestnuts. The trees of this genus are widely spread in tropical South America, Central America and Africa. Its wood has been extensively used as commercial timber, and its bark, flowers and seeds have been used to extract andiroba oil for centuries by the Amazonian people. Andiroba oil has about 65% unsaturated fatty acids and 9% linoleic acid. It has been traditionally used to repel insects, prevent mosquitos from biting, and to treat skin problems (including skin cancer).[2] It also has analgesic,[3] antimalarial,[4] anti-inflammatory,[5] anti-allergic,[6] and antiplasmodial[7] activities.

Y. Matsui *et al.* reported a new gedunin and two new limonoids (**3.5 - 3.7**) from the seeds of *Carapa guianensis* which showed inhibitory activity to RAW264.7 cells.[8] Compound **3.8** was isolated from the seeds of *Carapa procera* by M. Dioum *et al.* in 2016.[9] It displayed strong

anticlonogenic activity. T. Inoue *et al.* isolated three gedunin-type limonoids (**3.4**, **3.9** and **3.10**) from seeds of *Carapa guianensis* which significantly reduce triglyceride levels in hepatocytes.[10]

3.2 Results and Discussion

3.2.1 Isolation of Compounds 3.1, 3.2, 3.3, 3.4

The crude extract of the wood of *Carapa guianensis* had good antiplasmodial activity against chloroquine resistant *Plasmodium falciparum* strain, Dd2, with an IC_{50} of about 2.5 μg/mL. Liquid-liquid partition of 105 mg of crude extract as previously described gave 20 mg hexanes fraction, 51 mg dichloromethane fraction and 29 mg aqueous methanol fraction. All three fractions exhibited moderate antiplasmodial activities. Evaluation of these fractions by TLC on silica gel showed that the hexanes and dichloromethane fractions shared similar patterns and major compounds. These fractions were thus combined and applied to reversed phase C_{18} HPLC. The four known limonoids **3.1** – **3.4** were isolated by this method.

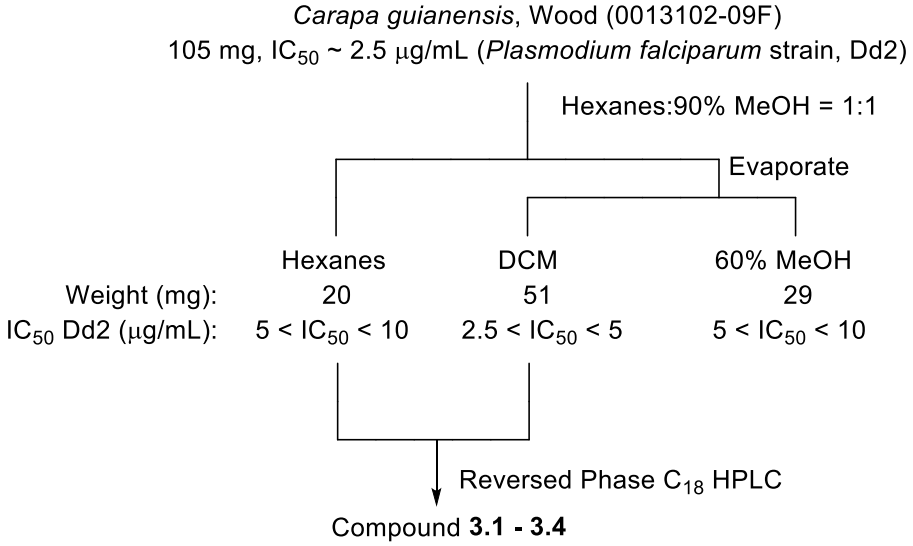

Figure 3-2. Bioassay-guided Separation of *Carapa guianensis*.

3.2.2 Structure Elucidation of Compound 3.1

Compound **3.1** was isolated as a colorless oil. It had the molecular formula $C_{32}H_{38}O_{11}$ based on its HRESIMS ions at *m/z* 599.2490 $[M+H]^+$ and *m/z* 621.2304 $[M+Na]^+$. So compound **3.1** was a highly unsaturated compound with 14 degrees of unsaturation.

The ^1H NMR spectrum of compound **3.1** contained signals for three protons at δ_H 7.40 (H-24), 7.42 (H-25) and 7.14 (H-1) located in the aromatic proton range. However, its UV spectrum did not show aromatic ring absorption. Therefore, along with protons with signals at δ_H 5.99 and 6.32, five double bond protons were identified in the structure, which indicated the existence of three double bonds. This was confirmed from the ^{13}C NMR spectrum, which had signals for six double bond carbons at δ_C 109.9, 119.9, 127.3, 141.5, 143.5 and 154.2.

As mentioned above, H-24 (δ_H 7.40) and H-25 (δ_H 7.42) had large chemical shifts compared with normal double bond protons and led to the conclusion that they were linked to an oxygen. In the ^1H NMR and COSY spectra, H-24 (δ_H 7.40), H-25 (δ_H 7.42), and H-26 (δ_H 6.32) were coupled with each other with coupling constants of J = 1.7 and 0.8. And they were also correlated with a quaternary double bond carbon C-23 (δ_C 119.9). All this information supported the structure of a furan ring. And because only correlations from H-17 (δ_H 5.61) to C-23 (δ_C 119.9) and C-24 (δ_C 143.5) and C-26 (δ_C 109.9) were observed in the HMBC spectrum, the furan ring should link at position 17 (**3.11**).

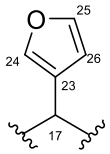

3.11

Signals in ^1H NMR spectrum indicated the presence of 8 methyl groups (δ_H 1.27, 3H, s; δ_H 1.17, 3H, s; δ_H 1.43, 3H, s; δ_H 1.48, 3H, s; δ_H 1.23, 3H, s; δ_H 2.04, 3H, s; δ_H 2.12, 3H, s; δ_H 2.13,

3H, s). Three of these groups with signals at δ_H 2.04, 2.12 and 2.13 were correlated with carbons at δ_C 169.8, δ_C 170.0 and δ_C 170.2 in the HMBC spectrum. And in the HSQC spectrum, the chemical shift of their carbons were δ_C 21.1, δ_C 21.4 and δ_C 21.7, respectively. These indicated that they were the methyl groups of three acetoxy groups. The remaining methyl groups were all singlets, so there were five quaternary methyl groups in the structure.

Aside from the three carbonyls in the acetoxy groups, there were two additional singlet carbonyl carbons with signals at δ_C 203 and 166.6 in ^{13}C NMR spectrum, which indicated the presence of a ketone and an ester group in the structure.

In the HMBC spectrum, the carbonyl carbon C-3 (δ_C 203) correlated with double bond protons H-1 (δ_H 7.14) and H-2 (δ_H 5.99). This showed the presence of an *α,β*-unsaturated ketone in the structure. The HMBC spectrum showed correlations between H_3-18 (δ_H 1.27) and H_3-19 (δ_H 1.17) to quaternary carbon C-4 (δ_C 44.8). Correlations from H_3-18 and H_3-19 were also observed to carbonyl carbon C-3 (δ_C 203.4) and C-5 (δ_C 49.1). Additional correlations were observed from H-2 (δ_H 5.99) to C-4 (δ_C 44.8) and from H-1 (δ_H 7.14) to C-3 (δ_C 203.4), C-5 (δ_C 49.1) and C-10 (δ_C 41.3). These correlations taken together indicate that compound **3.1** contains a 6-membered ring as shown in partial structure **3.12**.

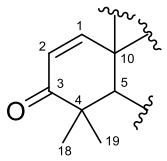

3.12

The second carbonyl carbon C-16 (δ_C 166.6) had a smaller chemical shift than carbonyl carbon C-3 (δ_C 203.4). Its chemical shift was very similar with that of carbonyl carbons in the acetoxy groups, which indicated that carbonyl C-16 was linked with an oxygen. In the HMBC

spectrum, carbonyl C-16 only correlated with H-15 (δ_H 3.68), and H-15 correlated with the two quaternary carbons C-13 (δ_C 38.0) and C-14 (δ_C 69.6). Also C-13 and C-14 both correlated with CH-17 (δ_H 5.61), which was linked to the furan ring. In addition, the proton chemical shift of H-17 is δ_H 5.61, which indicated that CH-17 was an oxygen bearing CH group and forms part of a six-membered ring as shown in the partial structure **3.13**.

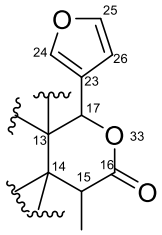

3.13

In the ^{1}H NMR spectrum, H-15 had a proton chemical shift at δ_H 3.68, which indicated it was oxygenated. A three-member ring formed by CH-15, C-16 and O-33 would be very unstable, so CH-15 must be linked with another oxygen. Unlike normal ring carbons with chemical shifts under 50 ppm, C-14 had a carbon resonance at δ_C 69.6, which indicated that C-14 and CH-15 may be connected with a same oxygen. All this information indicated the presence of an αβ-epoxy-δ-furyl-δ-lactone (**3.14**) in the structure of compound **3.1**.

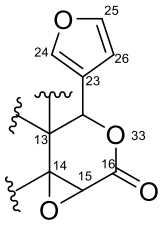

3.14

At this point all oxygen atoms and three double bonds have been assigned, and only two unsaturated degrees and six carbons remain to be assigned. These carbons can be assigned to two

additional rings, and this assignment was supported by the HMBC correlations and COSY correlations.

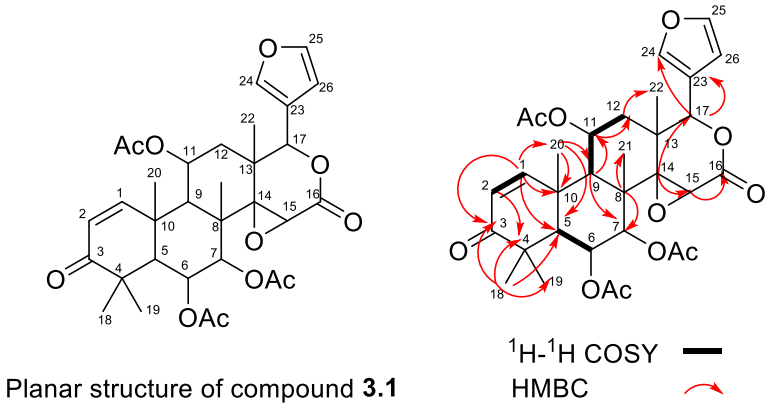

Planar structure of compound **3.1**

NOESY correlations were used to determine the relative stereochemistry of compound **3.1**. The CH-24, CH_3-22 and CH-11 were correlated with each other, but the correlation between CH-11 and CH_3-20 was missing. CH_3-20 had correlations with CH-6 and CH-7, and CH-7 had correlations with CH_3-21 and CH-15. Therefore, the furan ring, CH_3-22, the 6-acetoxy group and the 7-acetoxy group were cofacial, while the 11-acetoxy group, CH_3-20, CH_3-21 and epoxide were on the opposite side of the structure.

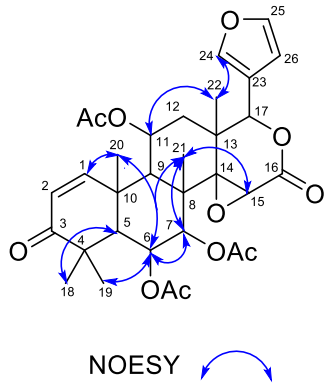

The absolute stereochemistry of compound **3.1** was determined to be the same as the compound reported by Connolly et al. in 1966.[11] This was confirmed by comparing the specific rotation of compound **3.1** ($[\alpha]_D$ +88° (c 0.1, MeOH)) with that of the literature compound ($[\alpha]_D$

+58º (c 0.13, MeOH)). Compound **3.1** is a derivative of gedunin, and it is reported with antimicrobial activity. Even though it was isolated 50 years ago, very little work has been done on it, and no complete NMR spectra have been reported.

Table 3-1. NMR spectroscopic data of **3.1**.

	Compound **3.1**		
Position	δ_C, type[b]	δ_H (*J* in Hz)[a]	HMBC
1	154.2, CH	7.14, d (10.1)	3, 5, 10, 20
2	127.3, CH	5.99, d (10.1)	3, 4, 10
3	203.4, C		
4	44.8, C		
5	49.1, CH	2.51, d (12.4)	1, 3, 4, 6, 7, 10, 18, 19, 20, 6-O$\underline{C}$OCH$_3$
6	69.6, CH	5.38, dd (2.6, 12.4)	5, 7, 10, 6-O$\underline{C}$OCH$_3$
7	73.7, CH	4.92, d (2.6)	6, 8, 21, 7-O$\underline{C}$OCH$_3$
8	42.9, C		
9	42.1, CH	2.59, d (5.0)	5, 8, 10, 11, 20, 21
10	41.3, C		
11	66.2, CH	5.80, dt (5.0, 5.9)	9, 11-O$\underline{C}$OCH$_3$
12	36.3, CH$_2$	1.55, s	11, 13, 22
		2.34, dd (4.4, 9.7)	9, 11, 13, 14, 22
13	38.0, C		
14	69.6, C		
15	55.3, CH	3.68, s	13, 14, 16
16	166.6, C		
17	78.0, CH	5.61, s	13, 14, 22, 23, 24, 26
18	20.7, CH$_3$	1.27, s	3, 4, 5, 19
19	31.9, CH$_3$	1.17, s	3, 4, 5, 18
20	24.1, CH$_3$	1.43, s	1, 5, 10
21	20.2, CH$_3$	1.48, s	7, 9, 14
22	17.2, CH$_3$	1.23, s	12, 13, 14, 17
23	119.9, C		
24	143.5, CH	7.40, dd (1.7, 0.8)	23, 25, 26
25	141.5, CH	7.42, dd (1.7, 1.7)	23, 24, 26
26	109.9, CH	6.32, dd (0.8, 1.7)	23, 24, 25
6-O$\underline{C}$OCH$_3$	169.8, C		
6-OCO$\underline{C}$H$_3$	21.1, CH$_3$	2.13, s	6-O$\underline{C}$OCH$_3$
7-O$\underline{C}$OCH$_3$	170.0, C		
7-OCO$\underline{C}$H$_3$	21.4, CH$_3$	2.12, s	7-O$\underline{C}$OCH$_3$
11-O$\underline{C}$OCH$_3$	170.2, C		
11-OCO$\underline{C}$H$_3$	21.7, CH$_3$	2.04, s	11-O$\underline{C}$OCH$_3$

[a]Data(δ) measured at 500 MHz; s = singlet, d = doublet, m = multiplet. *J* values are in Hz and are omitted if the signals overlapped as multiplets.
[b]Data(δ)measured at 125 MHz.

3.2.3 Structure Elucidation of Compounds 3.2 to 3.4

Compounds **3.2** to **3.4** were isolated as colorless oils similar to compound **3.1**. Compound **3.2** had the molecular formula $C_{30}H_{35}O_9$ based on its HRESIMS ion at *m/z* 541.2438 $[M+H]^+$. Compound **3.3** had the same molecular formula based on its HRESIMS ion at *m/z* 541.2438 $[M+H]^+$. Compound **3.4** had the molecular formula $C_{28}H_{33}O_7$ based on its HRESIMS ion at *m/z* 483.2381 $[M+H]^+$. Therefore, compounds **3.2** and **3.3** are isomers. The difference in molecular weight between compound **3.1** and compounds **3.2**/**3.3** was 58 ($C_2H_2O_2$), which was equal to the loss of one acetoxy group. Similarly, the difference between compound **3.2**/**3.3** and compound **3.4** was also 58 ($C_2H_2O_2$), which indicated the loss of another acetoxy group.

These conclusions were confirmed by comparing their ^{1}H NMR spectra with that of compound **3.1**. From their ^{1}H NMR spectra, compounds **3.2**, **3.3** and **3.4** all had five methyl groups as in compound **3.1**. The presence of proton signals around δ_H 7.4 (H-24, H-25) and 6.3 (H-26) indicated the presence of a furan ring as in compound **3.1**. The similar chemical shifts of H-15 and H-17 (**3.1**: H-15 δ_H 3.68, H-17 δ_H 5.61; **3.2**: H-15 δ_H 3.59, H-17 δ_H 5.61; **3.3**: H-15 δ_H 3.61, H-17 δ_H 5.62; **3.4**: H-15 δ_H 3.53, H-17 δ_H 5.62) showed the presence of an αβ-epoxy-δ-furyl-δ-lactone. The similar chemical shifts of H-1, H-2 (**3.1**: H-1 δ_H 7.14, H-2 δ_H 5.99; **3.2**: H-1 δ_H 7.13, H-2 δ_H 5.92; **3.3**: H-1 δ_H 7.08, H-2 δ_H 5.95; **3.4**: H-1 δ_H 7.09, H-2 δ_H 5.88;) also indicated the presence of an *α,β*-unsaturated ketone. All this information indicated the highly similar structures of compounds **3.1**-**3.4**. The differences turned out to be the number of acetoxy groups in each compound as shown in Figure 3-3.

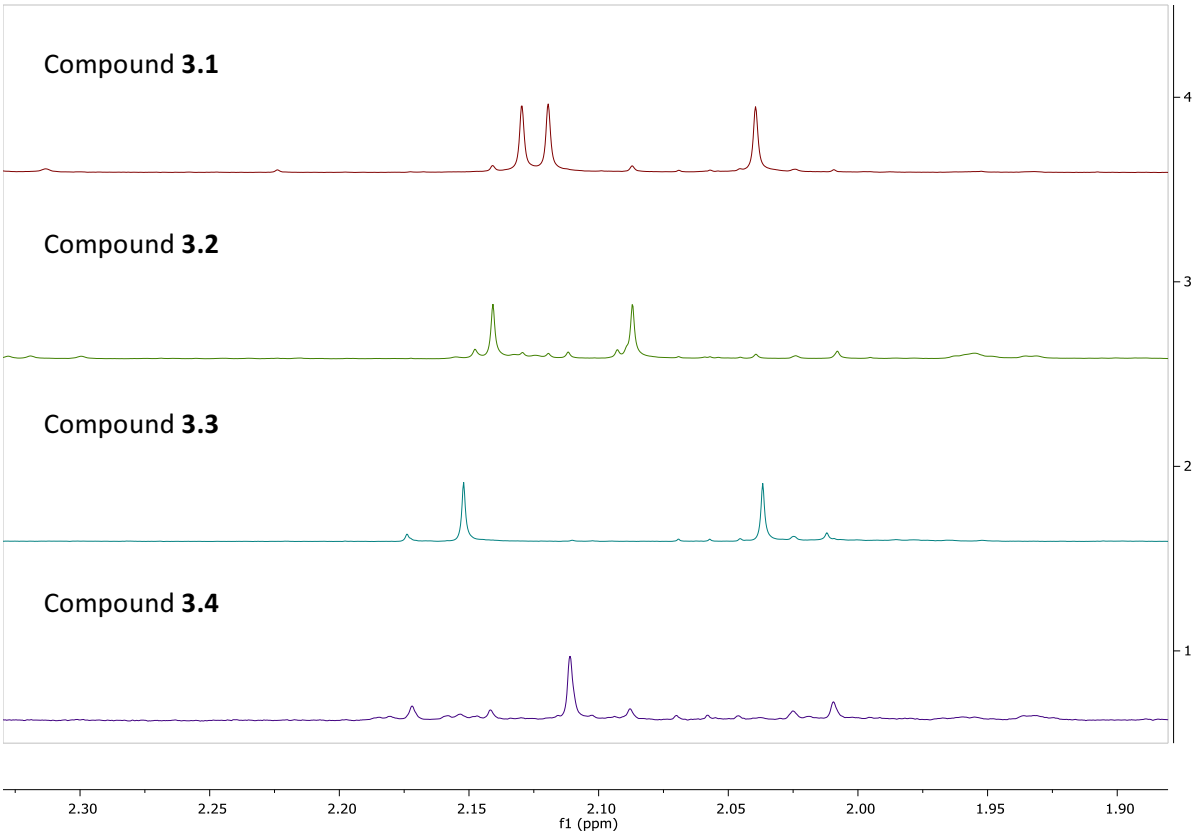

Figure 3-3. Selected range of ^{1}H NMR spectra of compounds **3.1** to **3.4** in the 1.90-2.30 ppm range.

The protons with signals at δ_H 5.38, 4.92 and 5.80 were assigned as H-6, H-7 and H-11, respectively, in the structure of compound **3.1**. In the ^{1}H NMR spectrum of compound **3.2**, the remaining signal of H-7 (δ_H 4.59) and H-11 (δ_H 5.80) and the missing signal of H-6 around 5.38 indicated the absence of the 6-acetoxy group in the structure of compound **3.2**. This led to the structure of compound **3.2**, which lost one acetoxy group at position 6 compared with compound **3.1**. For compound **3.3**, signals for two acetoxy groups appeared in its ^{1}H NMR spectrum, and the remaining proton signal for H-6 (δ_H 5.29), H-7 (δ_H 4.89), and the replacement of the proton signal at δ_H 5.80 for H-11 with signals for two protons at around 1.8 ppm indicated the absence of the 11-acetoxy group in the structure, compared with compound **3.1**. For compound **3.4**, a signal for only one acetoxy groups remained in its ^{1}H NMR spectrum, and signals for both H-6 around δ_H

5.38, and H-11 around δ_H 5.80 were missing. This led to the structure of compound **3.4**, with only one acetoxy group remaining in the position 7.

In summary, compounds **3.1** to **3.4** had very similar structures. Compound **3.4** is known as gedunin, with only one acetoxy group on position 7.[12] Compounds **3.1** to **3.3** are thus gedunin derivatives. Compared with compound **3.4**, compound **3.3**[15] had an additional acetoxy group at position 6, and compound **3.2**[11] had an additional acetoxy group at position 11, and compound **3.1**[11] had two additional acetoxy groups at both positions 6 and 11. Their absolute stereochemistry were determined by comparing their specific rotation with those in the literature. The specific rotation of compound **3.2** is $[\alpha]_D$ +52º (c 0.1, MeOH), while the literature value is $[\alpha]_D$ +33º (c 0.14, MeOH). The specific rotation of compound **3.3** is $[\alpha]_D$ +24º (c 0.1, MeOH), while the literature value is $[\alpha]_D$ +22.4º (c 0.26, MeOH). And the specific rotation of compound **3.4** is $[\alpha]_D$ +28º (c 0.1, MeOH), while the literature value is $[\alpha]_D$ +6.8º (c 0.32, MeOH). Although these compounds were isolated a long time ago, no complete NMR data have been reported.

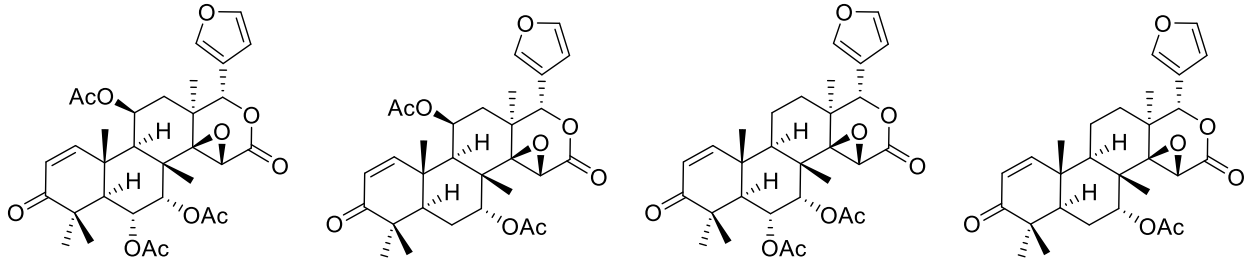

3.1 **3.2** **3.3** **3.4**

3.3 Bioactivities

The antiplasmodial activities of compounds **3.1** to **3.4** were determined against the Dd2 strain of *Plasmodium falciparum*. All four compounds showed good antiplasmodial activity, with IC_{50} values of 2.0 ± 0.3 μM, 2.1 ± 0.1 μM, 2.1 ± 0.2 μM, and 2.8 ± 0.2 μM, respectively.

Compound **3.4**, also known as gedunin, was first reported in 1960 by Akisanya et al.[12] It was then reported to have various biological activities, including antimalarial[13] and anti-inflammatory[14] activity. Various gedunin derived compounds were then isolated. 6α,11β-diacetoxygedunin (**3.1**) and 11β-acetoxygedunin (**3.2**) were reported by J. Connolly *et al.* in 1966.[11] 6α-Acetoxygedunin (**3.3**) was reported by D. Lavie et al. in 1972.[15] Compound **3.1** has been less studied and has only been reported to have antimicrobial activity,[16] so this is the first report of its antiplasmodial activity. Compounds **3.2** and **3.3** have been reported with antiplasmodial activity,[13,17] and compound **3.3** also has anti-inflammatory activity.[14]

Table 3-2. Antiplasmodial activity of compound **3.1** to **3.4**.

Compound	*P. falciparum* Dd2 strain, IC_{50} (μM)
3.1	2.0 ± 0.3
3.2	2.1 ± 0.1
3.3	2.1 ± 0.2
3.4	2.8 ± 0.2

3.4 Experimental Section

3.4.1 General Experimental Procedures

Mass spectra were measured on an Agilent 6220 LC-TOF-MS in the positive ion mode. NMR spectra were obtained in $CDCl_3$ on Bruker AVANCE 500 spectrometer. Semi-preparative HPLC was carried out on an instrument with a Shimadzu SCL-10A controller, Shimadzu LC-10AT pumps, SPD-M10A UV detector, and SEDEX 75 ELSD detector, with a semi-preparative C_{18} Varian Dynamax column (250 × 10 mm).

3.4.2 Plant Material

The wood parts of *Carapa guianensis* were collected at Groete Greek, 27 km from Bartica, Essequibo, Guyana by S. Tiwari under the auspices of the New Yourk Botanical Garden. The voucher specimen is St01017d.

3.4.3 Extraction and Isolation

Dried, powdered wood of *Carapa guianensis* (Meliaceae) was exhaustively extracted with EtOH at room temperature for 24 hours and the extract was then partitioned between aquous methanol and dichloromethane. The dichloromethane fraction was found to have antiplasmodial activity with an IC_{50} value around 3 μg/mL, and shipped to Virginia Tech as crude extract 0013102-09F. A 105 mg sample was suspended in 100 mL 90% aqueous MeOH, and then extracted with hexanes (3 × 100 mL portions) to give 20 mg of a hexanes-soluble fraction with an IC_{50} value between 5 and 10 μg/mL. The remaining materials were evaporated under vacuum and dissolved in 60% aqueous MeOH. This fraction was then extracted with dichloromethane (3 × 100 mL portions) to give 51 mg of a CH_2Cl_2–soluble fraction with IC_{50} value between 2.5 and 5 μg/mL. The residual aqueous MeOH soluble fraction was evaporated under vacuum, and yielded 29 mg of material with an IC_{50} value between 5 and 10 μg/mL. On TLC plate (silica gel developed with CH_2Cl_2 : MeOH = 20 : 1), the hexanes fraction and dichloromethane fraction shared a similar pattern and similar major compounds, which led to the combination of these two fractions prior to further purification. Around 10 mg combined fractions were applied to semi-preparative C_{18} HPLC column (10 × 250 mm) and eluted with aqueous acetonitrile from 50% to 70% over 30 minutes with a flow rate of 2.5 mL/min. Compound **3.1** (2.1 mg) was obtained at 18 min, compound **3.2** (2.7 mg) was obtained at 19 min, Compound **3.3** (1.3 mg) was obtained at 22.5 min, and compound **3.4** (0.5 mg) was obtained at 24 min.

3.4.4 Antimalarial Bioassays

The antimalarial bioassays were conducted in Dr. Cassera's group by the same procedures as described in chapter 2.

3.4.5 Spectroscopic Properties

Compound **3.1**: oil; $[\alpha]_D$ +88º (c 0.1, MeOH), [lit.[11] $[\alpha]_D$ +58º (c 0.13, MeOH)]; IR (film) ν_{max} 1739, 1674, 1218, 1032, 752 cm^{-1}; ^1H NMR (500 MHz, $CDCl_3$) see Table 3-1; HRESIMS *m/z* 599.2490 $[M+H]^+$ (calcd for $C_{32}H_{38}O_{11}^+$, 599.2448).

Compound **3.2**: oil; $[\alpha]_D$ +52º (c 0.1, MeOH), [lit.[11] $[\alpha]_D$ +33º (c 0.14, MeOH)]; ^1H NMR (500 MHz, $CDCl_3$) δ_H 7.13 (1H, d, *J* = 10.1, H-1), δ_H 5.92 (1H, d, *J* = 10.1, H-2), δ_H 4.59 (1H, t, *J* = 2.6, H-7), δ_H 2.53 (1H, d, *J* = 5.0, H-9), δ_H 5.80 (1H, dt, *J* = 5.0, 5.9, H-11), δ_H 1.56 (1H, m, H-12), δ_H 2.32 (1H, dd, *J* = 4.4, 9.7, H-12'), δ_H 3.59 (1H, s, H-15), δ_H 5.61 (1H, s, H-17), δ_H 1.37 (3H, s, H-18), δ_H 1.06 (3H, s, H-19), δ_H 1.46 (3H, s, H-20), δ_H 1.56 (3H, s, H-21), δ_H 1.24 (3H, s, H-22), δ_H 7.40 (1H, dd, *J* = 1.7, 0.8, H-24), δ_H 7.41 (1H, dd, *J* = 1.7, 1.7, H-25), δ_H 6.33 (1H, dd, *J* = 0.8, 1.7, H-26), δ_H 2.09 (3H, s, $OCOCH_3$), δ_H 2.14 (3H, s, $OCOCH_3$); HRESIMS *m/z* 541.2438 $[M+H]^+$ (calcd for $C_{30}H_{36}O_9^+$, 541.2393).

Compound **3.3**: oil; $[\alpha]_D$ +24º (c 0.1, MeOH), [lit.[15] $[\alpha]_D$ +22.4º (c 0.26, MeOH)]; ^1H NMR (500 MHz, $CDCl_3$) δ_H 7.08 (1H, d, *J* = 10.1, H-1), δ_H 5.95 (1H, d, *J* = 10.1, H-2), δ_H 2.54 (1H, d, *J* = 12.4, H-5), δ_H 5.29 (1H, dd, *J* = 2.6, 12.4, H-6), δ_H 4.89 (1H, d, *J* = 2.6, H-7), δ_H 2.54 (1H, m, H-9), δ_H 3.61 (1H, s, H-15), δ_H 5.62 (1H, s, H-17), δ_H 1.25 (3H, s, H-18), δ_H 1.17 (3H, s, H-19), δ_H 1.26 (3H, s, H-20), δ_H 1.27 (3H, s, H-21), δ_H 1.21 (3H, s, H-22), δ_H 7.41 (1H, m, H-24), δ_H 7.41 (1H, m, H-25), δ_H 6.33 (1H, brs, H-26), δ_H 2.04 (3H, s, $OCOCH_3$), δ_H 2.15 (3H, s, $OCOCH_3$); HRESIMS *m/z* 541.2487 $[M+H]^+$ (calcd for $C_{30}H_{36}O_9^+$, 541.2393).

Compound **3.4**: oil. $[\alpha]_D$ +28º (c 0.1, MeOH), [lit.[12] $[\alpha]_D$ +6.8º (c 0.32, MeOH)]; ^{1}H NMR (500 MHz, $CDCl_3$) δ_H 7.09 (1H, d, J = 10.1, H-1), δ_H 5.88 (1H, d, J = 10.1, H-2), δ_H 4.56 (1H, m, H-7), δ_H 3.53 (1H, s, H-15), δ_H 5.62 (1H, s, H-17), δ_H 1.16 (3H, s, H-18), δ_H 1.07 (3H, s, H-19), δ_H 1.22 (3H, s, H-20), δ_H 1.26 (3H, s, H-21), δ_H 1.07 (3H, s, H-22), δ_H 7.42 (1H, dd, J = 1.7, 0.8, H-24), δ_H 7.42 (1H, dd, J = 1.7, 1.7, H-25), δ_H 6.34 (1H, dd, J = 0.8, 1.7, H-26), δ_H 2.11 (3H, s, $OCOCH_3$); HRESIMS *m/z* 483.2381 $[M+H]^+$ (calcd for $C_{28}H_{34}O_7^+$, 483.2338).

3.5 Supporting Information

3.5.1 ^{1}H NMR spectrum of 3.1 ($CDCl_3$, 500 MHz)

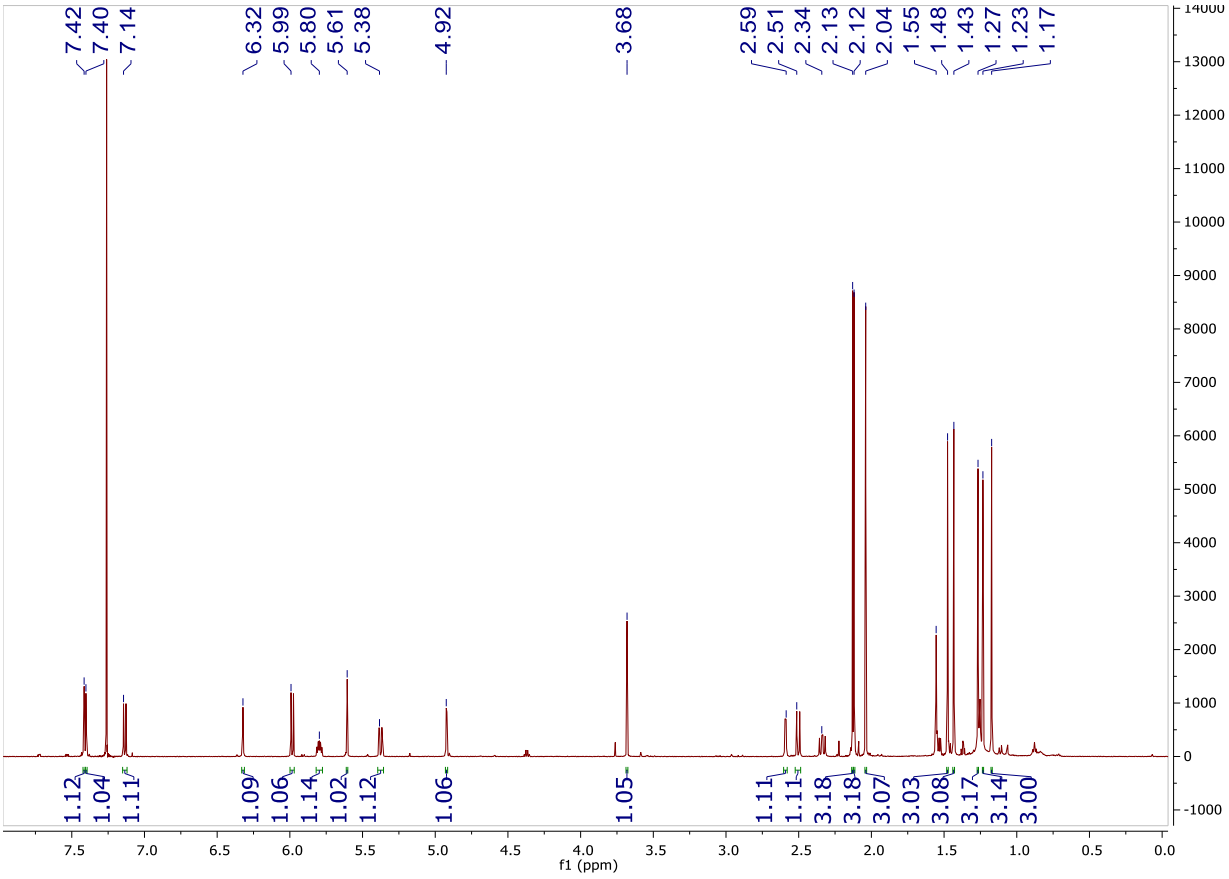

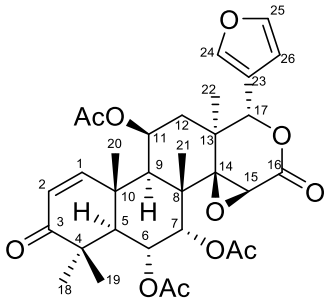

3.5.2 ^{13}C NMR spectrum of 3.1 ($CDCl_3$, 125 MHz)

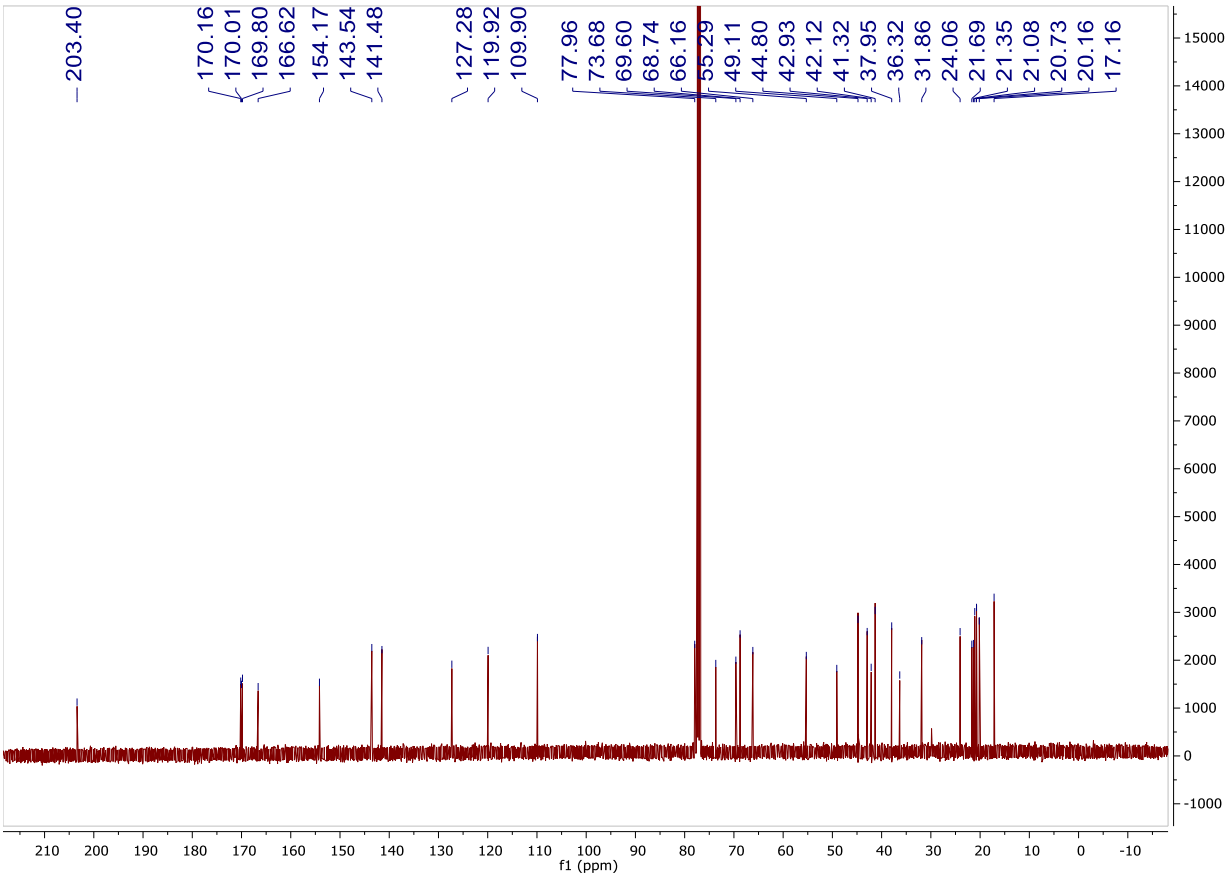

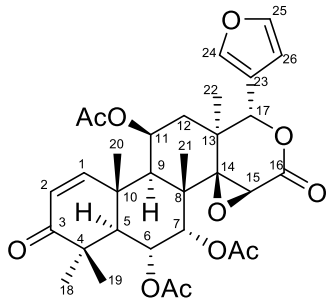

3.5.3 COSY spectrum of 3.1 ($CDCl_3$, 500 MHz)

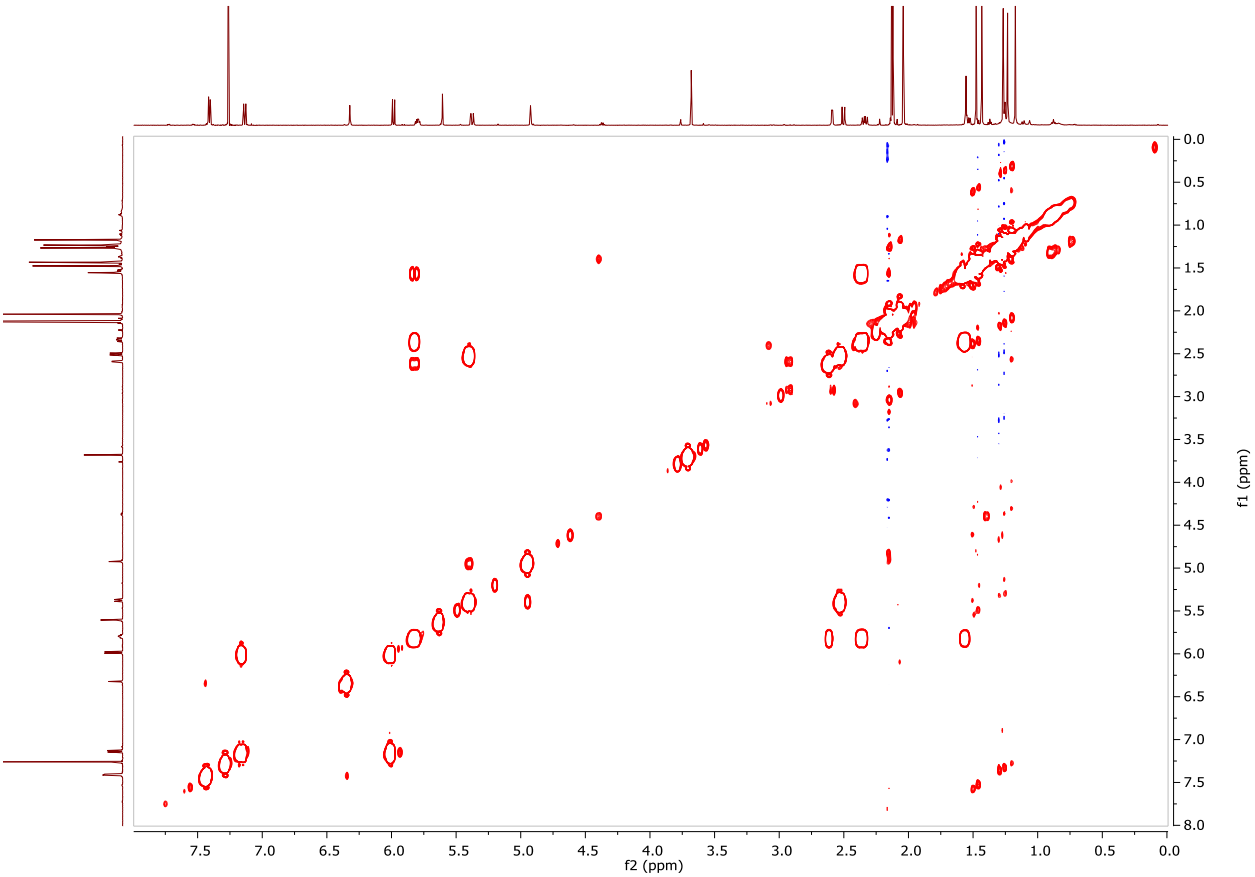

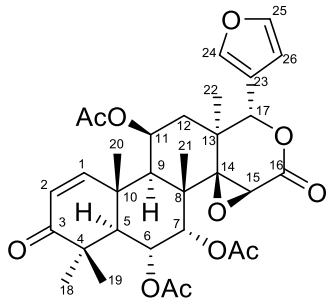

3.5.4 HSQC spectrum of 3.1 ($CDCl_3$, 500 MHz, 125 MHz)

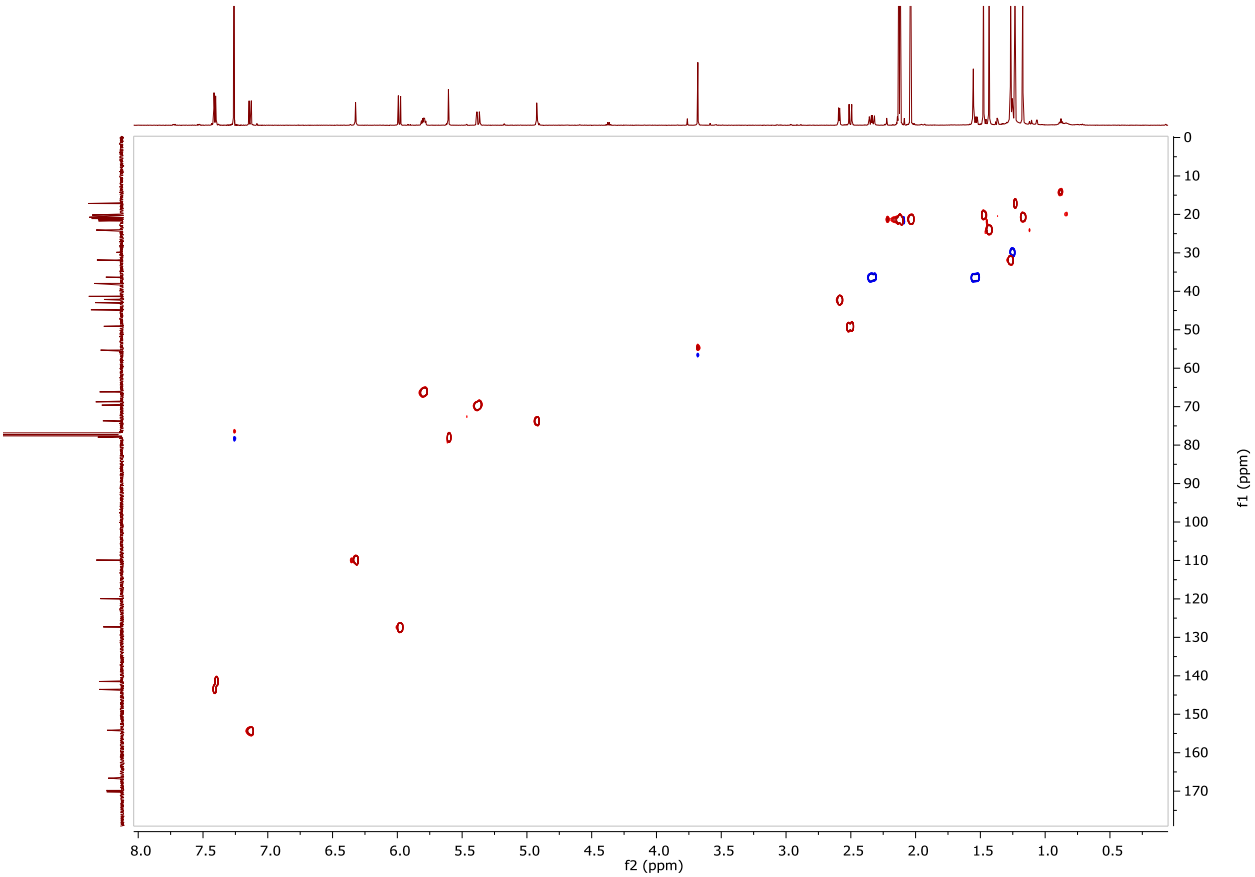

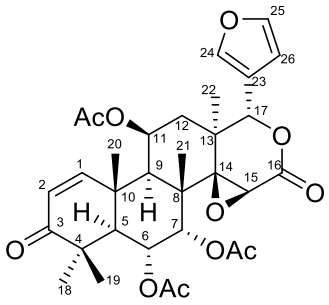

3.5.5 HMBC spectrum of 3.1 ($CDCl_3$, 500 MHz, 125 MHz)

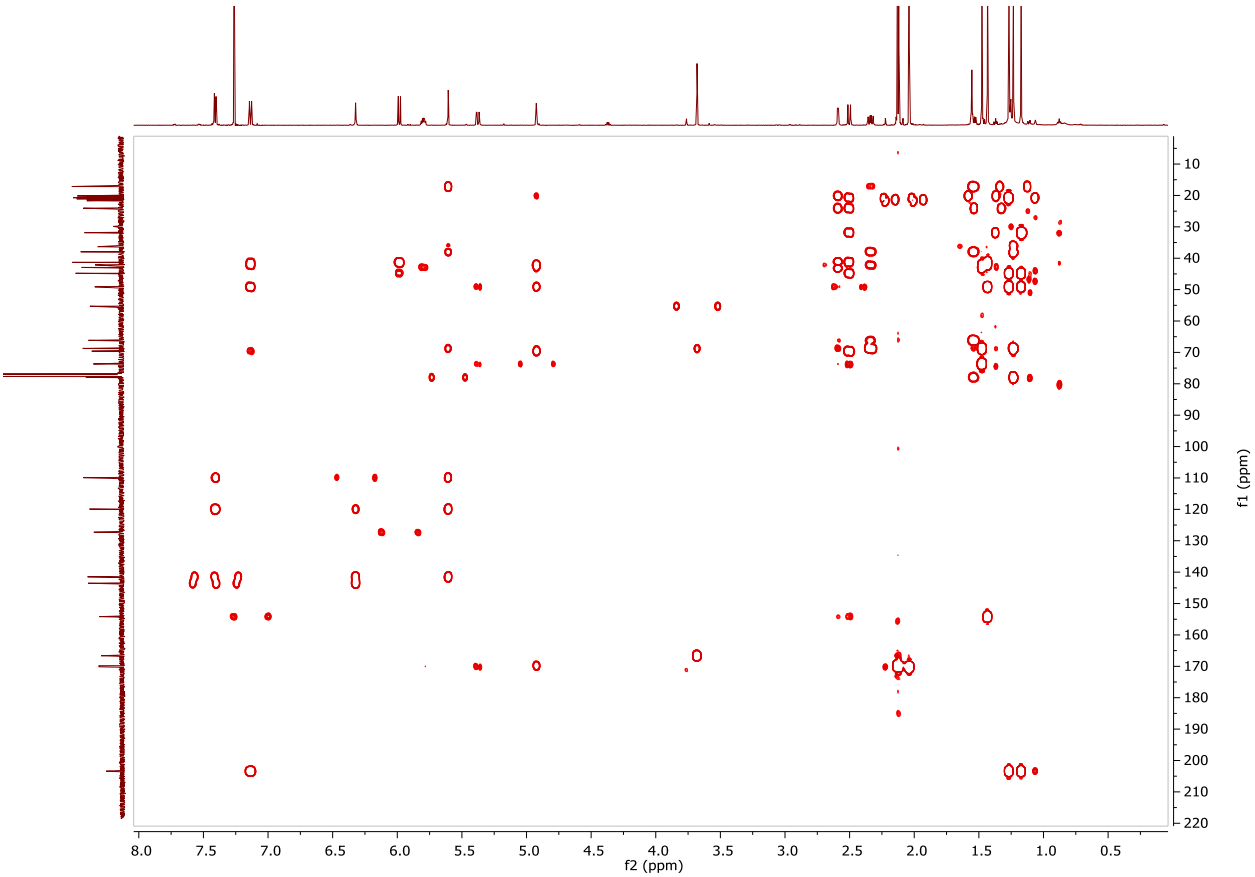

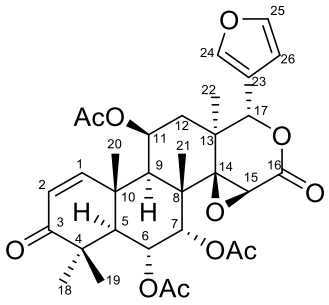

3.5.6 NOESY spectrum of 3.1 ($CDCl_3$, 500 MHz)

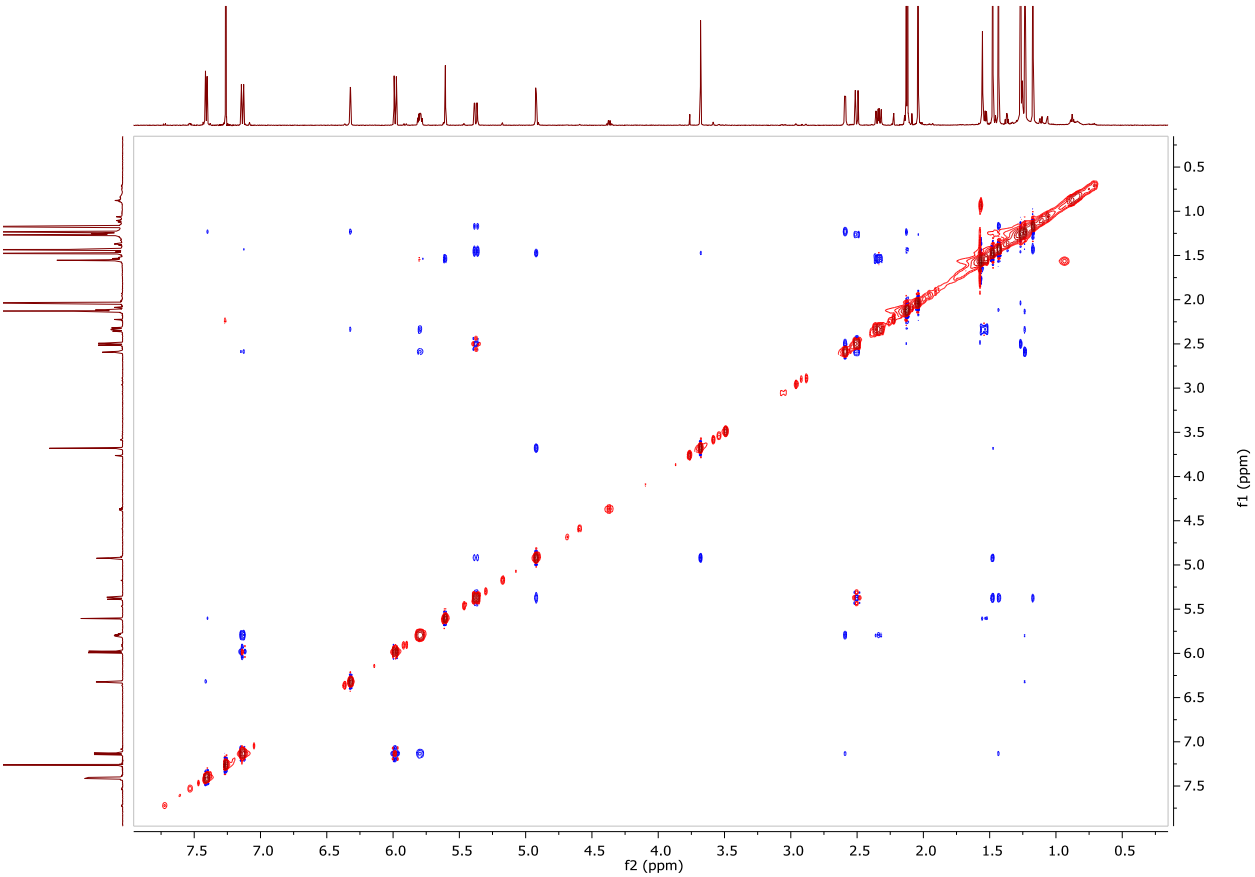

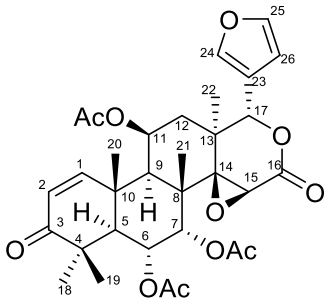

3.5.7 ^{1}H NMR spectrum of 3.2 ($CDCl_3$, 500 MHz) not pure

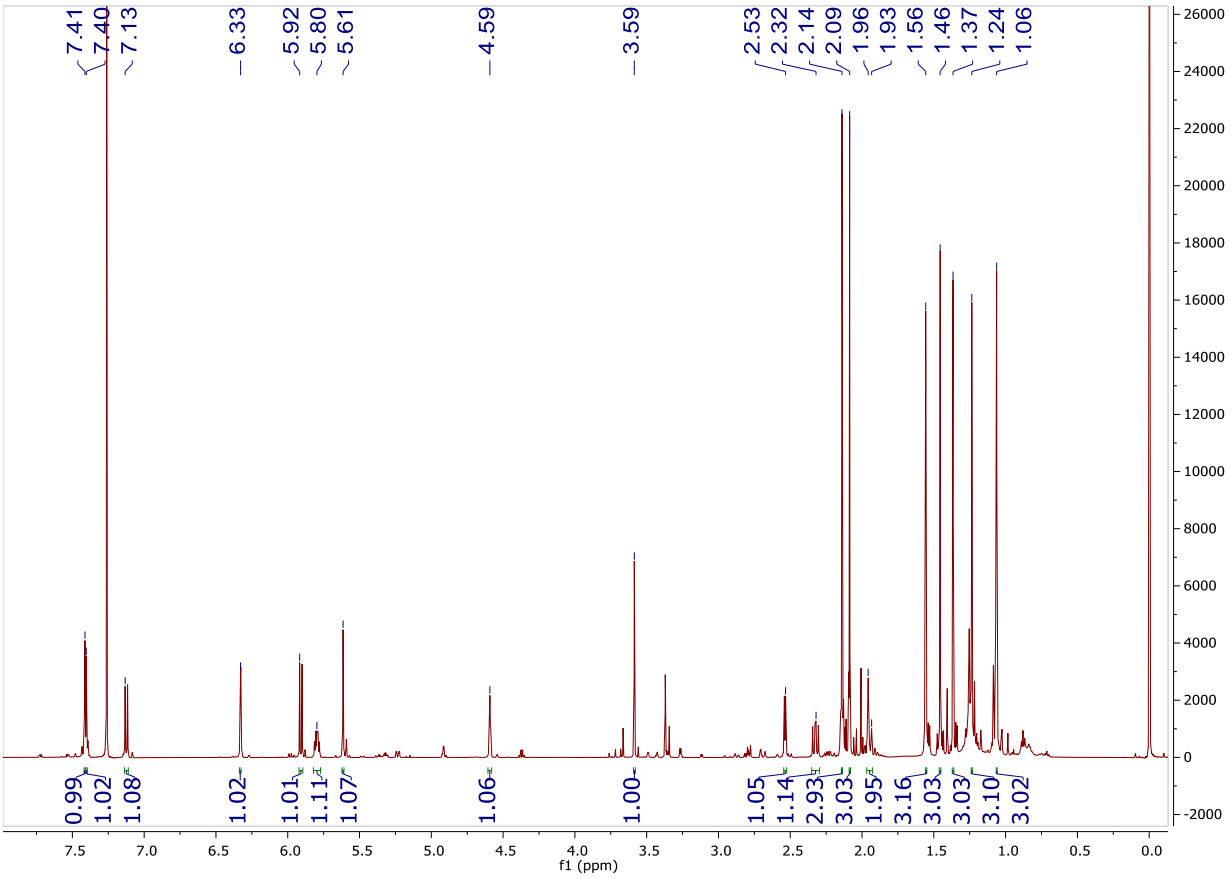

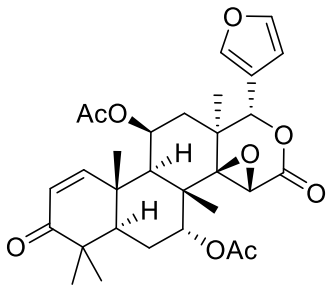

3.5.8 ^{1}H NMR spectrum of 3.3 ($CDCl_3$, 500 MHz) not pure

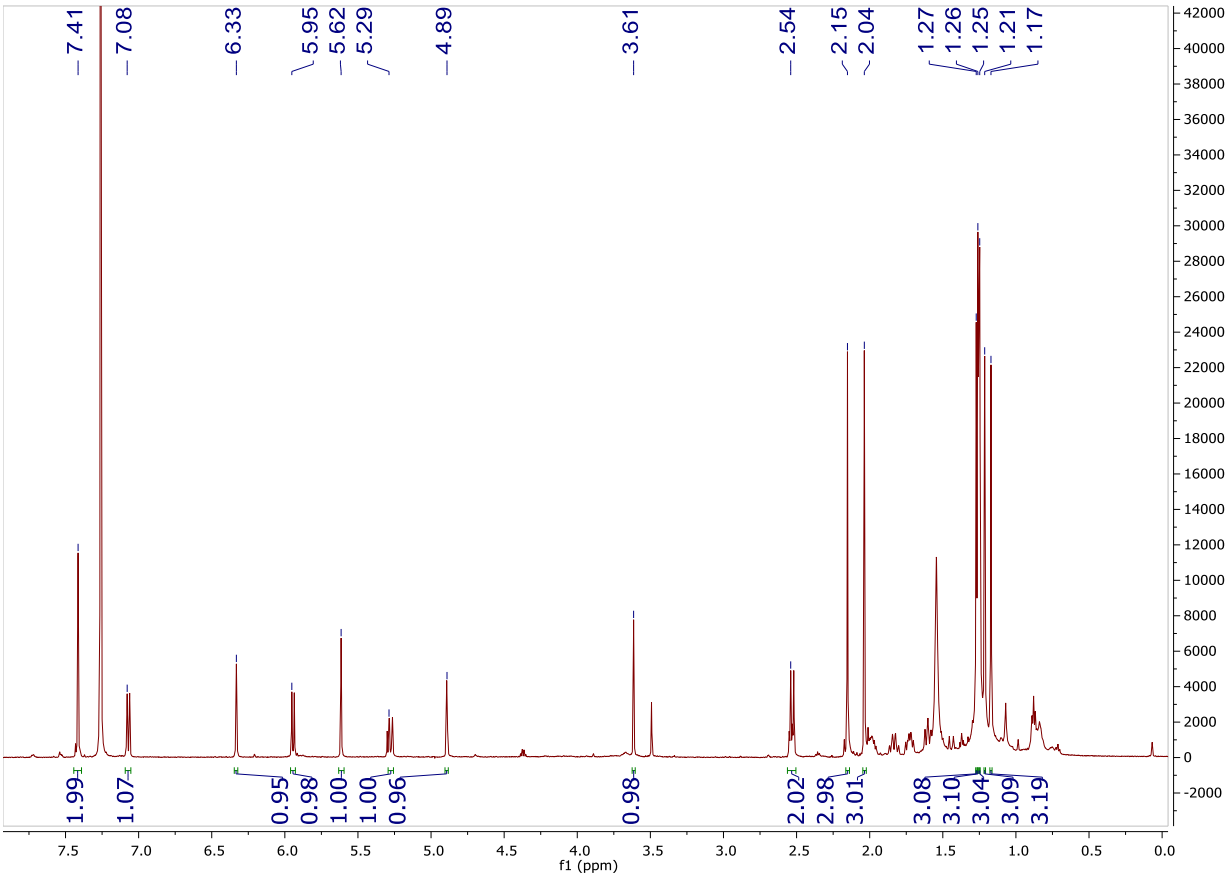

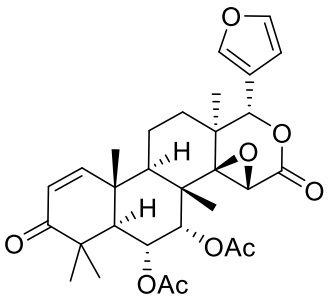

3.5.9 ^{1}H NMR spectrum of 3.4 ($CDCl_3$, 500 MHz) not pure

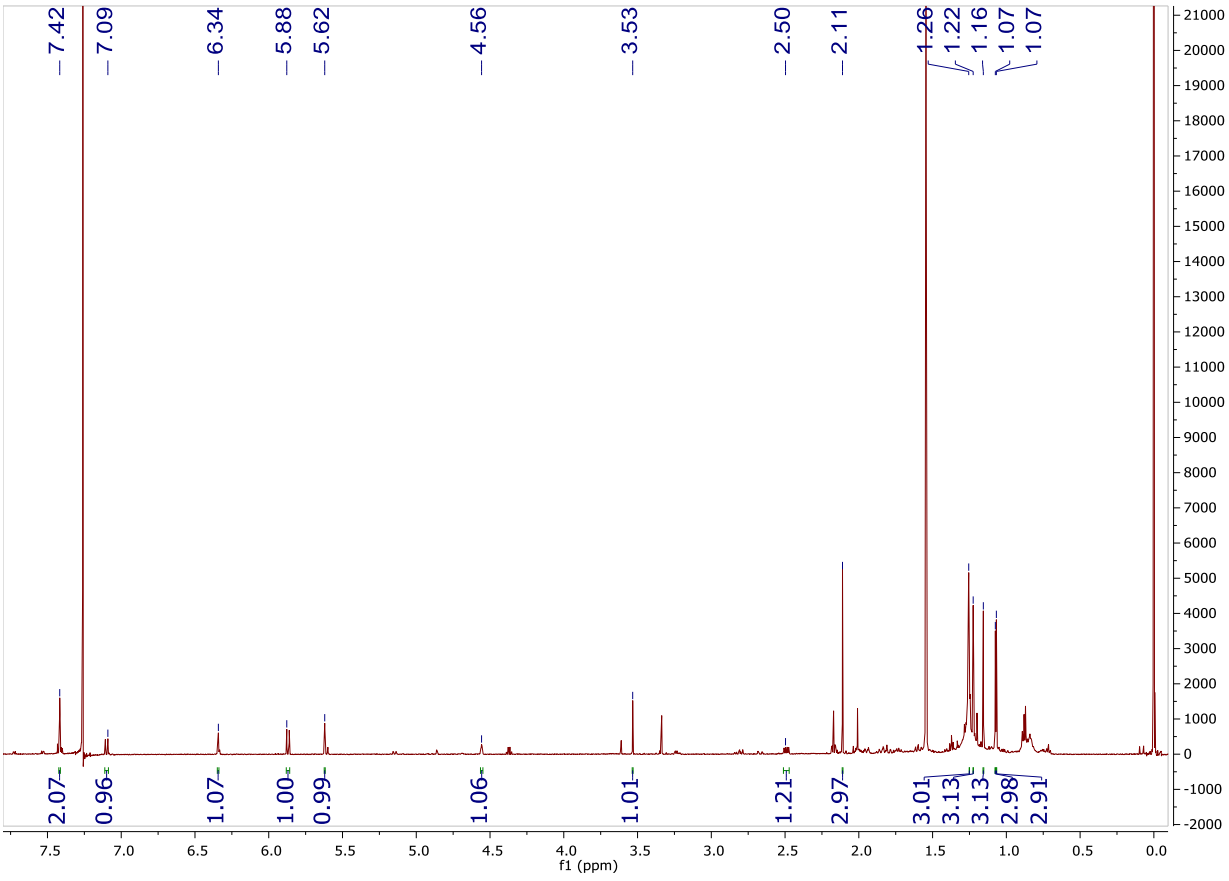

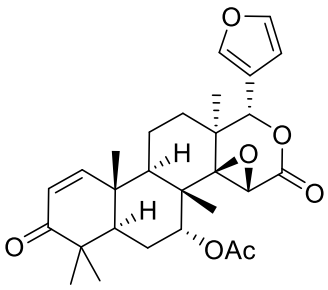

3.6 References

(1) Miyake, T.; Ishimoto, S.; Ishimatsu, N.; Higuchi, K.; Minoura, K.; Kikuchi, T.; Yamada, T.; Muraoka, O.; Tanaka, R. Carapanolides T-X from *Carapa guianensis* (Andiroba) Seeds. *Molecules* **2015**, *20*, 20955–20966.

(2) Sakamoto, A.; Tanaka, Y.; Yamada, T.; Kikuchi, T.; Muraoka, O.; Ninomiya, K.; Morikawa, T.; Tanaka, R. Andirolides W--Y from the Flower Oil of Andiroba (*Carapa guianensis*, Meliaceae). *Fitoterapia* **2015**, *100*, 81–87.

(3) Penido, C.; Costa, K. A.; Pennaforte, R. J.; Costa, M. F. S.; Pereira, J. de F. G.; Siani, A. C.; Henriques, M. das G. M. de O. Anti-Allergic Effects of Natural Tetranortriterpenoids Isolated from *Carapa guianensis* Aublet on Allergen-Induced Vascular Permeability and Hyperalgesia. *Inflamm. Res.* **2005**, *54*, 295–303.

(4) Bickii, J.; Njifutie, N.; Foyere, J. A.; Basco, L. K.; Ringwald, P. In Vitro Antimalarial Activity of Limonoids from *Khaya grandifoliola* C.D.C (Meliaceae). *J. Ethnopharmacol.* **2000**, *69*, 27–33.

(5) Penido, C.; Conte, F. P.; Chagas, M. S. S.; Rodrigues, C. A. B.; Pereira, J. F. G.; Henriques, M. Antiinflammatory Effects of Natural Tetranortriterpenoids Isolated from *Carapa guianensis* Aublet on Zymosan-Induced Arthritis in Mice. *Inflamm. Res.* **2006**, *55*, 457–464.

(6) Ferraris, F. K.; Rodrigues, R.; da Silva, V. P.; Figueiredo, R.; Penido, C.; das Graças, M. O. Modulation of T Lymphocyte and Eosinophil Functions in Vitro by Natural Tetranortriterpenoids Isolated from *Carapa guianensis* Aublet. *Int. Immunopharmacol.* **2011**, *11*, 1–11.

(7) Júnior, R. N. C. M.; Dolabela, M. F.; da Silva, M. N.; Póvoa, M. M.; Maia, J. G. S.

Antiplasmodial Activity of the Andiroba (*Carapa guianensis* Aubl., Meliaceae) Oil and Its Limonoid-Rich Fraction. *J. Ethnopharmacol.* **2012**, *142*, 679–683.

(8) Matsui, Y.; Kikuchi, T.; Inoue, T.; Muraoka, O.; Yamada, T.; Tanaka, R. Carapanolides J–L from the Seeds of *Carapa guianensis* (Andiroba) and Their Effects on LPS-Activated NO Production. *Molecules* **2014**, *19*, 17130-17140.

(9) Dioum, M. D.; Seck, M.; Silvestre, V.; Planchat, A.; Loquet, D.; Lohard, S.; Barille-Nion, S.; Remaud, G. S.; Robins, R. J.; Tea, I. A Ring-D-Seco-Tetranortriterpenoid from Seeds of *Carapa procera* Active against Breast Cancer Cell Lines. *Planta Med.* **2016**, *82*, 967-972.

(10) Inoue, T.; Matsui, Y.; Kikuchi, T.; Yamada, T.; In, Y.; Muraoka, O.; Sakai, C.; Ninomiya, K.; Morikawa, T.; Tanaka, R. Carapanolides M--S from Seeds of Andiroba (*Carapa guianensis*, Meliaceae) and Triglyceride Metabolism-Promoting Activity in High Glucose-Pretreated HepG2 Cells. *Tetrahedron* **2015**, *71*, 2753–2760.

(11) Connolly, J. D.; McCrindle, R.; Overton, K. H.; Feeney, J. Tetranortriterpenoids—II: Heartwood Constituents of *Carapa guianensis* Aubl. *Tetrahedron* **1966**, *22*, 891–896.

(12) Akisanya, A.; Bevan, C. W. L.; Hirst, J.; Halsall, T. G.; Taylor, D. A. H. 758. West African Timbers. Part III. Petroleum Extracts from the Genus *Entandrophragma. J. Chem. Soc.* **1960**, 3827–3829.

(13) Pereira, T. B.; e Silva, L. F. R.; Amorim, R. C. N.; Melo, M. R. S.; de Souza, R. C. Z.; Eberlin, M. N.; Lima, E. S.; Vasconcellos, M. C.; Pohlit, A. M. In Vitro and in Vivo Anti-Malarial Activity of Limonoids Isolated from the Residual Seed Biomass from *Carapa guianensis* (Andiroba) Oil Production. *Malar. J.* **2014**, *13*, 317-325.

(14) das Graças Henriques, M.; Penido, C. The Therapeutic Properties of *Carapa guianensis*.

Curr. Pharm. Des. **2014**, *20*, 850–856.

(15) Lavie, D.; Levy, E. C.; Zelnik, R. The Constituents of *Carapa guianensis* Aubl. and Their Biogenetic Relationship. *Bioorg. Chem.* **1972**, *2*, 59–64.

(16) Miyakado, M.; Kato, T.; Ohno, N.; Koshimizu, K. Alkaloids of *Urginea altissima* and their Antimicrobial Activity against *Phytophthora capsici*. *Phytochemistry* **1975**, *14*, 2717.

(17) Bray, D. H.; Warhurst, D. C.; Connolly, J. D.; O'Neill, M. J.; Phillipson, J. D. Plants as Sources of Antimalarial Drugs. Part 7. Activity of Some Species of Meliaceae Plants and their Constituent Limonoids. *Phytother. Res.* **1990**, *4*, 29–35.

Chapter 4. Identification of Inactive Compounds from Other Extracts

4.1 Introduction

The compounds mentioned in this chapter were isolated from extracts that had bioactivity in initial screening. But the isolated fractions or compounds were not active, or the structures of isolated compounds could not be completely elucidated.

4.2 Inactive Terpenoid from *Erica maesta* (Ericaceae)

4.2.1 Introduction to *Erica maesta* (Ericaceae)

Erica is a genus in the family Ericaceae. Members of this genus are evergreen shrubs, and can grow from 20 to 150 cm in height. Their leaves are small and needle-like, and their flowers are axillary. The seeds are small, and can survive in the soil for decades. Plants of the genus are widespread in South Africa and parts of Africa, Madagascar, the Mediterranean, and Europe. One inactive compound **4.1** was isolated.

Figure 4-1. Image of Ericaceae *Erica maesta*, Photography by Ando Ramahefaharivelo, from http://www.tropicos.org/Image/100225640

The *Erica* genus has not been extensively studied, and only a few bioactive compounds have been isolated from it. As one example, Bitchagno *et al*. reported a biflavonoid (Compound **4.6**) with moderate antibacterial activity.[1]

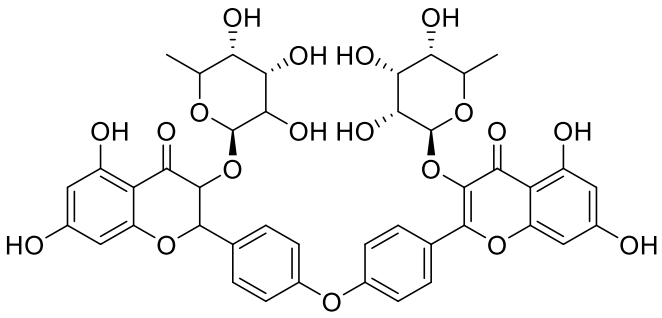

4.6

4.2.2 Isolation of Compound 4.1

The crude extract of *Erica maesta* was reported to have moderate antimalarial activity against chloroquine resistant *Plasmodium falciparum* strain Dd2. The liquid-liquid partition of 500 mg crude extract yielded 30.2 mg of a hexanes fraction with an IC_{50} value between 5 and 10 μg/mL, 70.7 mg of a dichloromethane-soluble fraction with an IC_{50} value greater than 10 μg/mL, and 455.5 mg of an inactive aqueous methanol fraction. The most active hexanes fraction was applied to a Si open column, and five fractions were obtained. TLC evaluation of these fractions showed that the last fraction with IC_{50} value around 10 μg/mL contained one major compound. Separation on a second Si open column yielded compound **4.1**.

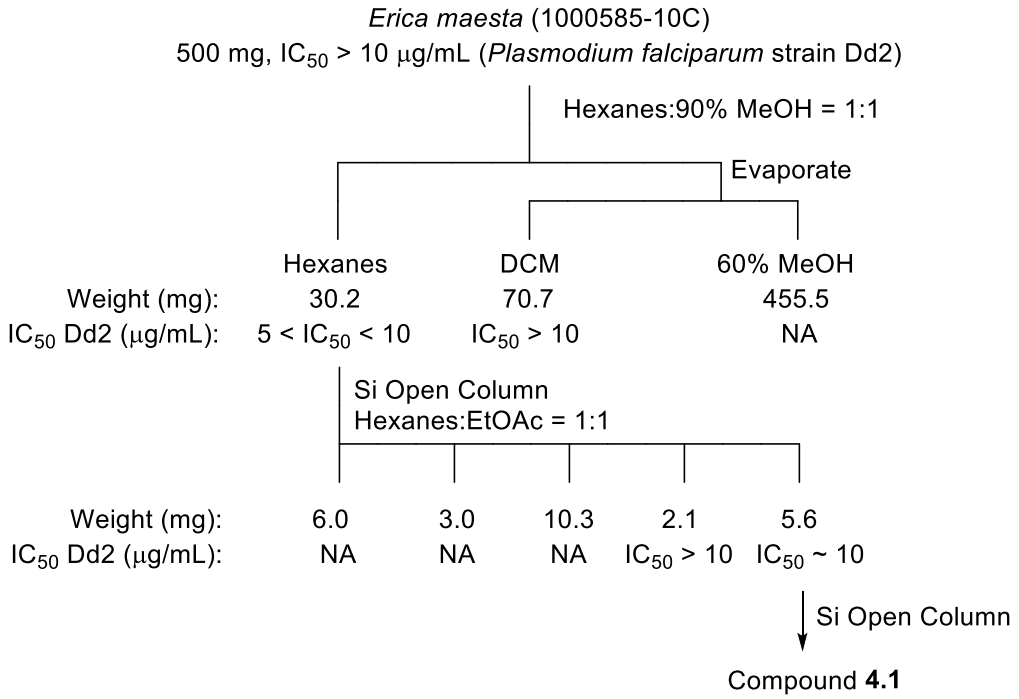

Figure 4-2. Bioassay-guided Separation of *Erica maesta*.

4.2.3 Structure Elucidation of Compound 4.1

Compound **4.1** had the molecular formula $C_{30}H_{48}O$ based on its HRESIMS ion at *m/z* 425.3783 $[M+H]^+$, indicating 7 degrees of unsaturation.

The ^1H NMR spectrum of compound **4.1** contained signals for seven methyl groups with resonances at δ_H 0.69, δ_H 0.93, δ_H 0.95, δ_H 1.02, δ_H 1.02, δ_H 1.07, δ_H 1.67. Since 30 carbons existed in the formula, these data are consistent with compound **4.1** being a triterpene. Signals for one terminal double bond at δ_H 4.67 and δ_H 4.69 were also observed. The ^{13}C NMR spectrum had a signal at δ_C 218.2 for a carbonyl group. Since **4.1** has seven degrees of unsaturation, it must be pentacyclic. Analysis of HMBC and COSY correlations led to the planar structure of **4.1**.

Compound **4.1** was previously isolated from a *Mallotus* species by Hui *et al.* in 1976,[2] but complete NMR spectra have not been reported. The partial NMR data reported by Chakravarty *et al.* indicated that the chemical shifts of the seven methyl groups were δ_H 0.692, δ_H 0.937, δ_H 0.952,

δ_H 1.022, δ_H 1.028, δ_H 1.078, δ_H 1.678, and the terminal double bond protons had signals at δ_H 4.698.[3] All these data matched well with my ^{1}H NMR spectrum. Also the absolute stereochemistry was determined based on the comparison of the specific rotation of **4.1** ($[\alpha]_D$ +10º (c 0.1, CH_2Cl_2)) with that of the literature compound ($[\alpha]_D$ +24.09º (c 0.498, CH_2Cl_2)).

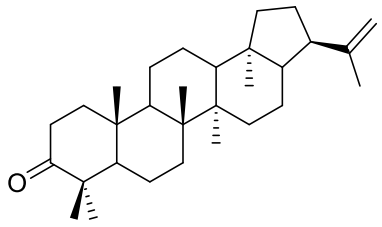

4.1

Table 4-1. NMR spectroscopic data of **4.1**.

	Compound **4.1**		
Position	δ_C, (J in Hz)[b]	δ_H, (J in Hz)[a]	HMBC
1	39.7, CH_2	1.93, m	3, 5, 10, 25
		1.56, m[c]	
2	34.3, CH_2	2.50, m	1, 3, 10
		2.41, m	1, 3, 10
3	218.2, C		
4	47.5, C		
5	55.0, CH	1.43, m[c]	
6	32.8, CH_2	1.38, m[c]	
		1.53, m[c]	
7	32.8, CH_2	1.46, m[c]	
		1.31, m[c]	
8	41.8, C	1.53, m[c]	
9	49.9, CH	1.24, m[c]	
10	37.0, C		
11	21.8, CH_2	1.43, m[c]	
		1.38, m[c]	
12	21.3, CH_2	1.62, m	
		1.38, m[c]	
13	49.0, CH	1.38, m[c]	
14	26.7, C		
15	24.1, CH_2	1.56, m[c]	
		1.31, m[c]	
16	21.0, CH_2	1.84, m	17, 18, 21
		1.38, m[c]	
17	54.0, CH	1.17, m[c]	
18	44.4, C		
19	40.4, CH_2	1.50, m[c]	
		1.25, m[c]	
20	27.5, CH_2	1.55, m[c]	
		1.30, m[c]	
21	47.5, CH	2.25, m	17, 20, 22, 29, 30
22	148.2, C		
23	19.9, CH_3	1.07, s	3, 4, 5, 24
24	21.3, CH_3	1.02, s	3, 4, 5, 6, 23
25	15.9, CH_3	0.95, s	1, 9, 10
26	16.6, CH_3	1.02, s	7, 8, 9, 14
27	16.7, CH_3	0.93, s	8, 13, 14
28	15.3, CH_3	0.69, s	13, 17, 18, 19
29	109.6, CH_2	4.67, brs	21, 22, 30
		4.69, brs	21, 22, 30
30	19.8, CH_3	1.67, s	21, 22, 29

[a]Data(δ) measured at 500 MHz; s = singlet, d = doublet, m = multiplet. *J* values are in Hz and are omitted if the signals overlapped as multiplets.
[b]Data(δ)measured at 125 MHz.
[c]Overlapping signals

4.2.4 Bioactivities

Compound **4.1** is a very nonpolar compound, which can only dissolve in low polarity solvents such as hexanes and dichloromethane. It is only very sparingly soluble in the antimalarial assay solvent, aqueous DMSO, which prevented it from being tested in this antimalarial assay. There are no reported bioactivity data for compound **4.1** in the literature.

4.3 Antiplasmodial Cerebrosides from *Hohenbergia antillana* (Bromeliaceae)

4.3.1 Introduction to *Hohenbergia antillana* (Bromeliaceae)

Hohenbergia is a genus of the Bromeliaceae family and the Bromelioideae subfamily. It is native to India and South America, including Colombia, Venezuela and Brazil. This genus has not been extensively studied, and no compounds have been isolated and reported until now. In my work, two known cerebrosides with tentative structures **4.2** and **4.3**, and with weak antiplasmodial activity, and two inactive glyceroglycolipids with tentative structure **4.4** and **4.5** have been isolated from this plant. Because the obtained information was not enough to determine the length of each chain and the position of the double bonds in the structures of **4.2** to **4.5**, and because the observed bioactivities were weak or non-existant, the extensive extra work needed to establish the exact structures was not carried out. As a result, the assigned structures are only tentative.

Figure 4-3. Image of *Hohenbergia* plant. Photography by David Stang, from http://www.tropicos.org/Image/100114400

4.3.2 Isolation of Compounds 4.2 to 4.5

The crude extract of *Hohenbergia antillana* was reported to have good antiplasmodial activity against chloroquine resistant *Plasmodium falciparum* strain Dd2, with an IC_{50} of 1.25 μg/mL. After liquid-liquid partition of about 1.3 g crude extract, 219 mg of a hexanes fraction, 395 mg of a dichloromethane fraction and 705 mg of an aqueous methanol fraction were produced. The dichloromethane fraction displayed the highest antimalarial activity with an IC_{50} value between 1.25 and 2.5 μg/mL. This fraction was further separated on a diol open column to yield nine fractions. Fraction 8 was the most active one with an IC_{50} value much less than 1.25 μg/mL. This fraction was applied to a reversed phase C_{18} HPLC column, and four known compounds were isolated from this procedure. Compound **4.2** had a retention time of 25.5 minutes, compound **4.3** had a retention time of 28 minutes, compound **4.4** had a retention time of 21 minutes, and compound **4.5** had a retention time of 23 minutes. But the severe loss of antiplasmodial activity was observed.

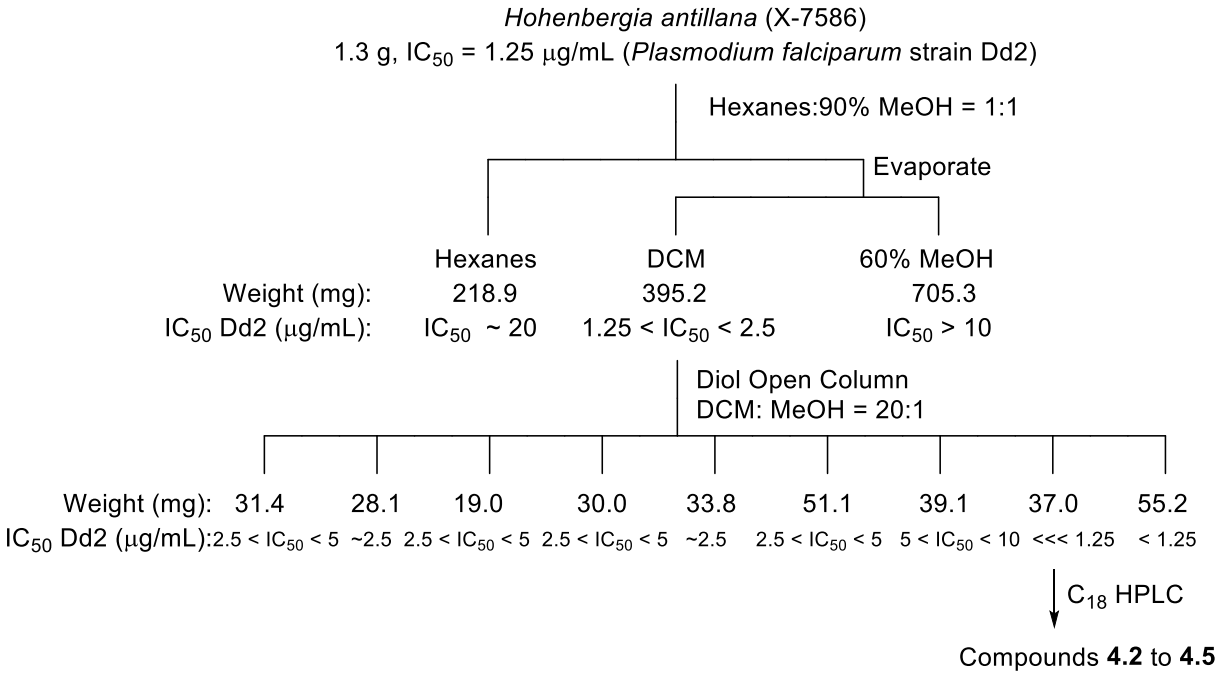

Figure 4-4. Bioassay-guided Separation of *Hohenbergia antillana*.

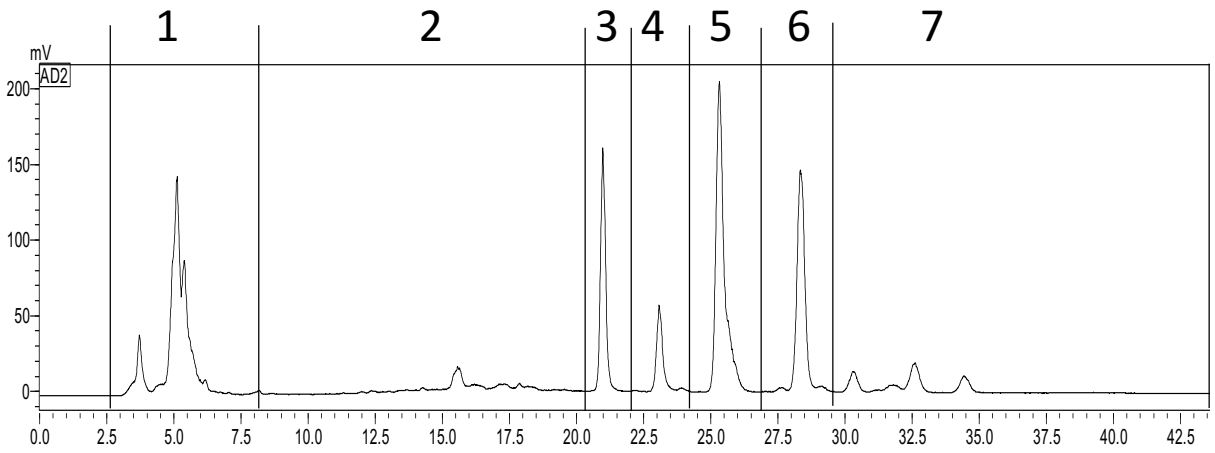

Fraction	1	2	3 compound **4.4**	4 compound **4.5**	5 compound **4.2**	6 compound **4.3**	7
IC_{50} (μg/mL)	> 10	NA	NA	NA	5 < x < 10	5 < x < 10	NA

Figure 4-5. HPLC Chromatogram (ELSD) of compound **4.2** to **4.5**.

4.3.3 Structure Elucidation of Compound 4.2

The structure of compound **4.2** shown in this chapter is a tentative structure. Since no experiments were conducted to determine the length of each chain and the position of the double bonds, the structure shown here is only one of the possible structures.

Compound **4.2** was isolated as a white powder. Its molecular formula was $C_{44}H_{83}NO_9$, based on the HRESIMS ion at *m/z* 792.5948 $[M+Na]^+$, indicating four degree of unsaturation.

In its ^1H NMR spectrum, two methyl groups were observed, and since they were triplets with coupling constants of 7.71 Hz, they were terminal methyl groups. A broad signal for the protons of long chains were observed with a chemical shift of 1.29 ppm. Based on this information, two long chains must exist in the structure of compound **4.2**.

The molecular weight of compound **4.2** is 769, an odd number, which indicated potential nitrogen atom in the structure. The proton signal at δ_H 3.99 (H-2) was for a nitrogen bearing

methine proton. In the HMBC spectrum, H-2 (δ_H 3.99) had a correlation with carbonyl C-1′ (δ_C 178.0). All this information indicated the presence of an amide linkage.

The carbon resonances at δ_C 105.0, 75.9, 78.8, 72.2, 78.7 and 63.4, along with the proton resonances at δ_H 4.26, 3.19, 3.35, 3.27, 3.27, 3.86/3.70 showed the presence of a glucopyranose moiety. In the HSQC, anomeric proton at δ_H 4.26 (1H, d, J = 7.73 Hz, H-1′′) was correlated to the carbon signal at δ_C = 105.0. Since its carbon resonance is higher than 100 ppm, the glucoside unit was in an β-configuration.[4]

In the ^{1}H NMR spectrum, signals for four double bonds protons were observed at δ_H 5.74, δ_H 5.50 and δ_H 5.38 (2H), and since only two unsaturated degrees remain after confirming the carbonyl and glucoside units, they must be two double bonds. In the HMBC spectrum, the correlation between C-4 (δ_C 131.1) and an oxygen bearing methine CH-3 (δ_H 4.13) was observed, which indicated that one double bond was adjacent to position 3. But because of its low bioactivity and the many previous studies on this type of compound,[5,6,7,8,9] no experiments were conducted to determine the position of the second double bond.

In summary, compound **4.2** is a glycosphingolipid. The NMR data I obtained (Table 4-2) matched very well with the literature values reported by Tao *et al* for structure **4.2**.[4] Also the specific rotation of compound **4.2** ($[\alpha]_D$ -4º (c 0.1, MeOH)) is very similar with that of the literature compound ($[\alpha]_D$ -3.7º (c 0.1, MeOH)). Based all this comparison, compound **4.2** is assigned the structure shown.

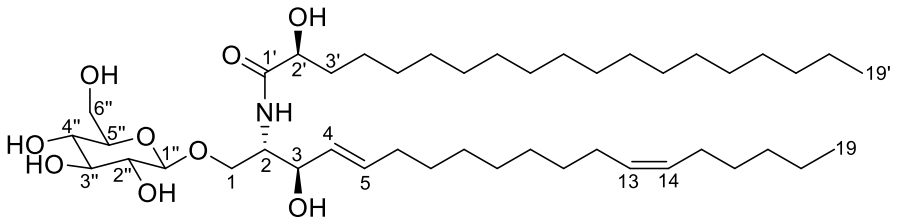

4.2

Table 4-2. NMR spectroscopic data of **4.2** and literature values.

	Compound **4.2**			Literature Value for **4.2**[4]	
Position	δ_C, type[b]	δ_H, (*J* in Hz)[a]	HMBC	δ_C	δ_H, (*J* in Hz)
1	70.5, CH_2	3.70, m	2, 3, 1′′	70.2	3.73, m
		4.13, m	2, 3, 1′′		4.08, m
2	55.0, CH	3.99, m	1, 3, 1′	55.1	3.99, m
3	72.8, CH	4.13, m	2, 4, 5	73.4	4.14, m
4	131.1, CH	5.50, m	3, 5	131.1	5.48, m
5	135.1, CH	5.74, m	4, 6	134.8	5.74, m
6	33.4, CH_2	2.08, m	5	33.6	2.05, m
7-11	30.0-31.5, CH_2	1.29, m		30.8-31.4	1.28, m
12	28.2, CH_2	2.08, m	13	28.8	2.03, m
13	131.7, CH	5.38, m	12, 14	132.5	5.36, m
14	132.3, CH	5.38, m	13, 15	131.9	5.36, m
15	28.8, CH_2	2.08, m	14	28.4	2.03, m
16-18	30.0-31.5, CH_2	1.29, m		30.8-31.4	1.28, m
19	15.3, CH_3	0.90, t (7.71)		15.0	0.89, t (7.1)
1′	178.0, C			177.7	
2′	73.6, CH	3.99, m	1′, 3′	73.6	3.99, m
3′	36.6, CH_2	1.56, m	1′, 2′	36.4	1.55, m
		1.72, m			1.72, m
4′-18′	30.0-31.5, CH_2	1.29, m		30.8-31.4	1.28, m
19′	15.2, CH_3	0.90, t (7.71)		15.0	0.89, t (7.1)
1′′	105.0, CH	4.26, d (7.73)	2′′, 1	105.2	4.27, d (7.6)
2′′	75.9, CH	3.19, m	1′′, 3′′, 4′′	75.5	3.20, m
3′′	78.8, CH	3.35, m	2′′, 4′′	78.5	3.36, m
4′′	72.2, CH	3.27, m	3′′, 5′′	72.0	3.30, m
5′′	78.7, CH	3.27, m	4′′, 6′′	78.4	3.28, m
6′′	63.4, CH_2	3.86, m	5′′	63.2	3.86, dd (12.0,
		3.70, m	5′′		3.67, dd (12.0,

[a]Data(δ) measured at 500 MHz; s = singlet, d = doublet, m = multiplet. *J* values are in Hz and are omitted if the signals overlapped as multiplets.
[b]Obtained from HMBC.

4.3.4 Structure Elucidation of Compounds 4.3 to 4.5

The ^{1}H NMR spectra of compounds **4.2** and **4.3** were very similar, which indicated that they had similar structures. Comparison of the molecular weights based on the HRESIMS data indicated that compound **4.2** had the formula $C_{44}H_{83}NO_9$ based on based on its sodiated molecular ion at 792.5948 $[M+Na]^+$, while compound **4.3** had formula of $C_{46}H_{87}NO_9$ based on its sodiated

molecular ion at 820.6250 $[M+Na]^+$. This showed that compound **4.3** had two more CH_2 groups in its structure than compound **4.2**. The structure shown is only one possible structure for compound **4.3**, since no further structure data were obtained to determine the length of each acyl chain and the position of the double bonds. However, the specific rotation of compound **4.3** ($[\alpha]_D$ -9º (c 0.1, MeOH)) matches well with that of the literature compound ($[\alpha]_D$ -3.8º (c 0.1, MeOH)), which indicates the similar structure of compound **4.3** and literature compound.[2]

Compounds **4.4** and **4.5** both had similar ^1H NMR spectra to that of compound **4.2**. Comparing their molecular weights obtained from the HRESIMS spectra, compound **4.4** had the formula of $C_{49}H_{88}NO_{15}$ based on its sodiated molecular ion at 939.5597 $[M+Na]^+$, and compound **4.5** had the formula $C_{49}H_{86}NO_{15}$ based on its sodiated molecular ion at 937.5846 $[M+Na]^+$.

The difference of molecular weight between compound **4.4** and compound **4.2** was 146.9649 ($C_5H_5O_6$ - N). Also the molecular weight of **4.4** is 916, an even number, which indicated the absence of nitrogen atom in its structure.

In its ^1H NMR spectrum, more proton signals were located in the oxygen-bearing range, and the proton signals of H-5′ (δ_H 3.71) and H-6′ (δ_H 3.71 and 3.90) were shifted upfield compared with those in compound **4.2** (H-5′′ δ_H 3.27; H-6′′ δ_H 3.70/3.86). This indicated a glycosidic linkage between C-1′′ and C-6′, and an additional glucopyranose moiety existing in the structure of **4.4**. Based on this information, dereplication was conducted by using SciFinder and the Dictionary of Natural Products databases, and structure **4.4** was identified as a possible match. Compound **4.4** has a similar specific rotation ($[\alpha]_D$ +75º (c 0.1, MeOH)) compared with that of the literature compound ($[\alpha]_D$ +47.6º (c 0.1, MeOH)) reported by Jung et al. in 1996. The comparison between the literature value and the ^1H NMR data of **4.4** are listed in Table 4-3, and they match very well.

Similar to compound **4.4**, compound **4.5** also had one more glucopyranose moiety in its structure from an analysis of its ^{1}H NMR spectrum. And because its molecular weight was 914, an even number, no nitrogen atom existed in its structure. The difference of molecular weight between **4.4** and **4.5** was only 2 (2H), which indicated that compound **4.5** had one more additional double bond than compound **4.4**. The specific rotation of compound **4.5** ($[\alpha]_D$ +69º (c 0.1, MeOH)) also matches well with that of the literature compound ($[\alpha]_D$ +47.6º (c 0.1, MeOH)) reported by Zhang et al. in 2012.[11] And this proves a similar structure between compound **4.5** and literature compound.

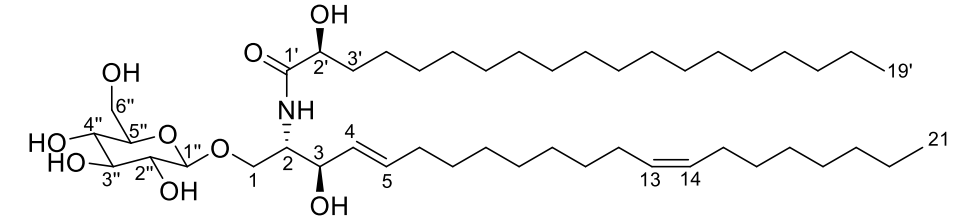

4.3

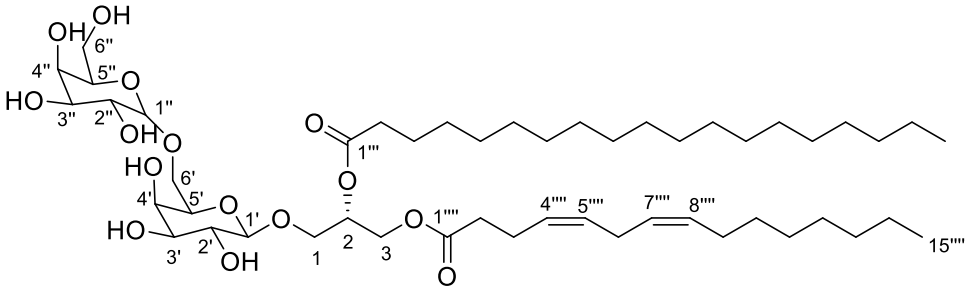

4.4

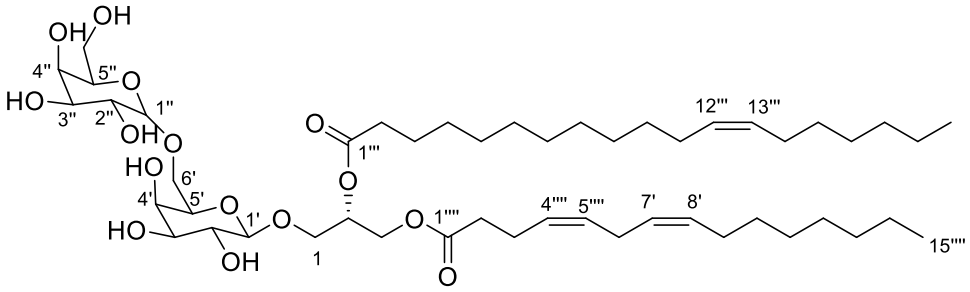

4.5

Table 4-3. NMR spectroscopic data of **4.4**.

	Compound **4.4**	Literature Value for **4.4**[10]
Position	δ_H (*J* in Hz)[a]	δ_H (*J* in Hz)[a]
1	3.90, m[b]	3.93, dd (11.0, 5.8)
	3.71, m[b]	3.73, dd (11.0, 6.2)
2	5.25, m	5.25, m
3	4.43, dd (12.0, 2.9)	4.43, dd (12.0, 3.0)
	4.21, dd (12.7, 6.7)	4.20, dd (12.0, 6.8)
1′	4.24, d (7.3)	4.23, d (7.5)
2′	3.48, m	3.50, dd (10.0, 7.5)
3′	3.48, m	3.47, dd (10.0, 3.5)
4′	3.90, m[b]	3.86, dd (3.5, 1.5)
5′	3.71, m[b]	3.73, t (6.2)
6′	3.90, m[b]	3.89, dd (6.3, 10.2)
	3.71, m[b]	3.66, dd (6.2, 10.2)
1′′	Overlap with water peak	4.84, d (3.8)
2′′	3.71, m[b]	3.78, dd (10.0, 3.8)
3′′	3.71, m[b]	3.72, dd (10.0, 3.5)
4′′	3.90, m[b]	3.88, dd (3.5, 1.5)
5′′	3.71, m[b]	3.70, t (5.9)
6′′	3.71, m[b]	3.72, dd (11.6, 6.1)
	3.71, m[b]	3.69, dd (11.6, 5.5)
2′′′	2.32, t (7.30)	2.33, t (7.4)
2′′′′	2.32, t (7.30)	2.30, t (7.4)
3′′′, 3′′′′	1.60, m	1.60, m
4′′′-18′′′, 10′′′′-14′′′′	1.29, m	1.30, m
3′′′′, 9′′′′	2.08, m	2.07, m
4′′′′, 5′′′′, 7′′′′, 8′′′′	5.34, m	5.34, m
6′′′′	2.82, t (6.74)	2.78, t (6.8)
19′′′	0.90, t (6.48)	0.90, t (6.8)
15′′′′	0.98, t (6.61)	0.90, t (6.8)

[a]Data(δ) measured at 500 MHz; s = singlet, d = doublet, m = multiplet. *J* values are in Hz and are omitted if the signals overlapped as multiplets.
[b]Overlapping signals

4.3.5 Bioactivities

The antiplasmodial activities of compounds **4.2** to **4.5** were evaluated against *Plasmodium falciparum* strain Dd2. Both compounds **4.2** and **4.3** showed weak antiplasmodial activity with IC_{50} values between 5 to 10 μg/mL. Compounds **4.4** and **4.5** were inactive in this assay. The severe loss of bioactivity may be due to an incomplete flush of the HPLC column, so some active

compounds with low polarity may still remain in the C_{18}-HPLC column, but this is quite unlikely since I flushed the column for a long time with MeOH after finishing the experiment. A second possible explanation is decomposition of an active compound on the HPLC column, and a third possible explanation is that the high activity noted for the active fraction after chromatography on the diol column was the result of an oversensitive assay, as has been observed previously in Kingston group (Yongle Du, personal communication).

Table 4-4. Antiplasmodial activity data of compound **4.2** to **4.5**.

Compound	*P. falciparum* Dd2 strain, IC_{50} (μg/mL)
4.2	$5 < IC_{50} < 10$
4.3	$5 < IC_{50} < 10$
4.4	NA
4.5	NA

4.4 Experimental Section

4.4.1 General Experimental Procedures

Mass spectra were measured on an Agilent 6220 LC-TOF-MS in the positive ion mode. NMR spectra were obtained in $CDCl_3$ and MeOD on Bruker AVANCE 500 spectrometer. Semi-preparative HPLC was carried out on an instrument with a Shimadzu SCL-10A controller, Shimadzu LC-10AT pumps, SPD-M10A UV detector, and SEDEX 75 ELSD detector, with a semi-preparative C_{18} Varian Dynamax column (250 × 10 mm).

4.4.2 Plant Material

The stems parts of *Erica maesta* were collected in Tsitsikamma National Park, South Africa in 1999 by Johan Ventner and R. Brand. The voucher specimen is JV09861b.

The whole plant of *Hohenbergia antillana* was collected at Puerto Rico at 18.28 N, 66.57W, Jayuya by Hannah Stevens of the New Yourk Botanical Garden. The specimen is HS00229.

4.4.3 Extraction and Isolation

Dried stems of *Erica maesta* (Ericaceae) were extracted with EtOH at room temperature for 24 hours. The ethanol fraction was found to have antiplasmodial activity with IC_{50} value around 5 μg/mL, and shipped to Virginia Tech as crude extract 1000585-10C. A 500 mg sample was suspended in 100 mL 90% aqueous MeOH, and then extracted with hexanes (3 × 100 mL portions) to give 30.2 mg of a hexanes-soluble fraction with an IC_{50} value between 5 and 10 μg/mL. The remaining materials were evaporated under vacuum and dissolved in 60% aqueous MeOH. This fraction was then extracted with dichloromethane (3 × 100 mL portions) to give 70.7 mg of a CH_2Cl_2–soluble fraction with IC_{50} value over than 10 μg/mL. The residual aqueous MeOH soluble fraction was evaporated under vacuum, and yielded 455.5 mg inactive materials. Then the most active hexanes-soluble fraction was applied to a silica open column, and eluted with hexanes : EtOAc = 1 : 1 to yield five fractions. The last fraction from this column turned out to be the most active one, with an IC_{50} value around 10 μg/mL and a major compound as determined by TLC (silica gel developed with hexanes : EtOAc = 1 : 1). A second silica gel open column separation yielded 3.3 mg of compound **4.1**.

Extract X-7586 was the whole part of *Hohenbergia antillana* (Bromeliaceae), obtained by the same method described above. The crude extract was found to have antiplasmodial activity with an IC_{50} value of 1.25 μg/mL. A 1.3 g sample was suspended in 100 mL 90% aqueous MeOH, and extracted with hexanes (3 × 100 mL portions) to give 218.9 mg of a hexanes-soluble fraction with an IC_{50} value around 20 μg/mL. The remaining materials were evaporated under vacuum and dissolved in 60% aqueous MeOH. This fraction was then extracted with dichloromethane (3 × 100 mL portions) to give 395.2 mg of a CH_2Cl_2–soluble fraction with an IC_{50} value between 1.25 and 2.5 μg/mL. The residual aqueous MeOH soluble fraction was evaporated under vacuum, and

yielded 705.3 mg of inactive materials. The most active CH_2Cl_2-soluble fraction was applied on a diol open column, and eluted with the solvent CH_2Cl_2 : MeOH = 20 : 1, and gave nine fractions. Fraction 8 turned out to be the most active one, with an IC_{50} value much less than 1.25 μg/mL. About 10 mg of this was then applied to a reversed phase C_{18} HPLC column (5 μm, 10 × 250 mm), and eluted with aqueous methanol from 80% to 100% over 30 minutes with a flow rate of 2.5 mL/min. Compound **4.2** (2.1 mg) was obtained at 25.5 min, compound **4.3** (1.6 mg) was obtained at 28 min, compound **4.4** (2.0 mg) was obtained at 21 min, and compound **4.5** (0.5 mg) was obtained at 23 min.

4.4.4 Antimalarial Bioassays

The antimalarial bioassays were conducted in Dr. Cassera's group by the same procedures as described in chapter 2.

4.5 Spectroscopic Properties

Compound **4.1**: white powder; $[\alpha]_D$ +10º (c 0.1, CH_2Cl_2), [lit.[2] $[\alpha]_D$ +24.09º (c 0.498, CH_2Cl_2)]; ^1H NMR (500 MHz, $CDCl_3$) see Table 4-1; HRESIMS *m/z* 425.3783 $[M+H]^+$ (calcd for $C_{30}H_{49}O^+$, 425.3739).

Compound **4.2**: white powder; $[\alpha]_D$ -4º (c 0.1, MeOH), [lit.[2] $[\alpha]_D$ -3.7º (c 0.1, MeOH)]; ^1H NMR (500 MHz, MeOD) see Table 4-2; HRESIMS *m/z* 792.5948 $[M+Na]^+$ (calcd for $C_{44}H_{83}NO_9Na^+$, 792.5960).

Compound **4.3**: white powder; $[\alpha]_D$ -9º (c 0.1, MeOH), [lit.[2] $[\alpha]_D$ -3.8º (c 0.1, MeOH)]; ^1H NMR (500 MHz, MeOD) δ_H 3.73 (1H, m, H-1), δ_H 4.14 (1H, m, H-1′), δ_H 3.99 (1H, m, H-2), δ_H 4.14 (1H, m, H-3), δ_H 5.48 (1H, m, H-4), δ_H 5.74 (1H, m, H-5), δ_H 2.07 (1H, m, H-6), δ_H 1.29 (10H, m, H-7-11), δ_H 2.07 (1H, m, H-12), δ_H 5.36 (1H, m, H-13), δ_H 5.36 (1H, m, H-14), δ_H 2.07 (1H, m, H-15), δ_H 1.29 (6H, m, H-16-20), δ_H 0.92 (3H, t, *J* =7.71, H-19), δ_H 3.99 (1H, m, H-2′), δ_H 1.62

(1H, m, H-3′a), δ_H 1.62 (1H, m, H-3′b), δ_H 1.29 (30H, m, H-4′-18′), δ_H 0.92 (3H, t, *J* = 7.71, H-19′), δ_H 4.25 (1H, d, *J* = 7.73, H-1′′), δ_H 3.21 (1H, m, H-2′′), δ_H 3.35 (1H, m, H-3′′), δ_H 3.27 (1H, m, H-4′′), δ_H 3.27 (1H, m, H-5′′), δ_H 3.88 (1H, m, H-6′′a), δ_H 3.73 (1H, m, H-6′′b); HRESIMS *m/z* 820.6250 $[M+Na]^+$ (calcd for $C_{46}H_{87}NO_9Na^+$, 820.6273)

Compound **4.4**: colorless oil; $[\alpha]_D$ +75º (c 0.1, MeOH), [lit.[10] $[\alpha]_D$ +89º (c 0.06, MeOH)]; ^{1}H NMR (500 MHz, $CDCl_3$) see Table 4-3. HRESIMS *m/z* 939.5997 $[M+Na]^+$ (calcd for $C_{49}H_{88}O_{15}Na^+$, 939.6015).

Compound **4.5**: colorless oil. $[\alpha]_D$ +69º (c 0.1, MeOH), [lit.[11] $[\alpha]_D$ +47.6º (c 0.1, MeOH)]; ^{1}H NMR (500 MHz, $CDCl_3$) δ_H 3.87 (1H, m, H-1a), δ_H 3.74 (1H, m, H-1b), δ_H 5.24 (1H, m, H-2), δ_H 3.87 (1H, m, H-3a), δ_H 4.21 (1H, m, H-3b), δ_H 4.25 (1H, m, H-1′), δ_H 3.48 (1H, m, H-2′), δ_H 3.48 (3H, m, H-3′), δ_H 3.87 (1H, m, H-4′), δ_H 3.74 (1H, m, H-5′), δ_H 3.87 (1H, m, H-6′a), δ_H 3.74 (1H, m, H-6′b), δ_H 4.45 (1H, d, *J* = 3.98, H-1′′), δ_H 3.74 (1H, m, H-2′′), δ_H 3.74 (1H, m, H-3′′), δ_H 3.74 (1H, m, H-5′′), δ_H 3.74 (2H, m, H-6′′), δ_H 2.33 (2H, m, H-2′′′, 2′′′′), δ_H 1.61 (2H, m, H-3′′′, 3′′′′), δ_H 1.29 (40H, m, H-4′′′-18′′′, 10′′′′-14′′′′), δ_H 2.08 (2H, m, H-3′′′′-9′′′′), δ_H 5.34 (6H, m, H-4′′′′, 5′′′′, 7′′′′, 8′′′′, 12′′′, 13′′′), δ_H 2.80 (1H, t, *J* = 6.92, H-6′′′′), δ_H 0.90 (6H, m, H-19′′′, 15′′′′). HRESIMS *m/z* 937.5846 $[M+Na]^+$ (calcd for $C_{49}H_{86}O_{15}Na^+$, 937.5859).

4.6 Supporting Information

4.6.1 ^{1}H NMR spectrum of 4.1 ($CDCl_3$, 500 MHz)

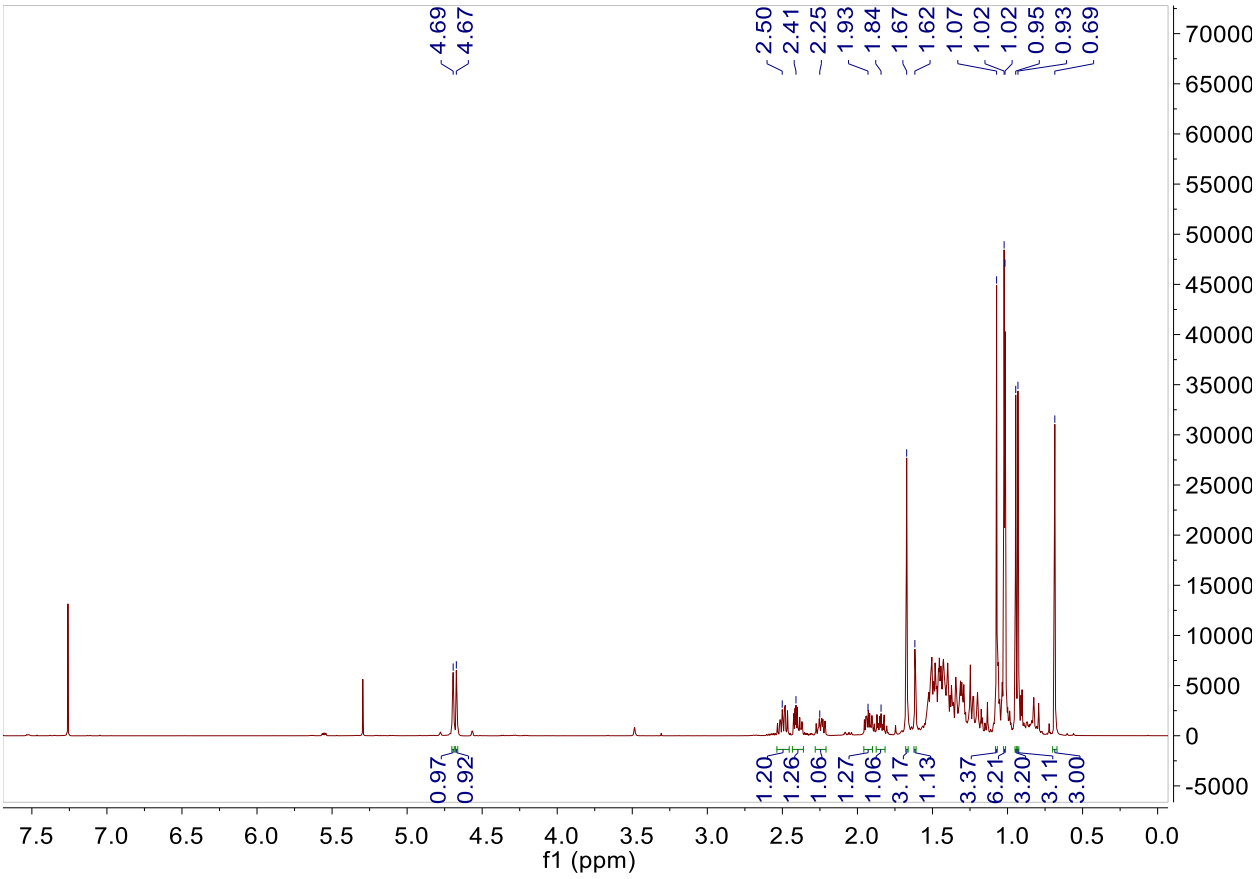

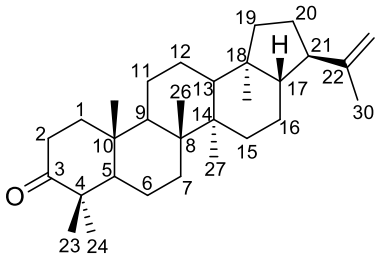

4.6.2 ^{13}C NMR spectrum of 4.1 ($CDCl_3$, 125 MHz)

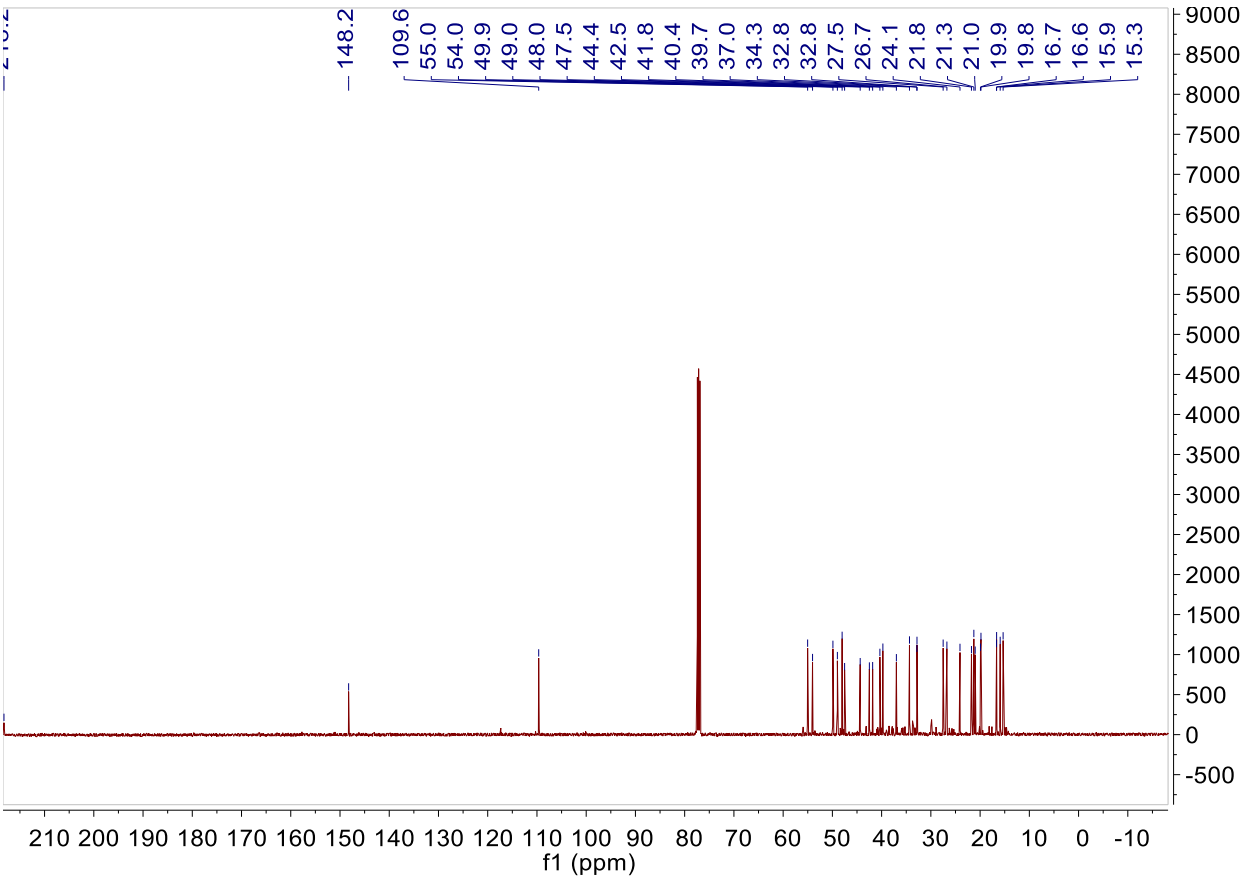

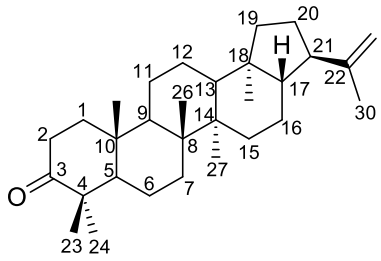

4.6.3 ^{1}H NMR spectrum of 4.2 (MeOD, 500 MHz)

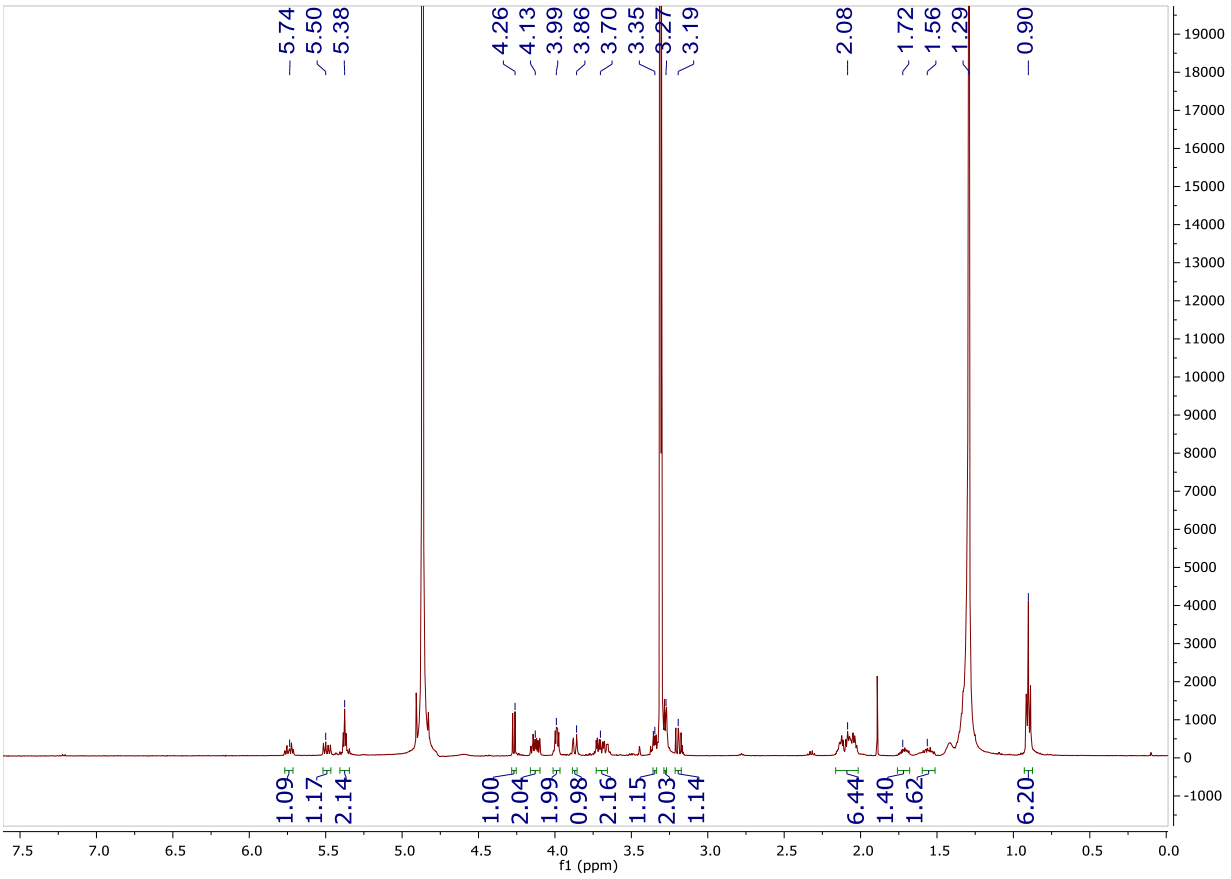

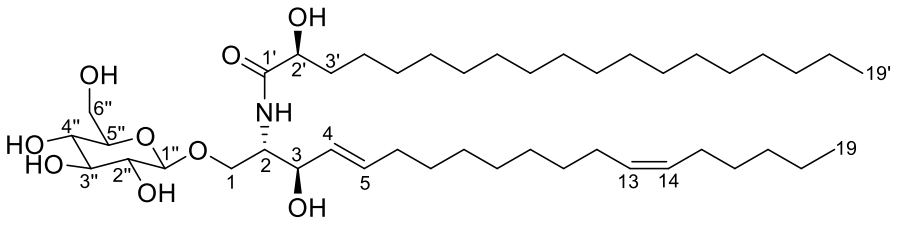

4.6.4 HSQC NMR spectrum of 4.2 (MeOD, 500 MHz 125 MHz)

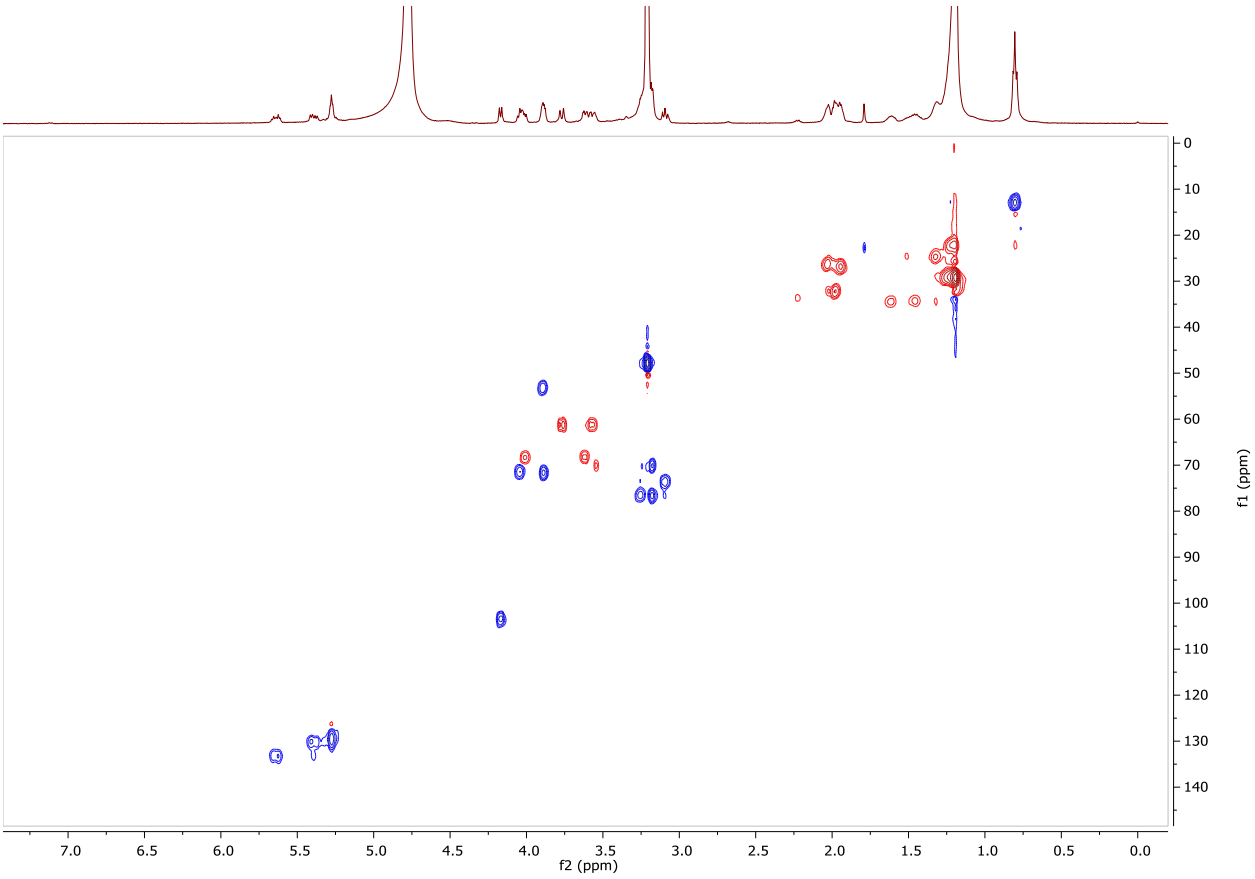

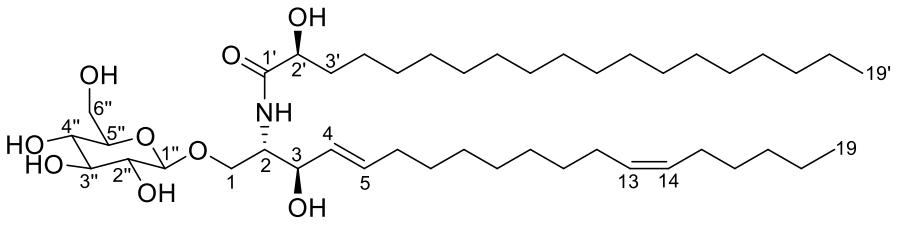

4.6.5 ^{1}H NMR spectrum of 4.3 (MeOD, 500 MHz) not pure

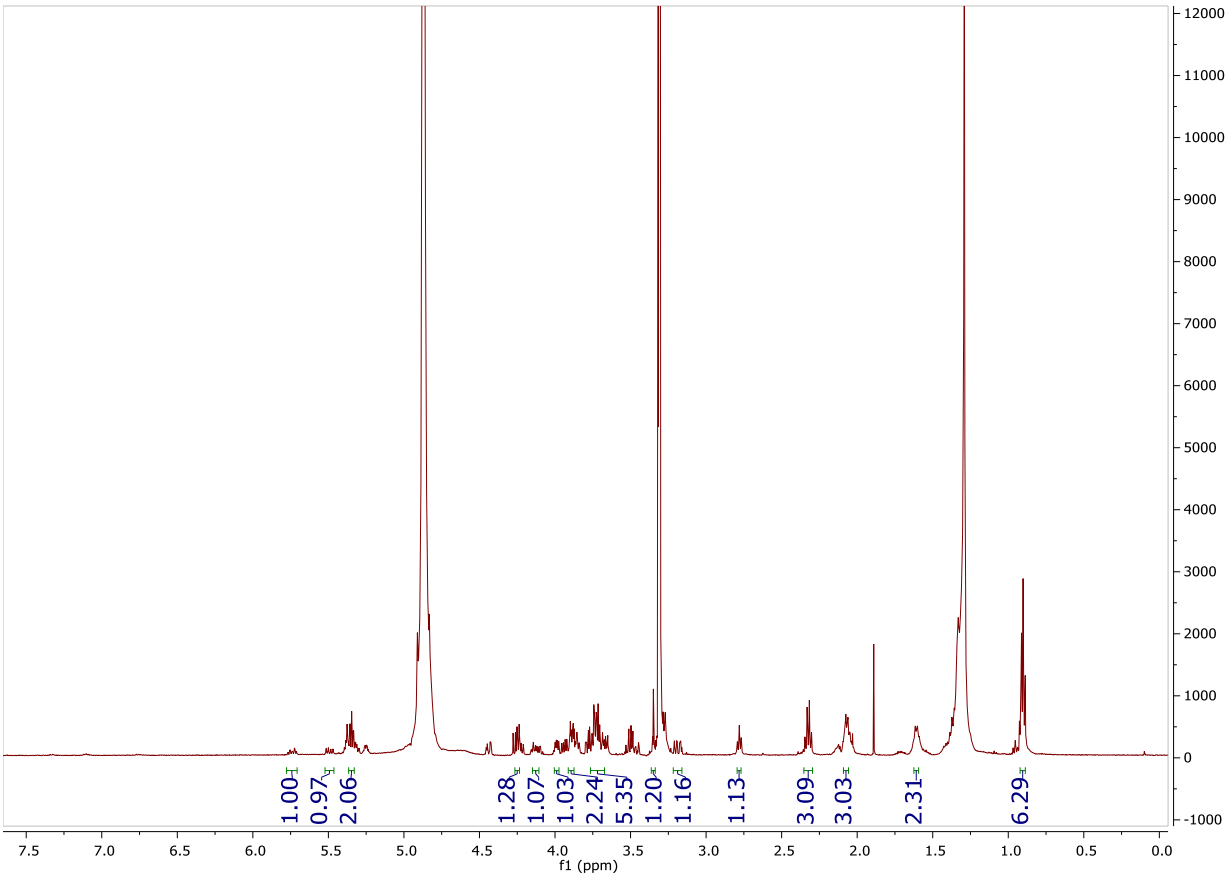

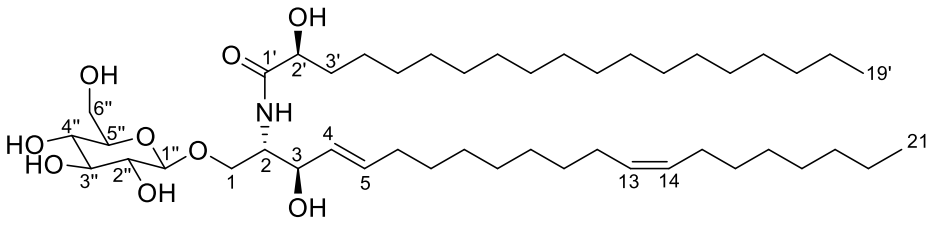

4.6.6 ^{1}H NMR spectrum of 4.4 (MeOD, 500 MHz) not pure

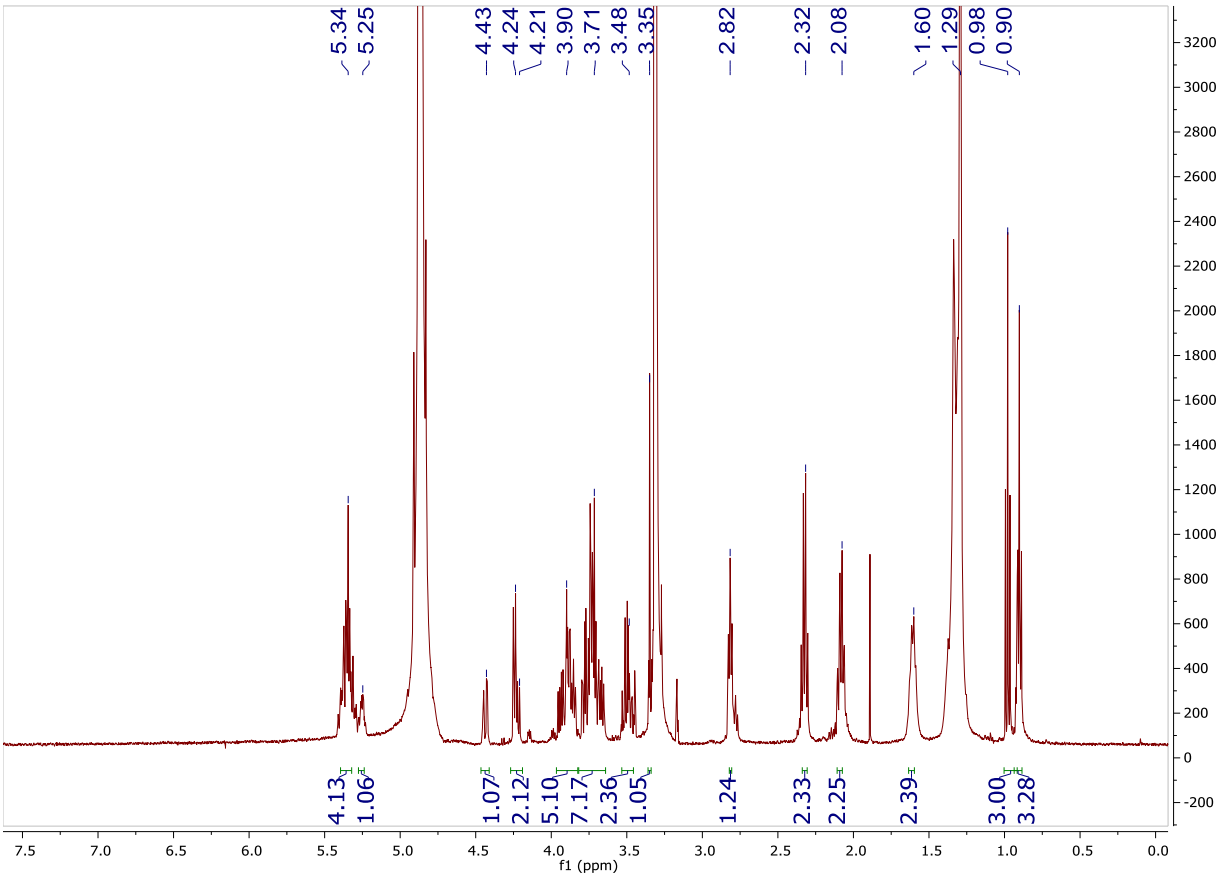

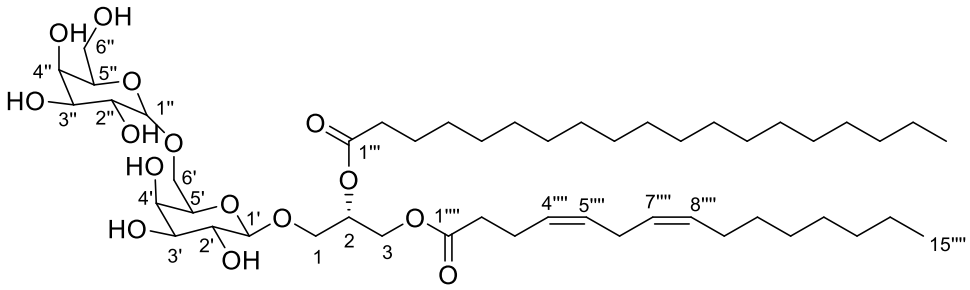

4.6.7 ^{1}H NMR spectrum of 4.5 (MeOD, 500 MHz)

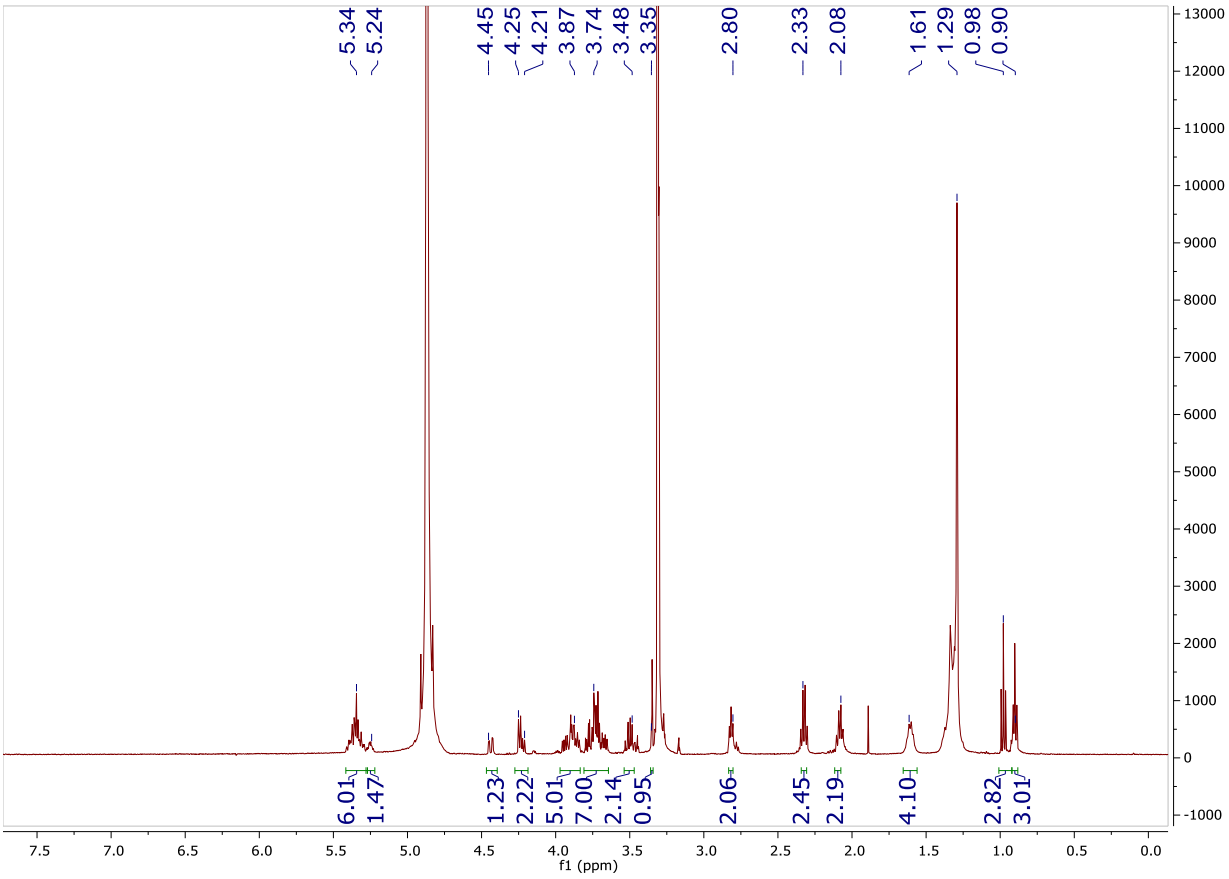

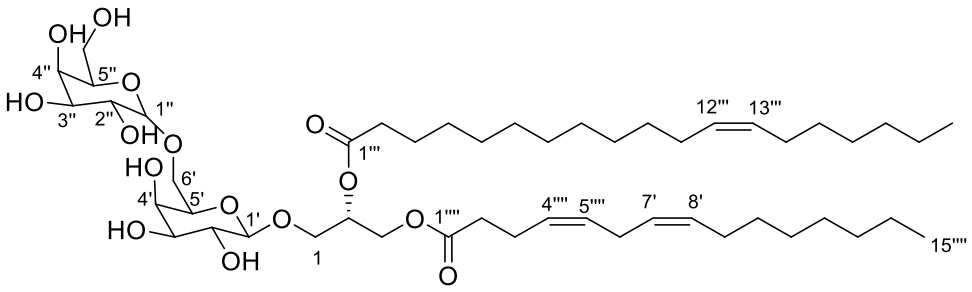

4.7 References

(1) Bitchagno, G. T. M.; Tankeo, S. B.; Tsopmo, A.; Mpetga, J. D. S.; Tchinda, A. T.; Fobofou, S. A. T.; Nkuete, A. H. L.; Wessjohann, L. A.; Kuete, V.; Tane, P. Ericoside, a New Antibacterial Biflavonoid from *Erica mannii* (Ericaceae). *Fitoterapia* **2016**, *109*, 206–211.

(2) Wai-Haan, H.; Man-Moon, L. Triterpenoids from Two Mallotus Species: A nor-Triterpene and Two New Acids. *Phytochemistry* **1976**, *15*, 985–986.

(3) Chakravarty, A. K.; Mukhopadhyay, S.; Das, B. Swertane Triterpenoids from *Swertia chirata*. *Phytochemistry* **1991**, *30*, 4087–4092.

(4) Tao, W.-W.; Yang, N.-Y.; Liu, L.; Duan, J.-A.; Wu, D.-K.; Qian, D.-W.; Tang, Y.-P. Two New Cerebrosides from the Pollen of *Typha angustifolia*. *Fitoterapia* **2010**, *81*, 196–199.

(5) Inagaki, M.; Oyama, A.; Arao, K.; Higuchi, R. Constituents of Crinoidea, 4. Isolation and Structure of Ceramides and Glucocerebrosides from the Feather Star *Comanthus japonica*. *Chem. Pharm. Bull.* **2004**, *52*, 1307–1311.

(6) Hue, N.; Montagnac, A.; Pa"\is, M.; Serani, L.; Laprévote, O.; Menou, J.-L.; Debitus, C. Structural Elucidation of Eighteen Cerebrosides from *Holothuria coronopertusa* in a Complex Mixture by High-Energy Collision-Induced Dissociation of $[M+ Li]^+$ Ions. *Eur. J. Mass Spectrom.* **2001**, *7*, 409–418.

(7) Shao, J.H.; Zhao, C.C.; Zhao, R. A New Cerebroside from *Anemone rivularis*. *Chem. Nat. Compd.* **2013**, *49*.

(8) Higuchi, R.; Jian, X. I. N. J.; Inukai, K.; Komori, T. Isolation and Structure of Six New Cerebrosides, Asteriacerebrosides A-F, and Two Known Cerebrosides, Astrocerebroside A and Acanthacerebroside C. *Liebigs Ann. der Chemie* **1991**, 745–752.

(9) Munesada, K.; Yuasa, M.; Suga, T. Cerebrosides of Frog Brain. Structure of the Ceramide Part of the Cerebrosides. *J. Chem. Soc. Perkin Trans. 1* **1991**, 189–194.

(10) Jung, J. H.; Lee, H.; Kang, S. S. Diacylglycerylgalactosides from *Arisaema amurense*. *Phytochemistry* **1996**, *42*, 447–452.

(11) Zhang, H.; Oh, J.; Jang, T. S.; Min, B. S.; Na, M. Glycolipids from the Aerial Parts of *Orostachys japonicus* with Fatty Acid Synthase Inhibitory and Cytotoxic Activities. *Food Chem*. **2012**, *131*, 1097-1103.